# X-Ray Video Imaging Quality Assessment Device

*Final Design for Prototyping and Testing Report*

**Client:** CancerCare Manitoba

**Project Sponsors:** Dr. Catriona Steele and Dr. Idris Elbakri

**Faculty Advisor:** Dr. Sean O'Brien, P.Eng.

**Course:** MECH 4860

**Course Instructor:** Dr. Paul E. Labossiere, P.Eng.

**Submission Date:** December 4th, 2019

**Team Number:** 9

**Team Members:**


Chandler J. del Carmen

Quinton E. Gitzel

Miriam Mazor

JC Ruiz

Alex (Shuo) Yang

# Executive Summary

The Imaging Physics department at CancerCare Manitoba is seeking to conduct an investigation pertaining to the image and frame quality produced in Fluoroscopy, a modality of x-ray imaging which captures multiple frames per second and sequences them into a video. Previously, a metronome was used in such an investigation, but proved insufficient due to the metronome's momentum varying over time. Thus, for the purpose of identifying Fluoroscopy frame issues which include missed, duplicated, averaged, or split frames, a specialized device was commissioned whose primary feature is a periodically repeating pattern which can be imaged by the fluoroscope, such that it is clearly disrupted at the instance of any of these frame issues.

The design team incorporated spiral geometry rotating at 60 [rpm], in order for the pattern to be continuous, as well as vary both angularly and radially, producing a unique image for each frame captured within a second-long cycle. The spiral takes up an area of 20 [cm] in diameter, maximizing the use of the area captured by the fluoroscope's image intensifier. The spiral is mounted directly onto a NEMA 6 Bipolar stepper motor, providing high precision at relatively low speeds, which eliminates the need for a drive mechanism and simplified the design. The rotation of the motor is controlled by an Arduino Uno – R3 control board and an Easy Driver – Stepper Motor Driver, all powered by a pair of 18650 Lithium Ion rechargeable batteries, providing a charge of up to 5.2 [hr] and a total lifespan of 300 charge cycles. All of these components are enclosed in an acrylic housing in order to prevent unnecessary user tampering, protect the components from any damage, and ensure appropriate visibility of the spiral when imaged by the fluoroscope. The enclosed assembly is mounted on a tripod to allow for height adjustability for compatibility with a variety of fluoroscope models.

The submission of this report marks the conclusion of the design phase of this project, with the prototype and testing phase officially commencing on January 6$^{th}$, 2020. To prepare, included in the report are a cost analysis totaling at $435.94 CAD and an assembly plan to guide the prototype manufacturing, as well as a preliminary failure modes and effects analysis to guide the team in the design of the testing plan.

# Table of Contents

# List of Figures

## List of Tables

# 1 Introduction

In partnership with the Imaging Physics Department at CancerCare Manitoba, over the course of two academic semesters, Team 9 must develop, design, prototype, and test a fluoroscopy quality assessment device, to identify quality losses as expressed by missed, duplicated, averaged, or split frames. This must be done by developing a device which employs a pattern which repeats itself in a periodic fashion, 19 needs and 21 metrics were identified. The critical constraint of the design is a budget of $2,250 for the purposes of prototyping and testing.

## 1.1 Client and Project Background

Fluoroscopy is an imaging modality in the field of radiology that produces an x-ray "movie" and is widely used in the medical field. This is done by capturing multiple x-ray frames within a second and sequencing the frames together. Oftentimes, fluoroscopy studies are viewed in real-time, but within the application of Speech-Language Pathology, Speech-Language Pathologists (SLPs) often engage in offline review of the video fluoroscopic studies (VFSS) they captured. Offline review often requires the processing and compression of the real-time VFSS and due to the various settings and filters applied during this process the compressed VFSS may experience various quality losses, including quality losses in the captured frames. This in turn effects the SLP's judgement of the VFSS, potentially resulting in a misdiagnosis.

As a preliminary step into a much larger investigation of quality losses present in fluoroscopy, CancerCare Manitoba has commissioned the team to design a device which employs a pattern moving in a periodic, continuous motion. The purpose of this tool is to identify the frame quality losses that may occur in a compressed VFSS. Currently, the solution to testing VFSS quality losses has been limited to a metronome, used during a study conducted by two of the project stakeholders, which they've determined to be insufficient. Another tool currently available for fluoroscopy quality loss assessment, but not specific to the application of VFSS is the Ludlum Model L-629-15 Rotating Spoke Test Tool, shown in Figure 1 below. The device demonstrates image distortions present in fluoroscopic examinations such as motion blur, contrast, or screen image lag [1].

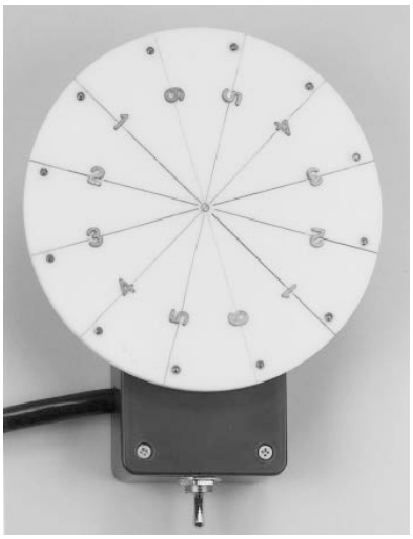

Figure 1: Ludlum model L-629-15 rotating spoke test tool (permission use granted) [1].

The Ludlum test tool is specialized for procedures using catheters. As such, the tool's features may not be as applicable to testing for the specific quality losses identified in VFSS and its purpose within Speech-Language Pathology.

## 1.2 Problem Statement

When specialists and clinicians suspect the presence of VFSS quality loss, their confidence in their interpretation and associated intervention is impacted. The team will design a fluoroscopy quality assessment tool to assist specialists and clinicians with identification, characterization, and quantification of video quality loss. The focus is specifically on frame quality loss, as expressed by the following four frame issues:

1. Missed frames
2. Duplicated frames
3. Averaged frames
4. Split frames

Missed and duplicated frames are simply when a frame was not recorded, or the same frame is shown multiple times. No illustration is available for these issues. Figure 2 below shows an example of an averaged frame for a fluoroscopy imaged metronome. This frame would have been created in the fluoroscopy imaging chain by interpolating two adjacent frames and replacing them with the interpolated frame.

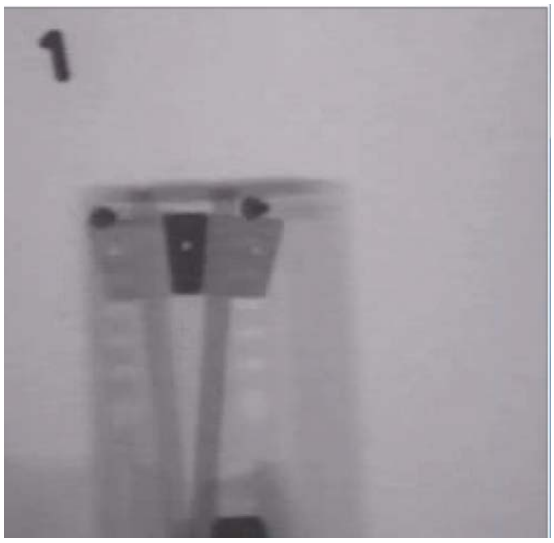

Figure 2: Example of an averaged frame (permission use granted) [2].

Figure 3 below shows an example of a split frame, where the imaged object is the same metronome as Figure 2, but now the hinged, long portion of the metronome has been split and appears broken (outlined in yellow).

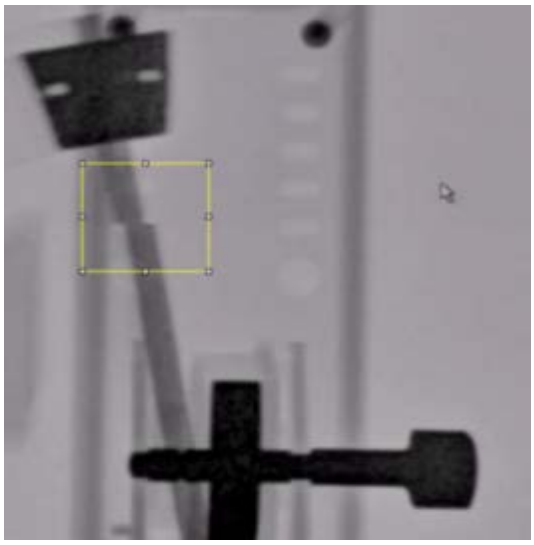

Figure 3: Example of a split frame (permission use granted) [2].

## 1.3 Objectives

The primary objectives of this design project are:

1. Identify and quantify the four frame quality losses by designing a tool whose primary feature is a continuous, periodically repeating pattern. As such, when the

pattern produced by the device is imaged by the fluoroscope, any deviations from its intended motion would indicate the presence of a frame quality loss.

2. This design will avoid operational complexities to be accessible for use by both Subject Matter Experts (SMEs) of radiology, as well as non-technical operators.
3. The designed device will be compact, allowing it to be transported across different facilities in a private vehicle, and be stored compactly in an equipment cupboard.

Secondary objectives are independent of meeting the primary objectives. Should time and resources permit, the team will design the device to be capable of identifying and indicating any resolution changes during the conversion process.

## 1.4 Scope

The design space for the quality assessment device within the fluoroscopic imaging chain represented in Figure 4 below is limited to between the filtration and the grid, essentially replacing the patient in the imaging chain.

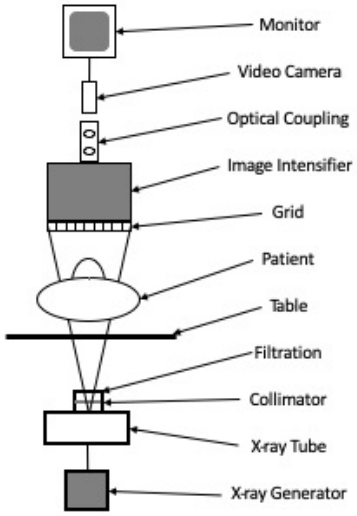


Figure 4: Components of a fluoroscopic imaging chain (redrawn from [3]).

Although the aspects of the video capture process are outside of the design space, they will be taken into consideration for the purpose of informing the team of the design's performance, as they will be used to capture the motion of the device. The design will not interface with the fluoroscope's electrical components nor explore any video compression algorithms. As a result, this will limit the solutions the team is able to employ as they must be completely independent from the fluoroscope's internal system. Other out of scope work includes

introducing new designs, tools, or methods into the patient exam process, determining fluoroscopy x-ray rate emitted from the x-ray generator and the tube, and providing solutions for the four frame issues.

The deliverables for this project as requested by the client are listed below in TABLE I, and categorized by the phase of the project to which they pertain.

TABLE I: CUSTOMER REQUESTED DELIVERABLES

| Design phase deliverables, September – December 2019) | Prototyping and testing phase deliverables, January – April 2020 |
|---|---|
| CAD model of device | Functional prototype |
| Bill of materials (BoM) | Prototype and testing plan |
| Manufacturing instructions | |

## 1.5 Customer Needs

TABLE II below details the 19 project needs, as well as the importance of each need, rated out of 5.

TABLE II: CUSTOMER NEEDS

| Needs # | Customer Needs | Importance |
|---|---|---|
| 1 | Device pattern position is unique for every frame captured within a second | 5 |
| 2 | Device is compatible for a frame rate of 15-30 fps | 5 |
| 3 | Device is able to be transported across different facilities via a private vehicle | 5 |
| 4 | Device pattern uses materials that are visible on x-ray | 5 |
| 5 | Device pattern is clear when outputted, recorded, and archived by the fluoroscope | 5 |
| 6 | Device is safe to use | 5 |
| 7 | Device pattern is clearly disrupted when a frame is averaged | 5 |
| 8 | Device pattern is clearly disrupted when a frame is split | 5 |
| 9 | Device pattern is clearly disrupted when a frame is missing | 4 |
| 10 | Device pattern is clearly disrupted when a frame is duplicated | 4 |
| 11 | Device operation is intuitive | 4 |
| 12 | Pattern maintains constant change in position between subsequent frames over time | 3 |
| 13 | Device is easy to clean | 2 |

| Needs # | Customer Needs | Importance |
|---|---|---|
| 14 | Device is easy to set up | 2 |
| 15 | Device is easy to take down | 2 |
| 16 | Device is compatible with and resistant to potential and present environmental effects | 2 |
| 17 | Device requires limited maintenance | 1 |
| 18 | Device looks sleek and professional as judged by Harry Ingleby, | 1 |
| 19 | Device is operational over many subsequent uses | 1 |

## 1.6 Engineering Metrics

TABLE III below details the 21 project metrics, nine of which have been highlighted as they have been identified as more difficult to conceptualize for a reader not familiar the specific application of the design, and additional details are provided in Appendix A.

TABLE III: ENGINEERING METRICS

| Needs # | Metric # | Engineering Metrics | Importance | Unit | Marginal Value | Ideal Value | Benchmark Value |
|---|---|---|---|---|---|---|---|
| 1 | 1 | Position change distance between subsequent frames | 5 | mm | 0.5 - 1 | < 0.7 | 0.6 |
| 1 | 2 | Overlap percentage between subsequent frames | 5 | % | < 10 | <5 | 2 |
| 2 | 3 | Pattern frequency | 5 | Hz | 0.9 | 1.1 | 0-4.2 |
| 3 | 4 | Longest dimension | 5 | m | 0.5 - 1.0 | < 0.7 | 0.6 |
| 3 | 5 | Overall volume | 5 | m^3 | < 0.5 | < 0.25 | 0.2 |
| 3 | 6 | Total mass | 5 | kg | < 8 | < 4.5 | 4 |
| 4 | 7 | Mean number of photons transmitted | 5 | $mm^2$ keV | $<1.500\times10^8$ | $<1.300\times10^8$ | $1.500\times10^8$ |
| 5 | 8 | Image sharpness as measured by spatial frequency response | 5 | line pairs/mm | < 0.5 | < 0.1 | 0.1 |

| Needs # | Metric # | Engineering Metrics | Importance | Unit | Marginal Value | Ideal Value | Benchmark Value |
|---|---|---|---|---|---|---|---|
| **6** | 9 | Accepted hazard level determined through safety hazard analysis | 5 | # | 2 | 1 | 2 |
| **7, 8, 9, 10** | 10 | Degree of frame discontinuity | 4 or 5 | % | > 90 | 95-100 | 100 |
| **11** | 11 | Device operation intuitiveness, as judged by Harry Ingleby, on a subjective scale of 10 | 4 | # | 5-10 | 8-10 | 10 |
| **12** | 12 | Steady state operation time period | 3 | minutes | > 6 | > 10 | 10 |
| **13** | 13 | Time to appropriately clean and disinfect | 2 | minutes | < 5 | < 2 | 2 |
| **14** | 14 | Assembly time | 2 | minutes | < 5 | < 3 | 1 |
| **15** | 15 | Disassembly time | 2 | minutes | < 5 | < 3 | 1 |
| **16** | 16 | Accepted environmental hazard level as determined by an environmental effect's analysis. (Scale of 1-5) | 2 | # | 3 | 1 | 4 |
| **17** | 17 | Replacement parts lead time | 2 | days | 7-21 | 7-14 | 7 |
| **17** | 18 | Maximum maintenance duration | 2 | minutes | 10 - 20 | <10 | 1 |
| **17** | 19 | Accepted service complexity level as determined through product service analysis (from 1-10 with 1 the easiest) | 2 | # | 1-5 | 1-3 | 2 |

| Needs # | Metric # | Engineering Metrics | Importance | Unit | Marginal Value | Ideal Value | Benchmark Value |
|---|---|---|---|---|---|---|---|
| **18** | 20 | Device operation aesthetics, as judged by Harry Ingleby, on a subjective scale of 10 | 2 | # | 5-10 | 8-10 | 10 |
| **19** | 21 | Device time in operation until maintenance is required | 2 | hours | >= 300 | >= 600 | 600 |

The bench marking conducted is based on the metronome presented earlier in Figure 2 and Figure 3 and originates from a study on Fluoroscopy frame quality in the context of VFSS conducted Dr. Catriona Steele and Melanie Peladeau-Pigeon at the Swallowing Rehabilitation Research Laboratory, as part of the Toronto Rehabilitation Institute, at University Health Network (UNH) [4]. The short fall of the metronome for identifying frame quality issues was due to its change in momentum, as its functionality required it to slow down, stop, and speed back up in order to change its motion direction. This results in the change in position between each position of the metronome as captured by the fluoroscope to vary and does not guarantee that every frame captured is unique, especially those that are at the edges of the motion where the metronome must come to a stop to change the direction of its motion.

## 1.7 Constraints and Limitations

TABLE IV lists and categorizes the constraints and limitations associated with the project.

TABLE IV: PROJECT CONSTRAINTS AND LIMITATIONS

| Category | Constraint |
|---|---|
| **Design Phase** | |
| | Must be completed by December 4, 2019 |
| | Budget of $400 for approved expenditures |
| **Prototyping and testing phase** | |
| | Must be completed by early April 2020 |
| | Budget of $2,250 for materials, manufacturing, and testing |

| Category | Constraint |
|---|---|
| | Testing must be conducted at either the University of Manitoba, or spaces to which the client provides access to, while complying with all relevant safety guidelines and regulations |
| **Travel** | |
| | For the purposes of travelling to client meetings, the team will be restricted to the use of their private vehicles, or public transportation provided by Winnipeg transit |
| **Software** | |
| | For the purposes of design, analysis, and deliverables production, the team will be constrained to software for which the University of Manitoba provides licenses |
| **Manufacturing** | |
| | Manufacturing capabilities will be primarily constrained to the machine shop at CancerCare to save on manufacturing costs |
| | Any manufacturing that has been approved by the client to be conducted outside of CancerCare, must be done within Winnipeg |
| **Parts purchasing** | |
| | Purchasing of off the shelf parts will be limited to Canadian vendors to reduce costs incurred from shipping and currency exchange |
| **The Device** | |
| | Must tolerate exposure to radiation |
| | Must be able to operate with a wide range of fluoroscopic machines which requires the device to meet the following:<br>• Imaged portion of the device must be fully visible by a 20 [cm] diameter image scanner<br>• Must operate either in a vertical or horizontal fluoroscope configuration<br>• Must securely operate at a height no lower than the minimum height of the fluoroscope Field of View (FOV). Minimum height of 1 [m] prescribed by the client |
| | Device must identify quality loss associated with the frame rate |
| | Device must use an accessible energy source |

# 2 Concept Development

The concept generation phase focused on coming up with different methods of employing the periodically repeating pattern, which is the primary objective of the designed device. To guide this process first four potential motion types were identified, including circular, lateral, linear and fluid. Concepts were developed under each of these categories, and the resulting top three concepts identified towards the conclusion of the concept generation phase included two circular motion concepts, and one lateral motion concept. Once these three top concepts were further assessed, it was identified that the best concept was one which incorporated circular motion by employing a rotating spiral which varied angularly and radially. For additional detailed information on the concept development phase, including the description of all concepts considered, see Appendix B.

## 2.1 Motion Types

The four different motion types identified in order to guide the concept generation phase are listed and described in TABLE VII below.

TABLE V: MOTION TYPES IDENTIFIED

| *CIRCULAR* | *LINEAR* | *LATERAL* | *FLUID* |
|---|---|---|---|
|  | 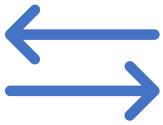 |  |  |
| Circular motion is a periodic continuous motion. Speed can be easily adjusted, and the motion can be easily established. It's the simplest motion type for the device. | Lateral motion is a unidirectional motion. The object's motion goes from one side of the sensor to the other end. It's a simple type of motion that | Linear motion is a unidirectional movement. The motion goes in the same path as the electrons emitted by the X-ray machine. The mechanism relies on the contrast | Fluid motion is a motion type where the material to be used is radiopaque fluids. The motion will be driven using pumps. |

| *CIRCULAR* | *LINEAR* | *LATERAL* | *FLUID* |
|---|---|---|---|
| | can be established for the device. | of the object for identification of the motion | |

Some examples of the concepts that were generated and their descriptions are tabulated are shown in TABLE VI. More preliminary concepts are illustrated in Appendix B.

TABLE VI: SAMPLE CONCEPTS FOR MOTION TYPES

| **Sample Design Space** | |
|---|---|
| 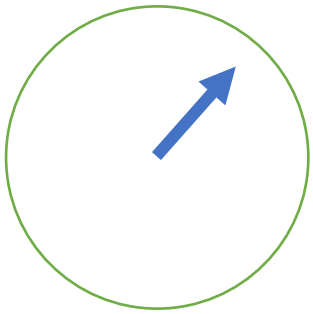 **Circular Motion: Simple Clock** | The idea was inspired by a simple cock set up as illustrated in the figure on the left. The clock hand runs with continuous motion in a constant speed. It potentially can carry out frames with identical pattern. The contrast of frame can be obtained from clock hand with inner empty. |
| 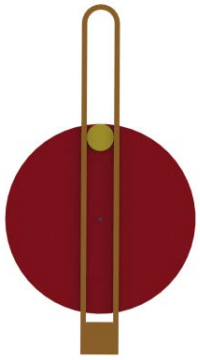 **Linear Motion: Slider and Pin** | Here, the idea is that to convert circular motion into lateral motion such that we can obtain a lateral pattern with less distractions comparing with the circular motion. |

| Sample Design Space | |
|---|---|
| 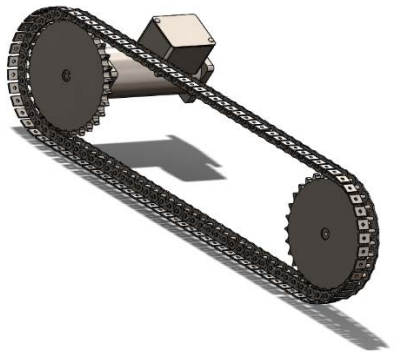 <br>**Lateral Motion: Chain Drive** | The idea is to have belt/chain drive system that expose to of X-ray as illustrated in the left. On the belt or chain, we attach it with a mantellic object for obtaining contrast. The driving system will be driven by an electrical motor where the motor is calibrated with a constant output speed. |
| 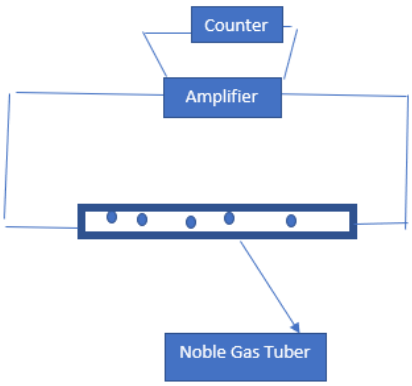 <br>**Miscellaneous Concept: Noble Gas** | The idea here is inspired by the Geiger counter system. As the x-ray pass through the noble gas tube, will ionize the noble gas inside to electrons. Electrons will flow along the cooper wire to the amplifier and convert into electrical single, counter will receive the signal and count it as a number. |

These types of motions were evaluated based on different criteria during the concept development phase of the project. The motion types of circular and lateral were selected as the main types of motion to go further in the development. The selection involved the metronome as the basis for the selection process and is demonstrated in TABLE VII below.

TABLE VII: MOTION TYPE ASSESSMENT

| | | Reference Concept | Concept Motion | | | |
|---|---|---|---|---|---|---|
| | Criteria | Metronome | Linear | Circular | Lateral | Fluid |
| 1 | Device Simplicity | 0 | - | 0 | 0 | - |
| 2 | Output Pattern Performance | 0 | - | + | + | + |

| | | Reference Concept | | Concept Motion | | |
|---|---|---|---|---|---|---|
| 3 | Variable Frame Rate Compatibility | 0 | + | + | + | + |
| 4 | Durability | 0 | 0 | 0 | 0 | - |
| 5 | Costs | 0 | - | - | - | - |
| 6 | Ease of Operation | 0 | - | + | + | 0 |
| 7 | Maintenance | 0 | - | 0 | 0 | - |
| | Sum +'s | 0 | 1 | 3 | 3 | 2 |
| | Sum 0's | 9 | 1 | 3 | 3 | 1 |
| | Sum -'s | 0 | 6 | 1 | 1 | 4 |
| | Net Score | 0 | -5 | 2 | 2 | -2 |
| | Rank | 2 | 4 | 1 | 1 | 3 |
| | **Continue?** | | **No** | **Yes** | **Yes** | **No** |

## 2.2 Top Three Concept Selection

The project entered its final design phase with three concepts still in consideration, referred to as the Spiral, Chain Drive, and Sinusoid, and a week was allocated to additional investigation into these concepts to ensure that sufficient due diligence given the time constraints is conducted in order to choose the final concept. This course of action was taken primarily due to the project's subsequent prototype and testing phase in the Winter 2020 semester. As such, higher risk is involved in the selection of the final concept, in comparison to other design groups in the course, where their conceptual design is handed off to their client at the conclusion of the Fall 2019 semester.

The additional work done during this additional week consisted of further preliminary investigation into the various components and processes required to manufacture the concepts, as well as additional client discussion. At the conclusion of the additional week spent on concept, the final concept chosen to be fully designed in detail and carried forward to the prototype and testing phase was the Spiral concept. In the below sections where the preliminary components for each concept are listed, components or systems that are common to all concepts, such as

control units and motors are excluded. Additional details for each of the top three concepts are provided in Appendix B.

### 2.2.1 Spiral

The Spiral concept, illustrated in Figure 5, is based on an Archimedean Spiral, a circular geometry which varied angularly and radially. When rotated, the position changes of the spiral would create the periodically repeating pattern required by the device. Originally, the Spiral concept was conceptualized with a gear drive actuating the rotational motion of the Spiral, but since the gear mechanism has been removed from the concept by mounting the spiral directly on the motor, and adjusting the geometry of the spiral so as to not interfere with the motor once the device is imaged by the fluoroscope.

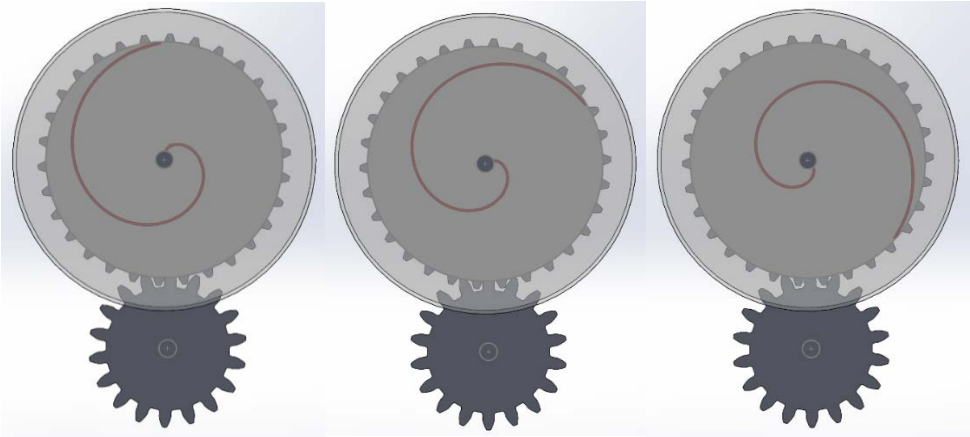

Figure 5: Spiral concept front view at varying rotational positions.

TABLE VIII below details the preliminary parts list and cost estimate for the Spiral concept, which incorporates primarily automated and rapid manufacturing processes, such as 3D printing and Laser-Cutting. This was identified as a major benefit as it would allow the team to rapidly manufacture the design, and rapidly manufacture design changes during the Prototype and Testing phase of the project.

TABLE VIII: SPIRAL CONCEPT PRELIMINARY PARTS LIST AND COST ESTIMATE

| Component | Purchase or Manufacture | Unit Cost [$USD/unit] | Quantity | Combined Cost [$USD] |
|---|---|---|---|---|
| **Acrylic sheet for casing (3 [mm] thickness, 18'x24')** | Purchase, Laser cut | 18 | 2 | 36 |
| **Spiral** | Manufacture, 3D Print | 25 | 1 | 25 |
| **Grid** | Manufacture, 3D Print | 25 | 2 | 50 |
| **Motor mount** | Manufacture, 3D Print | 40 | 1 | 40 |
| **Estimated Cost** | | | | **151** |

### 2.2.2 Chain Drive

The Chain Drive concept, a schematic for which is shown in Figure 6 below, utilizes a roller chain with to engage in lateral motion. The roller links seen in Figure 6**.** below include attachments for the mounting of unique shapes such that when the chain is engaged in motion, the position change of these shapes creates the periodically repeating pattern required for the device.

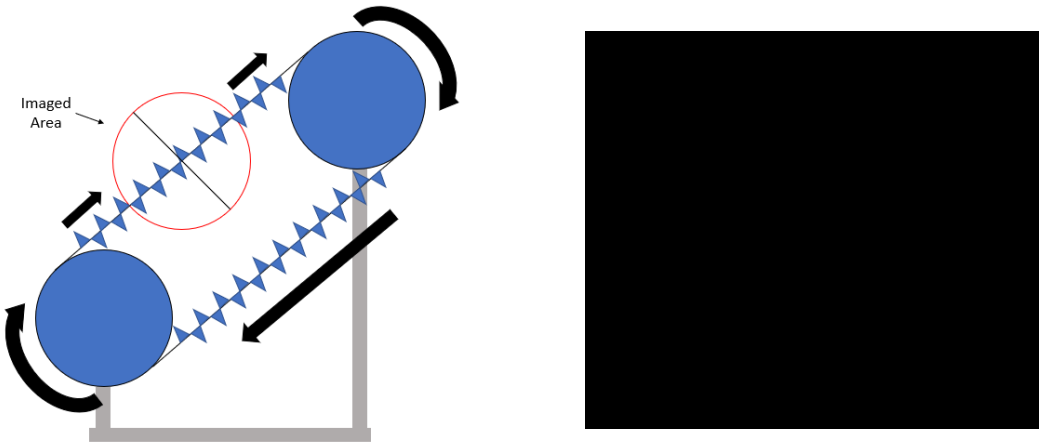


(a) (b)

Figure 6: (a) Diagonally mounted chain drive concept and (b) Roller link attachments.

TABLE IX below details the preliminary parts list and cost estimate for the Chain Drive concept. It has been found that for this concept, virtually all components are off-the-shelf purchased components, with some limited additional machining or adjustments. Although this virtually eliminates manufacturing needs for the design, this increases components lead times, as well as more importantly limits the team's ability to rapidly incorporate design changes during the prototype and testing phase of this project.

TABLE IX: CHAIN DRIVE CONCEPT PRELIMINARY PARTS LIST AND COST ESTIMATE

| Component | Purchase or Manufacture | Unit Cost [$USD/unit] | Quantity | Combined Cost [$USD] |
|---|---|---|---|---|
| **Roller chain [5]** | Purchase | 20.00 | 1 | 20.00 |
| **Roller chain attachment [6]** | Purchase | 5.00 | 30 | 150.00 |
| **Large sprocket [7]** | Purchase | 20.00 | 1 | 20.00 |
| **Small sprocket [7]** | Purchase | 20.00 | 1 | 20.00 |
| **Shaft [8]** | Purchase and machine | 30.00 | 2 | 60.00 |
| **Bearing [9]** | Purchase | 10.00 | 2 | 20.00 |
| **Retaining ring [10]** | Purchase | 10.00 | 2 | 20.00 |
| **Chain guard [11]** | Purchase | 20.00 | 1 | 50.00 |
| **Base [12]** | Purchase laser cut | 50.00 | 1 | 20.00 |
| **Tensioner [13]** | Purchase and cut | 100.00 | 1 | 100.00 |
| **Estimated Cost** | | | | **480.00** |

### 2.2.3 Sinusoid

The Sinusoid concept, a side view of which is provided in Figure 7 below, is inspired by how a moon revolves around a planet, while the planet is also rotating, creating a sinusoidal motion in a specific perspective. This type of motion can be achieved mechanically by rotating a spring type object, supported by a shaft and a pair of bearings.

Figure 7: Sinusoid concept side view.

TABLE X below details the preliminary parts list and cost estimate for the Chain Drive concept. The biggest flaw identified with the Sinusoid design is that for crucial feature, the spring, the design would depend on the capabilities of the spring manufacturer, imposing additional lead time and potentially costs on the team, as the spring would be manufactured outside of both the University of Manitoba and CancerCare, and would be a low quantity production.

TABLE X: SINUSOID CONCEPT PRELIMINARY PARTS LIST AND COST ESTIMATE

| Component | Purchase or Manufacture | Unit Cost [$USD/unit] | Quantity | Combined Cost [$USD] |
|---|---|---|---|---|
| **Sinusoid Spring** | Purchase | N/A | 1 | N/A |
| **Shaft [8]** | Purchase and machine | 30.00 | 1 | 30.00 |
| **Bearing [9]** | Purchase | 10.00 | 2 | 20.00 |
| **Grid** | 3D Print | 25.00 | 1 | 25.00 |
| **Acrylic for Casing** | Purchase and laser cut | 18.00 | 2 | 32.00 |
| **Motor Mount** | 3D Print | 40.00 | 1 | 40.00 |
| **Total Estimated Cost** | | | | **Over 147.00** |

# 3 Detailed Design

Following the submission of this report at the conclusion of the Fall 2019 academic term, the prototype and testing phase of this project will officially commence on January 6th, 2020, with the beginning of the Winter 2020 academic term, providing the team with 3 months to prototype, test, change, and re-test the design. The team took the design approach that allowed for rapid prototype manufacturing and the investigation of alternative components at an economical price point, using machine automated processes such as 3D printing and laser cutting, which are readily available to the team through either CancerCare or the University of Manitoba. The team's device

operates by using a 3D PLA filament combined with particles of bismuth that provides high contrast when viewed under x-ray. The final design is shown below in Figure 8.

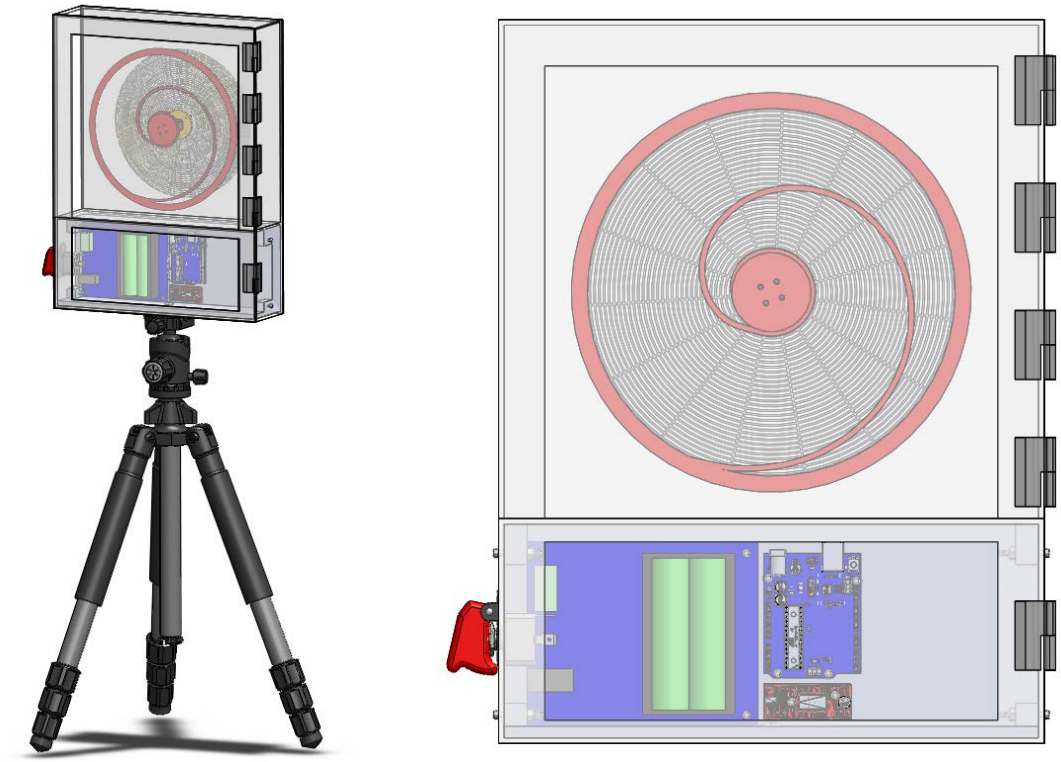

(a) (b)

Figure 8: Final design, (a) Device mounted on tripod, (b) front view.

## 3.1 Design Overview

The device consists of 19 major components as illustrated and listed in Figure 9 and TABLE XI respectively. Most components are all contained within an acrylic housing that is laser cut and bonded using acrylic cement. The grid, locating pin, quick release mount, and tripod are contained outside the housing to allow for quick removal for storage and ease of changing the grid between framerates.

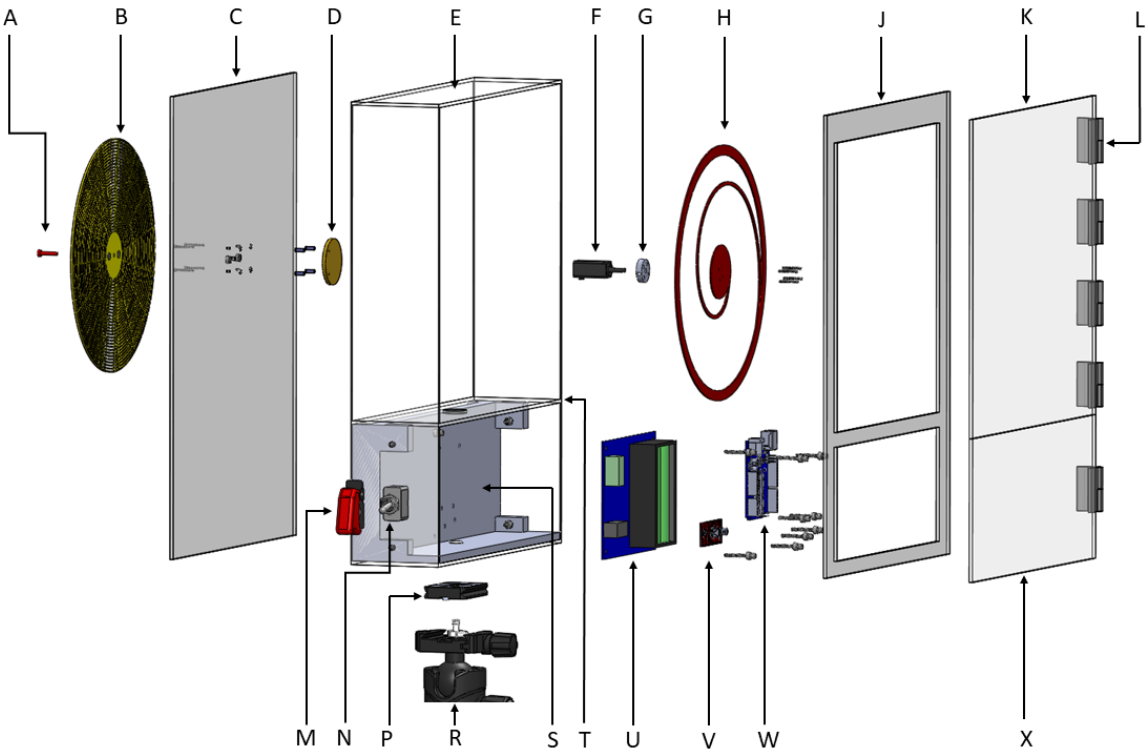


Figure 9: Frame rate quality assessment device exploded view of major device components.

TABLE XI: IDENTIFICATION OF MAJOR DEVICE COMPONENTS IN EXPLODED VIEW

| ID | Component | ID | Component |
|---|---|---|---|
| **A** | Grid Locating Pin | **M** | Safety Switch Cover |
| **B** | Grid | **N** | Power Switch |
| **C** | Rear Housing Plate | **P** | Quick Release Mount |
| **D** | Motor Mount | **R** | Tripod |
| **E** | Central Housing | **S** | Electronic Hub Mount |
| **F** | NEMA 6 Stepper Motor | **T** | Electronic and Spiral Separation Plate |
| **G** | Spiral Mount Hub | **U** | Battery Charger |
| **H** | Spiral | **V** | Motor Controller |
| **J** | Front Housing Plate | **W** | Arduino Uno |
| **K** | Spiral Access Door | **X** | Electronic Access Door |
| L | Self-Closing Hinge | | |

## 3.2 Spiral and Grid

#### *3.2.1.1 Geometry and Assembly*

The primary feature of the design is the radially and angularly varied spiral geometry, which rotates at 60 [rpm], thus producing a unique image for each position captured by the

fluoroscope image intensifier within a one second long period. The spiral's geometry is based on an Archimedean Spiral, but rather than the spiral beginning at the center of its rotation, its beginning is offset by a radius of 20 [mm] from the center. This allows for direct mounting of the spiral onto the motor, which eliminates variance in motion and added complexities inherent in the use of transmission drives such as gears, belts, and chains; but renders the area taken up by the motor restricted for use for pattern geometry. Thus, this area has been termed the "dead-zone" and designated to be 40 [mm] in diameter to allow for a change in the selected motor during prototype and testing.

The spiral component is a 3 [mm] thick, almost free-floating geometry, supported by an outer hoop of 200 [mm] internal diameter, and the inner circle 40 [mm] in diameter, which also serves to mount the spiral onto the motor. The internal diameter of the support hoop was set to 200 [mm] to maximize the area used and captured by the fluoroscope's image intensifier, as provided by the client. Bismuth PLA is used for the manufacturing of the spiral as it shows well under x-ray providing the needed contrast, as well as readily available for use by the client.

Figure 10 below demonstrates the securement of the spiral component to the motor, located at the "dead-zone" of the spiral component, which includes four 3 [mm] holes for interfacing with the 3D printed spiral mounting hub using M3-0.5 socket cap screws. The hub is then mounted directly onto the motor shaft, which is secured to the 3D printed mounting plate using a set screw. Finally, the motor mounting plate is attached to the outer acrylic walls of the device using four M3-0.5 socket cap screws.

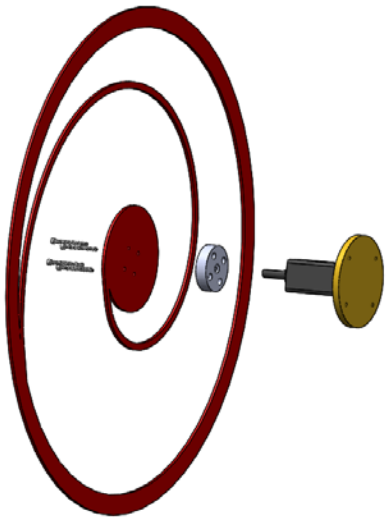

Figure 10: Mounting mechanism of spiral onto motor.

The only component other than the spiral meant to be visible within the field of view of the fluoroscopy study is the grid pictured in Figure 11 below.

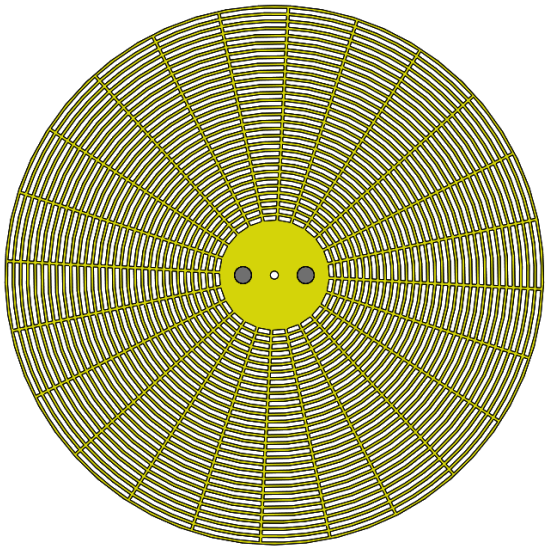

Figure 11: Grid geometry containing two 1/4" magnets.

The purpose of this grid is to serve as a reference frame for the rotating spiral, acting like “graph-paper”. Its outer diameter is 200 [mm], equal to the internal diameter of the spiral support hoop. The subdivisions of the grid are based on the frame rate setting of the fluoroscopy study, with the above Figure 11 possessing 30 subdivisions for a 30-fps setting. The line width for the grid component is 1 [mm], as recommended for the manufacturing process chosen. Additional grids will be manufactured for other fps settings that will be encountered during the testing phase of the project, including 25 fps. Similarly, to the spiral, the grids are 3D printed Bismuth PLA. The grid is mounted onto the rear of the acrylic enclosure with a pair of epoxy embedded magnets and aligned using the grid locating pin as illustrated in Figure 12.

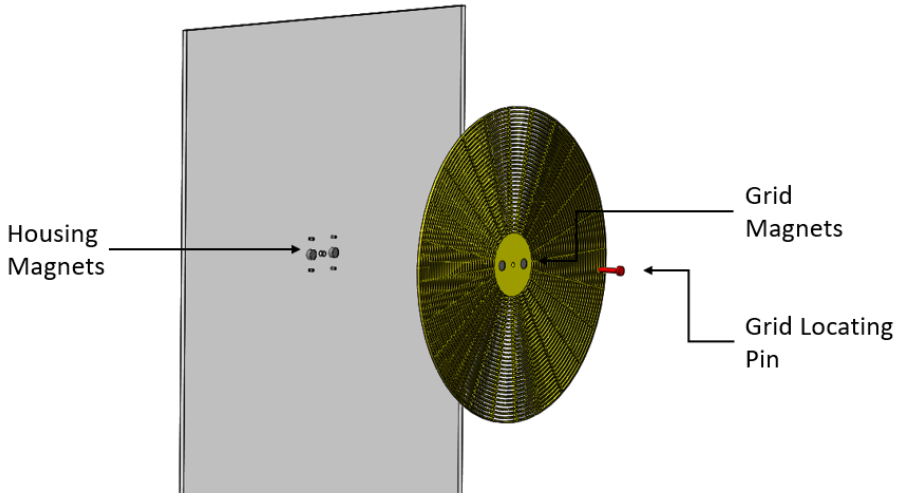


Figure 12: Grid attachment onto rear housing with embedded magnets and locating pin.

#### *3.2.1.2 Functionality*

The rotation of the spiral produces a unique position for each frame captured by the fluoroscope, advancing though one increment of the grid per frame, successfully targeting the four frame issues the project is concerned with. Figure 13**.** illustrates how the device would look under x-ray as the spiral rotates and is contrasted against the grid.

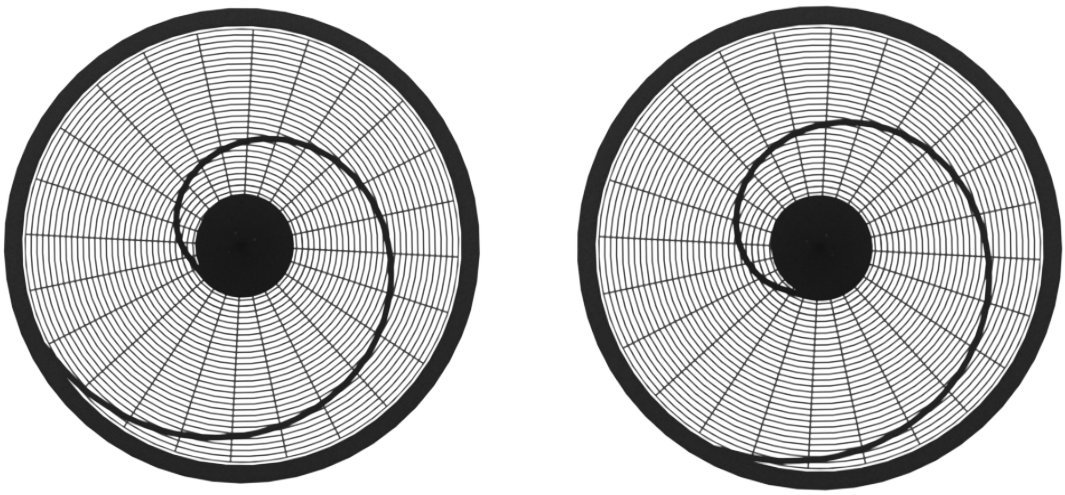

(a) (b)

Figure 13: Expected x-ray frame for device FOV during operation with missed frames. (a) initial frame, (b) advanced 2 frames.

Figure 14 simulates how the device will identify a split and averaged frame. A split frame will divide the spiral with a clear gap similarly to how the metronome performed. Two averaged

frames will result in merging the frames together, creating a darker spiral where the merged image overlaps, surrounded by a lighter boundary.

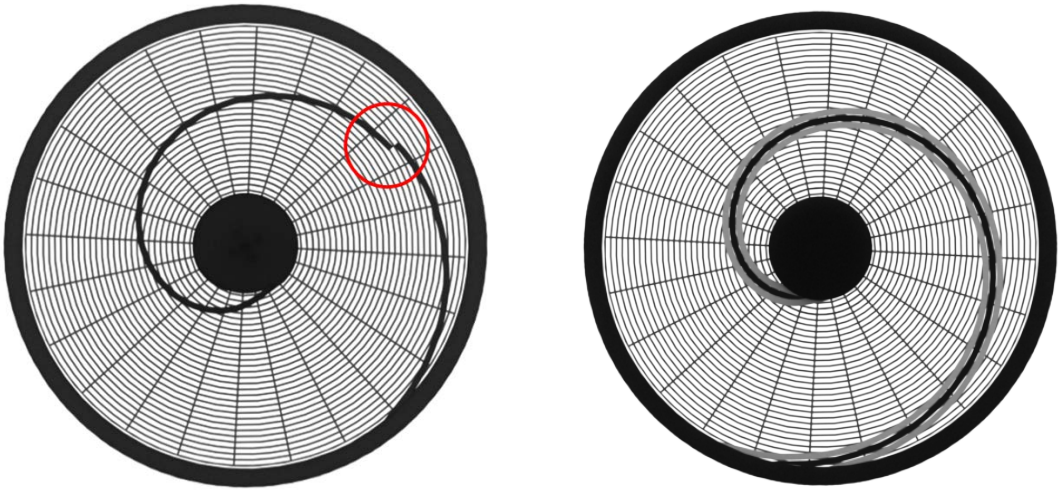

(a) (b)

Figure 14: (a) Output of a split frame halfway through the spiral, (b) output of two average frames.

One design aspect of concern to the imaged pattern quality is the motor wire which crosses the FOV vertically downwards. Since the wire is metallic, it radiopaque and expected to interfere with the pattern during a fluoroscopy in some capacity. This design choice is justified by using the wire as a reference point to the position of the spiral. The vertical alignment of the wire will be secured in place with minimal amounts of epoxy.

#### *3.2.1.3 Attenuation and Materials*

The primary purpose of our design is to identify frame quality loss in fluoroscopy through a periodically repeating pattern produced by the device, as seen in the output fluoroscopy study. As such, the contrast of the pattern during the fluoroscopy study (metric seven) is a key metric in determining the dimensioning and material used for the pattern geometry. The contrast of the pattern as outputted by the fluoroscope is defined as the difference in brightness of an object, relative to surrounding objects in its field.

Within x-ray imaging, contrast (brightness or darkness) is determined by the number of photons that pass through the object, and the number of photons transmitted by an object depend on its thickness, density, material atomic number, and the energy of the individual photons. When x-rays are directed onto objects, the projected photons will naturally interact with

the particles inside the matter and their energy will be absorbed or scattered, resulting in contrast on the image. Equation 1 below characterizes photon ease of transmission through an object, and TABLE XII described the meaning of each variable.

$$I = I_o e^{\frac{\mu}{\rho}x} \qquad \text{Equation 1}$$

TABLE XII: VARIABLES DETERMINING PHOTON TRANSMISSION

| Variable | Meaning |
|---|---|
| $\boldsymbol{I_o}$ | Initial photon intensity |
| $\boldsymbol{\mu}$ | Material attenuation coefficient |
| $\boldsymbol{\rho}$ | Material density |
| $\boldsymbol{x}$ | Material thickness |
| $\boldsymbol{I}$ | Intensity of photons transmitted through material |

The photon intensity $I$ is measured in keV, a measure of the voltage difference between the x-ray tube anode and cathode, also referred to as tube potential, and is directly related to the peak energy of photons in the resultant x-ray beam. The attenuation coefficient $\mu$ is a material property characterizing the ease through which photons can penetrate through a given material, with a decrease in this material property meaning that the medium is relatively transparent to the x-ray beam. Overall, Equation 1 communicates that relative darkness and therefore contrast to surrounding objects is achieved using thicker (1), higher density (2), larger atomic number objects (3), and lower energy input photons (4).

Of these variables, the one that the design cannot control is $I$, as it is a fluoroscope setting. Regarding this variable, the client was consulted and quoted a recommended range of 30-40 keV, and consequently, in order to design for worst case scenario, 40 keV was used since better contrast is achieved at the lower end of the keV range. For the remaining three variables, material selection and thickness were taken into consideration and varied during the attenuation analysis.

In order to obtain high contrast for key pattern features of the device when imaged by the fluoroscope, the team was recommended to utilize metals for the fabrication of these components, as all metals are radio-opaque and image well. In order to determine an appropriate thickness for these features in the direction of penetration of the x-ray beam, as well as assess

the performance of the material used, an online X-Ray Spectra Simulation tool was used, provided on the OEM Siemens Healthineers website [14]. This simulation was run with tungsten used for the input anode material, as used in fluoroscopy systems.

In order to establish a baseline for the contrast of the fluoroscope output image of our device, the simulation was first run using Human Bone as the selected material, with a 10 [mm] thickness, since bones are an object commonly imaged using a fluoroscope. Figure 15: Photons energy distribution of Bone under x-ray . below illustrates the photon energy distribution expressed in mean number of photons and measured in $mm^2$ keV, where a peak of about $1.5000 \times 10^8$ [$mm^2$ keV] was measured, within the provided input energy range of 30 – 40 [keV].

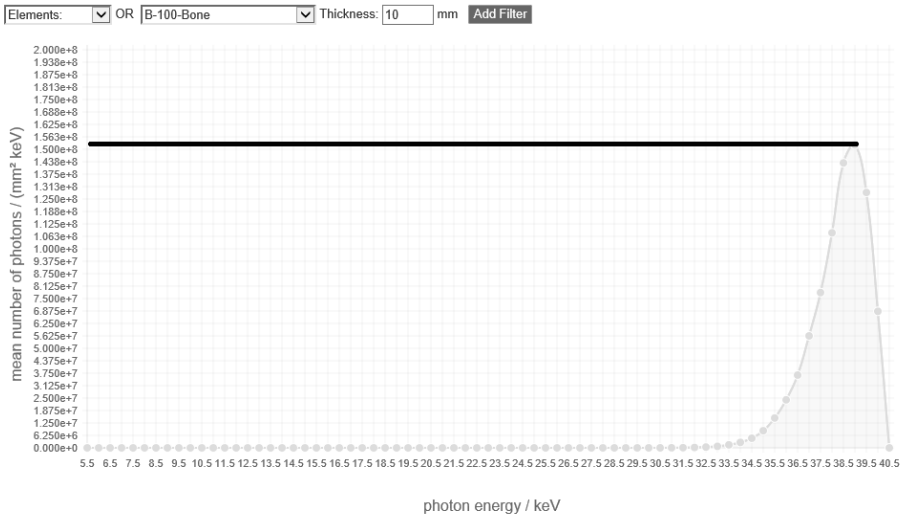


Figure 15: Photons energy distribution of Bone under x-ray [14].

The mean number of photons describes how much light is able to penetrate the object under x-ray, therefore a lower mean number of photons creates a darker image, and higher contrast. After several iterations using this tool, varying material and thickness, it was determined that Iron with a thickness of 3 [mm] would be sufficient to achieve a comparable but lower mean number of photons than Human Bone with a 10 [mm] thickness. Figure 16: Photons energy distribution of Iron under x-ray . below demonstrates the photon energy distribution for iron at this thickness, with a peak of about $1.313 \times 10^8$ [$mm^2$ keV] within the provided input energy range of 30 – 40 [keV], exceeding the performance of the 10 [mm] thick bone in terms of contrast, as less photons are able to penetrate the iron, creating higher contrast.

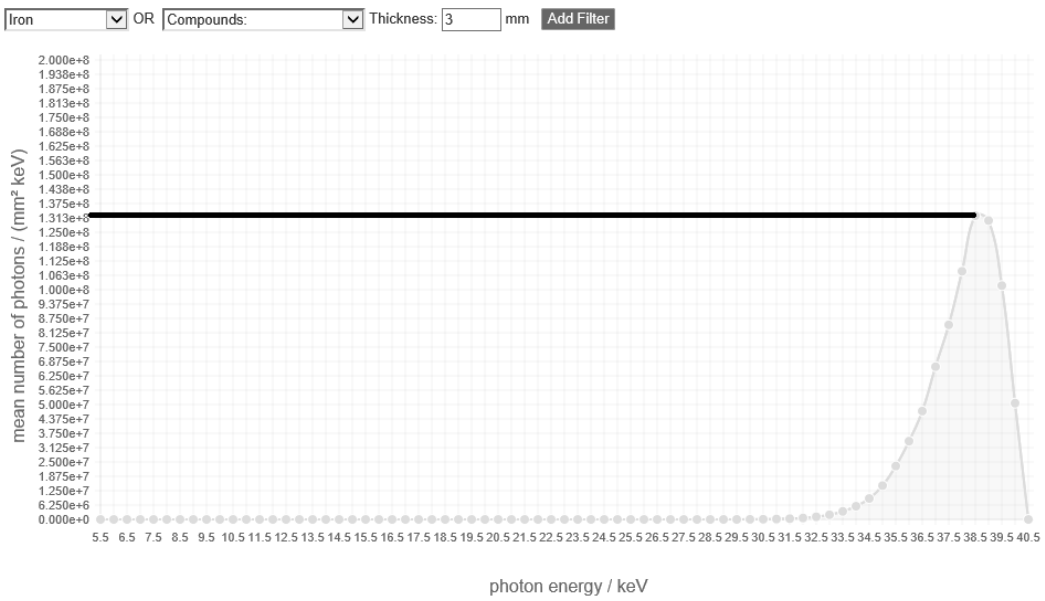


Figure 16: Photons energy distribution of Iron under x-ray [14].

After proposing a preliminary design to the client's manufacturing division, viable in-house material options and manufacturing processes were discussed for the fabrication of key pattern features. With the goal of economical, rapid prototyping in mind, it was decided to make use of 3D printed Bismuth PLA filament, which has both a higher atomic number and material density than iron, which would result in superior contrast and subsequent image contrast than the iron used in the simulation.

## 3.3 Acrylic Housing

The components of the design are contained in an acrylic enclosure is to prevent unnecessary tinkering with key components of the device, protection of these components during transportation, and drop damage protection. Acrylic was chosen as it is a clear, durable, and easy to manufacture. The enclosure material must be clear in order to allow for internal component visibility for both the naked eye and the fluoroscopy study. Acrylic's durability protects internal device components from potential damage during transportation. The acrylic enclosure is also easily manufacturable within the university by laser cutting the profiles into three [mm] thick sheets and attaching the sheets to create the enclosure.

The acrylic housing is bonded using TAP acrylic cement at each of the housing plates edges and permanently bonds the pieces by melting them together into one piece. The bonding of the

assembly is preferred over mechanical fasteners to prevent the housing coming apart and providing more strength from unexpected drops. Mechanical fasteners only provide clamping force which induce stress concentrations onto the housing, and if dropped may break where the bolts pass through the acrylic. Additionally, if the fasteners were overtightened, they may crack the acrylic. The access doors are bonded with spring self-closing acrylic hinges using acrylic cement. This provides easy access to replacing components while ensuring operator safety.

## 3.4 Tripod and Design Mount

The device is attached to a tripod to achieve the customer requirement to achieve a device height of one meter. The Orion Paragon-Plus Heavy-Duty Tripod was selected as it has a range of 31.5 [in] to 68 [in]. The team's device weighs 4.5 [lb], and the tripod has a weight rating of 10 [lb] resulting in a factor of safety of 2.2. The tripods tri-braced legs enhance device stability and reduces the risk of damage due to tipping. The quick-release shoe attaches to the 3D printed electrical housing lock nut using a standard ¼"-20 bolt as illustrated in Figure 17.

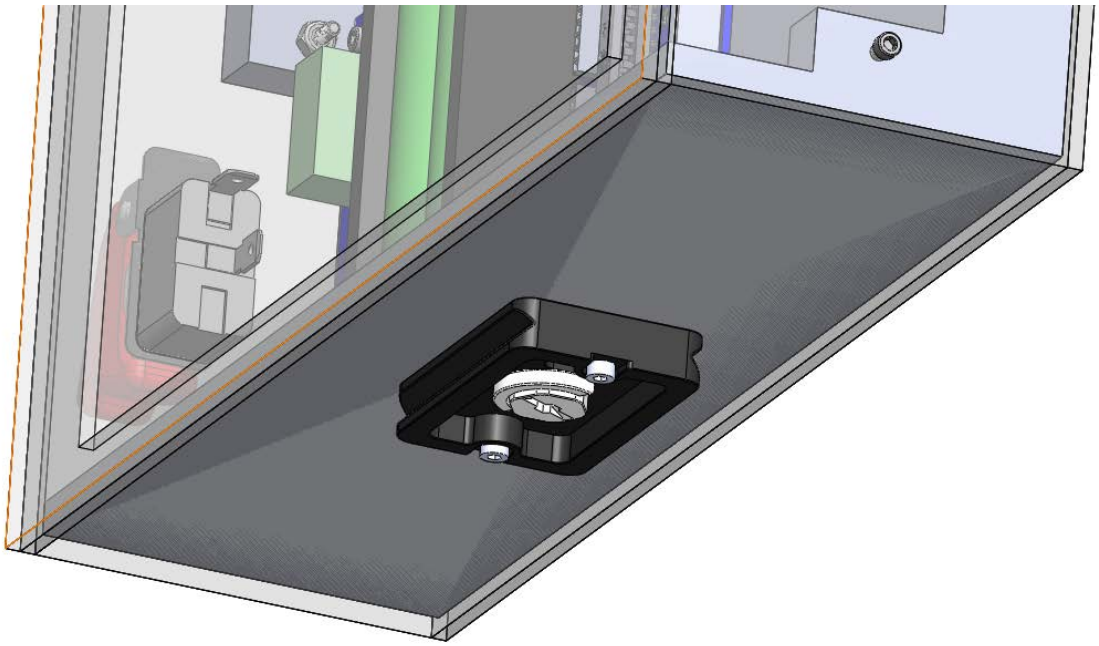

Figure 17: Quick release shoe and device connection.

The quick-release shoe illustrated in Figure 18, allows for the device to easily separate from the tripod for storage or to operate flat on the x-ray machine. The tripods graduated

reference marks and bubble level allow for consistent repeatable setups when diagnosing an x-ray machine.

Figure 18: Quick release functionality [15].

## 3.5 Motor

For the purpose of creating the periodically repeating pattern caused by the rotation of the spiral at 60 [rpm], five motor types were considered, including Brushed DC, Brushless DC, Stepper, Servo, and Synchronous. Motors were chosen online and evaluated based on the selection criteria, additional details for which can be found in Appendix B.

The suitable motor types identified were stepper and servo motors. Stepper motors are extremely precise due to their high number of discrete steps and are best suited for low speed applications such as this design. Servo motors provide highly accurate speed due to their closed feedback loop which allows for correction any errors due to external factors. The error correction of this motor, however, can possibly introduce uncertainty in the produced motion, lowering confidence in the device's ability to identify frame quality loss.

The top two motors are the NEMA 6 Bipolar stepper motor and the EzRobot servo motor. The performance of both motors will be evaluated during the upcoming prototype and testing phase of this project. The stepper motor will serve as the primary choice for the design, and the servo motor will be investigated as an alternative depending on the effect of the servo motor's built in error correction on the performance of the design.

## 3.6 Electrical Systems

The device will have an electrical system that consists of a battery management system, an Arduino microcontroller, and a motor driver. The electrical system's function is to control the speed of the motor in order to ensure that it can consistently run at 60 [rpm]. The power source is a rechargeable lithium ion battery cells that is connected to a charger and can provide 5.2 [hr] of power between recharges, and 300 charging cycles [16]. The charger has a on board LED to indicate battery levels and the batteries are charged through a barrel jack connection in the device. A toggle switch on the device turns the power on and off and a cover is included to prevent accidental toggle switch

### 3.6.1 Arduino Controller

For the controlling the input values to the motor, the Arduino Uno – R3 was selected, providing a 3.3 [V] or 5 [V] logic signal and possessing a digital I/O with PWM capability. It includes pre-installed ports to easily connect components for the prototype, has an input voltage of 7-12 V, and both digital and analog inputs. Power is provided to the Arduino solely through its pin connections, with a maximum current draw of 200 [mA].

### 3.6.2 Stepper Motor Driver

The motor driver that was selected is the Easy Driver – Stepper Motor Driver. It is compatible with four, six, and eight wire stepper motors of any voltage. Additionally, it has a power supply range from 6V to 30V and can drive bi-polar motors which would have 4-wire cables. This motor driver has an additional built in feature to adjust the maximum current provided to the motor, using the attached potentiometer, based on the motor's current rating.

### 3.6.3 Power Source – 18650 Lithium Ion Battery

The controllers chosen for use in the design require DC power at low current and voltage. Additionally, the customer had requested the device to a rechargeable battery that is embedded in the design but can be easily replaced once the battery reaches its charging cycle limit.

The batteries chosen for the design are 18650 Lithium Ion batteries, which are rechargeable and can be connected in series to increase the voltage should it be required. At a 2600 [mAh] capacity, these batteries can discharge 2.6 [A] in peak and 0.5 [A] in steady state, with two 3.7 [V] in series, providing a total voltage of 7.4 [V], making it compatible with the Arduino controller chosen [16]. These batteries can also be charged while embed in the device using the

power pack PCB with an integrated charger, therefore removal won't be required for recharging. The batteries last for 300 charge cycles and replaceable. The batteries have a 2.6Ah capacity and the maximum current draw from the system is 0.5A. The lifespan on the batteries before replacement is 1560 hours.

### 3.6.4 Electrical Setup

#### *3.6.4.1 Hardware Setup*

The motor driver has two mounting holes to mechanically secure the board. The chosen stepper motor is a 4-wire stepper motor. The wiring connection based on the motor's data sheet [17] is shown in TABLE XIII below.

TABLE XIII: STEPPER MOTOR WIRING CONNECTION

| A+ | A- | B+ | B- |
|---|---|---|---|
| Black | Green | Red | Blue |

These wires are then to be connected into the motor driver on the four top right pins as shown in Figure 19 below.

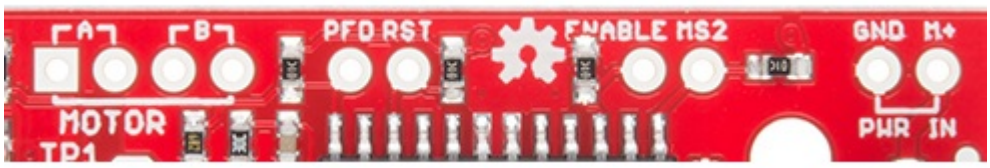


Figure 19: Motor driver board top pins - motor connections (permission use granted) [18]

The motor pins functions are as follows, from left to right:

- Coil A+ - H-Bridge 2 Output A. Half of connection point for bi-polar stepper motor coil A.
- Coil A- - H-Bridge 2 Output B. Half of connection point for bi-polar stepper motor coil A.
- Coil B+ - H-Bridge 1 Output A. Half of connection point for bi-polar stepper motor coil B.
- Coil B- - H-Bridge 1 Output B. Half of connection point for bi-polar stepper motor coil B.

After the motor is connected to the motor driver, the power supply may be connected. The selected 18650 Lithium Ion batteries are to be connected to the GND and M+ connections of the motor driver that can be seen in Figure 19. The batteries will be secured in a power pack and charger circuit board, further described in section 5 Assembly Plan.

This board has the capability of supplying 7.4 [V] DC and can charge the batteries with 5-12 [V] DC at a minimum of 1 [A]. Through its Auxiliary Cell Power Output, two pin screw terminals are attached on the left bottom corner for easy interfacing with the motor driver. The charging port is a barrel jack female connector on the bottom right.

Once the power source is connected to the motor driver, motor driver may be connected to the Arduino UNO R3 microcontroller. To do so, each of the pin connections must be connected to the digital points of the controller, as listed in TABLE XIV below.

TABLE XIV: MOTOR DRIVER TO MICROCONTROLLER CONNECTIONS AND FUNCTIONS [18]

| Microcontroller | Motor Driver | Function |
|---|---|---|
| **D2** | STEP | Logic Input. This is where the signal on how fast the rotation can go |
| **D3** | DIR | Logic Input. This is where the signal on which direction will the rotation take |
| **D4** | MS1 | Logic Input. This is for the micro step functionality |
| **D5** | MS2 | Logic Input. This is for the micro step functionality |
| **D6** | ENABLE | Logic Input. This is the trigger for controlling the motor |

Once the microcontroller, motor driver, power source, and stepper motor are connected, the setup can be tested prior to integration with the mechanical components of the device. A block diagram of the electrical layout is shown in Figure 20 below.

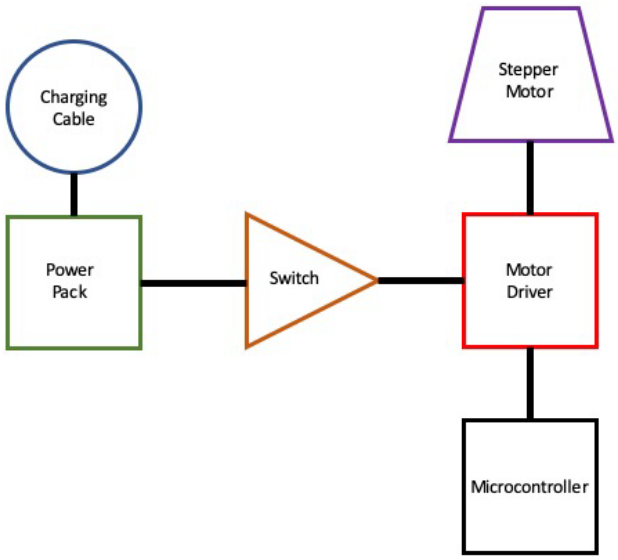


Figure 20: Electrical diagram for quality frame assessment device.

#### 3.6.4.2 *Software Setup*

Once the hardware is all connected, the next step is to upload the inputs to the microcontroller. The full instruction for the Arduino coding is available in the motor driver website. In the prototyping phase of this project, further testing will be done for optimization purposes and the code will be modified based on proper inputs that will produce the optimal rotation speed.

# 4 Cost Analysis

The total cost for the first prototype device is $433.37 CAD which is within the $2,250 prototype and testing budget set by CancerCare Manitoba. This is the initial cost of the device with most of the costs coming from purchasing electrical components and a tripod. The fabrication cost was minimized to allow for multiple iterations to be fabricated during the prototype testing phase, during which the electrical and housing components are expected to remain unchanged during iterations. The spiral and grid components will be the main components requiring further investigation and will not majorly impact the project cost. A summary of the total cost is illustrated in TABLE XV.

TABLE XV: DEVICE TOTAL COST

| Section | Cost (CAD) | % of Cost |
|---|---|---|
| **Raw Material** | $74.98 | 17.2 |
| **Fabrication Cost** | $24.50 | 5.6 |
| **Purchased Components** | $336.46 | 77.18 |
| **Total** | $435.94 | 100.00 |

## 4.1 Raw Material

The device requires minimal raw materials for the prototyping phase as illustrated in TABLE XVI. During further prototyping new raw materials will not need to be purchased as the device housing is not expected to undergo changes. The bonding agent amounts purchased will be sufficient to last the entire prototyping phase, and as new housings would only require additional acrylic sheets to be purchased.

TABLE XVI: RAW MATERIAL COST

| Name | Description | QTY | Unit Cost |
|---|---|---|---|
| **Acrylic Sheet [2'x2'] [19]** | Device housing material | 2 | $13.56 |
| **TAP Acrylic Cement [1 pt] [20]** | Bonds acrylic housing components | 1 | $13.75 |
| **Hypo-Type Solvent Cement Applicator [20]** | Used to apply TAP Acrylic Cement | 2 | $3.50 |
| **5 min Epoxy [21]** | Bonds magnets to acrylic housing | 1 | $30.61 |
| **Total** | | | $74.98 |

## 4.2 Fabricated Cost

Fabrication costs have been minimized by using laser cutting and 3D printing. These methods allow the team rapidly prototyping changes and refine the design during the testing phase, and do not incur high machining costs as they are automated processes. The laser cut components will be done by the team at the University of Manitoba's FAB Lab, at the current price of laser cutting of $0.60/min. The spiral and grid will be printed on CancerCare Manitoba's AON3D printer with their Bismuth filament while the other components will be printed using the team's 3D printer. The 3D printed components are what the team is expecting to iterate the most during the testing phase. A summary of the fabricated parts is illustrated in TABLE XVII.

TABLE XVII: COST OF FABRICATED COMPONENTS

| No. | Name | Description | Manufacturing Type | QTY | Unit Cost |
|---|---|---|---|---|---|
| **HOS01** | Front Plate | Housing | Laser Cutter | 1 | $3.00 |
| **HOS02** | Back Plate | Housing | Laser Cutter | 1 | $2.00 |
| **HOS03** | Side Plate | Housing | Laser Cutter | 2 | $0.50 |
| **HOS04** | Top Plate | Housing | Laser Cutter | 2 | $0.50 |

| No. | Name | Description | Manufacturing Type | QTY | Unit Cost |
|---|---|---|---|---|---|
| **HOS05** | Separation Plate | Separates electrical hub from spiral | Laser Cutter | 1 | $0.50 |
| **HOS06** | Top Access Door | Spiral access door | Laser Cutter | 1 | $1.50 |
| **HOS07** | Bottom Access Door | Electrical Access Door | Laser Cutter | 1 | $1.50 |
| **HOS08** | Spiral Support Plate | Support | Laser Cutter | 1 | $1.50 |
| **PAT01** | Spiral | Pattern Identification | 3D Printed, CancerCare | 1 | $5.00 |
| **PAT02** | Grid | Pattern Identification | 3D Printed, CancerCare | 1 | $6.00 |
| **MOT01** | Motor Mount Plate | Motor to Housing Mount | 3D Printed, Team Printer | 1 | $0.25 |
| **MOT02** | Spiral Mount Plate | Motor to Spiral Mount | 3D Printed, Team Printer | 1 | $0.25 |
| **ECE08** | Electronic Hub Mount | Holds Electronics | 3D Printed, Team Printer | 1 | $1.00 |
| **Total** | | | | | $24.50 |

## 4.3 Purchased Parts

Purchased parts are the most expensive part of the device cost. The high cost comes from selecting a sturdy tripod which will not tip during operation and from the electrical components. These are expected to be one-time purchases and not change between iterations of the device. The purchased parts are illustrated in TABLE XVII. Specification sheets for relevant components are provided in Appendix C.

TABLE XVIII: PURCHASE LIST

| No. | Name | Description | QTY | Unit Cost |
|---|---|---|---|---|
| **ECE01** | Motor Driver | Stepper Motor Driver [22] | 1 | $ 19.88 |

| No. | Name | Description | QTY | Unit Cost |
|---|---|---|---|---|
| **ECE02** | Arduino | Microcontroller [23] | 1 | $ 30.52 |
| **ECE03** | Battery | 18650 2600mah 3.7V [16] | 2 | $17.29 |
| **ECE04** | Power Pack | Power Pack/Charger 18650 [24] | 1 | $39.73 |
| **ECE05** | Charging Cable | 5V 2A Barrel Jack to Wall [25] | 1 | $7.91 |
| **ECE06** | Toggle Switch | Quick Disconnect Switch [26] | 1 | $6.49 |
| **ECE07** | Switch Cover | 1/2" Safety Switch [27] | 1 | $27.77 |
| **HOS09** | Clear Acrylic Hinge | Self-closing Acrylic Hinge [20] | 5 | $1.25 |
| **HOS10** | Tripod | Orion Paragon-Plus Heavy Duty with Quick Release [15] | 1 | $149.99 |
| **HOS11** | Magnets | ¼" Rare Earth Magnets [28] | 4 | $0.65 |
| **HOS12** | Hardware | M3-0.5 Socket Cap Screw (3-Pack) [29] | 7 | $0.65 |
| **HOS13** | Tripod Locknut | ¼" -20 Lock Nut (3-Pack) [30] | 1 | $1.18 |
| **HOS14** | Hex Nut | M3 Hex Nut (2-Pack) [31] | 10 | $0.50 |
| | | | **Total** | **$336.46** |

# 5 Assembly Plan

To manufacture the device, several components must be made using the raw materials purchased in Section 4 and assembled. These steps are to give a brief overview of how the team intends to manufacture the device during the next academic semester.

The device consists of the following three main components:

- Electrical mount and components
- The Acrylic Housing
- The spiral and grid pattern

## 5.1 Electric Component Integration

The electrical components consist of purchased components as detailed in Section 4.1 that are to be mounted onto a 3D printed electrical stand illustrated in Figure 21.

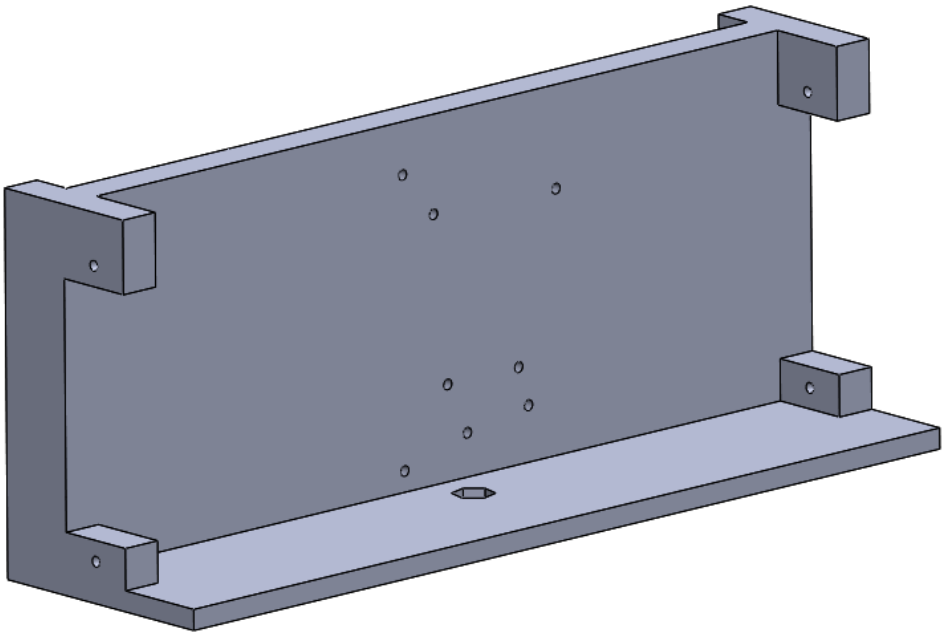

Figure 21: Electrical stand for attaching power charger, Arduino Uno, and motor controller.

The Arduino, motor control board, and battery power pack are attached to the mount with 4-40 screws and appropriately wired as illustrated in Figure 22. A 1/4"-20 lock nut is friction fit into the center of the mount and epoxied in place. The assembly is set aside to be placed into the acrylic housing.

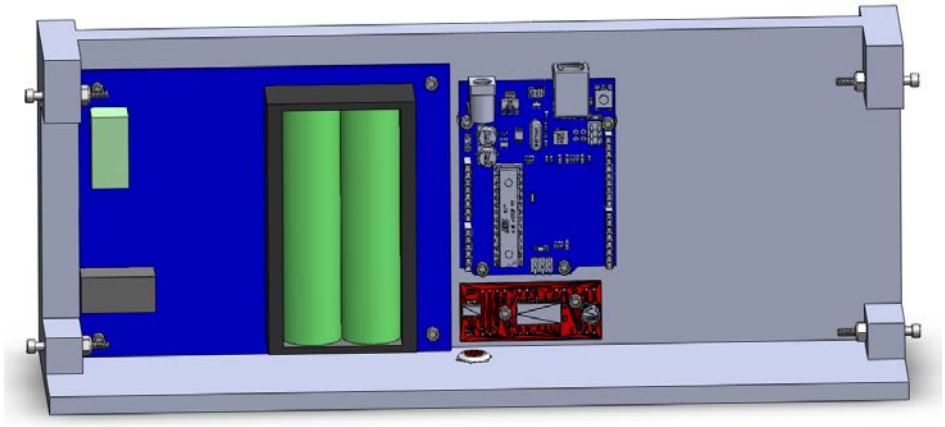

Figure 22: Electrical stand with boards mounted.

## 5.2 Acrylic Housing manufacturing

The device housing is made out of 3 [mm] acrylic sheets that are laser cut at the University of Manitoba's FAB Lab to reduce on manufacturing costs. Housing components are restricted to

a maximum size of 32”x18” to accommodate the available laser cutters. The eight components listed in TABLE XIX are cut out from 2 acrylic sheets.

TABLE XIX: ACRYLIC HOUSING COMPONENTS

| Component | Quantity | Outer Area |
|---|---|---|
| **Front Panel** | 1 | 15.7”x11.8” |
| **Rear Panel** | 1 | 15.7”x11.8” |
| **Side Walls** | 2 | 15.4”x3.15” |
| **Top and Bottom Walls** | 2 | 3.15”x11.6” |
| **Wall between Spiral and Electronics** | 1 | 3.15”x11.6” |
| **Spiral Access Door** | 1 | 11.8”x10.8” |
| **Battery Access Door** | 1 | 11.8”x4.8” |

The Rear panel and side walls are attached by clamping the components together and applying TAP Acrylic Cement to permanently bond them as illustrated in Figure 23. The housing is to be left to cure for 24 hours.

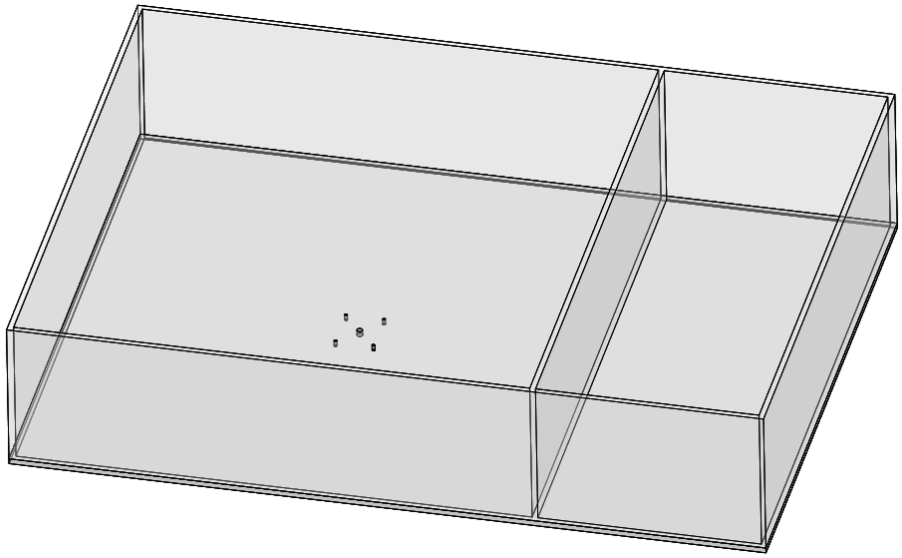

Figure 23: Bottom half of device housing.

The electical housing is installed into the lower half of the housing and the motor and 3D printed motor mount is attached into the upper section housing as illustrated in Figure 24. The

motor is connected to the motor controller and then tested to ensure proper operation before further assembly.

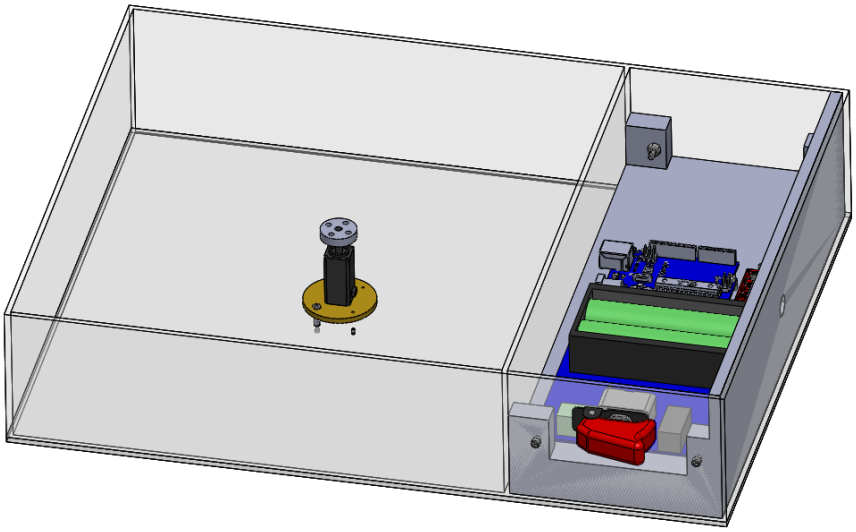

Figure 24: Housing with added electric components.

The front panel is bonded to the rest of the housing using the TAP acrylic cement. After curing, the five clear acrylic self-closing hinges are attached to the two doors and bonded. The magnets that fit into the housing are set aside until later when the grid is attached. The result is illustrated in Figure 24.

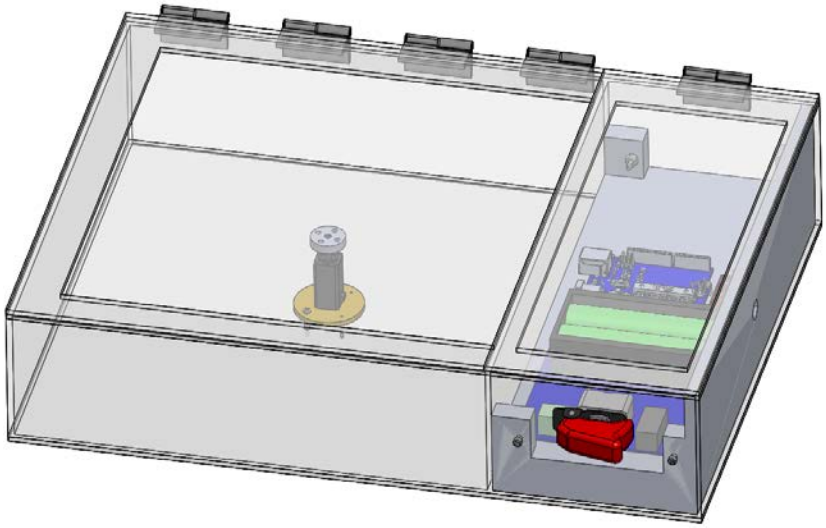

Figure 25: Complete housing.

## 5.3 3D printed spiral and grid

The spiral and grid are to be 3D printed using Cancer Care Manitoba's AON3D printer with high contrast bismuth PLA. The spiral is mounted and secured to the motor mount using bolts. The grid is then attached onto the rear housing plate with two embedded magnets that are epoxied in place. To ensure the pair of magnets are sufficiently contacting each other the magnets are loosely placed into the acrylic housing. The magnets are then epoxied in place while the grid is placed flush with the housing. A grid locating pin is placed into the center of the grid and slots into the housing.

## 5.4 Tripod Mounting

As described in Section 3.4, the assembled device is attached to the tripods quick release mount with a ¼" -20 bolt that threads into the nut inside the electrical component 3D printed electrical housing.

# 6 Failure Modes and Effects Analysis

The first deliverable for the upcoming Prototype and Testing Phase of this project includes a testing plan and in order to identify and design the tests needed to be conducted on the device and in which priority order, a Failure Modes and Effects Analysis (FMEA) was conducted. TABLE XX below details the failure modes identified for the design thus far. It is important to note that additional failure not predicted by the team will likely be identified during the next phase of this project.

TABLE XX: POTENTIAL FAILURE MODES

| | Potential Failure Mode | Potential Effects | Potential Causes | Current Controls |
|---|---|---|---|---|
| **A** | Motor does not rotate at 60 rpm consistently | • Design cannot perform | • Motor electrical or mechanical failure<br>• Motor specifications are incompatible with design needs<br>• Motor controller is incompatible with motor | • Testing<br>• Planning<br>• Development of secondary motor option |

| | Potential Failure Mode | Potential Effects | Potential Causes | Current Controls |
|---|---|---|---|---|
| B | Poor contrast between pattern, grid, and other visible components | • Pattern is incapable of identifying quality losses | • Poor pattern design<br>• Poor material selection<br>• Poor quality of motion capture<br>• Motion blur is too great in captured image | • Testing<br>• Development of secondary and tertiary designs<br>• Adjustability of motor control |
| C | Design is too large to fit between fluoroscope's image intensifier and x-ray tube | • Design cannot perform | • Variance between theoretical design and physical parts<br>• Fluoroscope adjustability is less than expected | • Testing<br>• Design Constraints<br>• Development of secondary and tertiary designs |
| D | Spiral unmounts from motor shaft during operation | • Design cannot perform<br>• Operator injuries | • Poor Assembly<br>• Insufficient component mounting | • Testing<br>• Design encasement |
| E | Quality loss identification method becomes inconsistent over time | • Quality loss identification is invalid | • Variance over time of pattern or grid dimensions from original measurements<br>• Poor pattern design | • Testing<br>• Development of secondary and tertiary designs |
| F | Device is operable during maintenance | • Operator injuries | • Electrical or mechanical fault<br>• Operator blunder | • Safety switch<br>• Testing |
| G | Device topples over and impacts the ground | • Device is damaged<br>• Device is inoperable | • Operator blunder<br>• Tripod base not fully deployed<br>• Device vibration results in imbalance | • Rigid Housing to withstand damage<br>• Testing |

| | Potential Failure Mode | Potential Effects | Potential Causes | Current Controls |
|---|---|---|---|---|
| **H** | Spiral does not support itself under gravity | • Design cannot perform<br>• Unable to operate device | • Part thickness not sufficient<br>• Material choice too flexible | • Testing<br>• Add extra support material |

After considering the above failure modes and analyzing their causes and effects, risk priority numbers (RPN) must be assessed. To assess the RPN, the severity, frequency and likelihood of detection of each failure mode should be considered on a scale of 1 to 10 [32]. The RPN is then simply a function of the severity, frequency, and likelihood of detection ($severity \times frequency \times detection = RPN$). TABLE XXI below shows the RPN assessment of the above potential failure modes.

TABLE XXI: RISK PRIORITY NUMBERS OF POTENTIAL FAILURE MODES

| Failure Mode | Severity | Frequency | Detection | Risk Priority Number |
|---|---|---|---|---|
| **A** | 2 | 2 | 1 | 4 |
| **B** | 8 | 3 | 4 | 96 |
| **C** | 2 | 1 | 1 | 2 |
| **D** | 9 | 2 | 2 | 54 |
| **E** | 8 | 3 | 5 | 120 |
| **F** | 9 | 1 | 1 | 9 |
| **G** | 9 | 2 | 1 | 18 |
| **H** | 2 | 3 | 1 | 6 |

After assessment, the highest priorities include failure modes regarding poor pattern visibility, and pattern inconsistency as both are critical to the success of the design. Disassembly of the design during operation is a notable failure mode as it risks the safety of the operator and should be a higher priority. The failure modes have been plotted with regards to criticality in Figure 26 below.

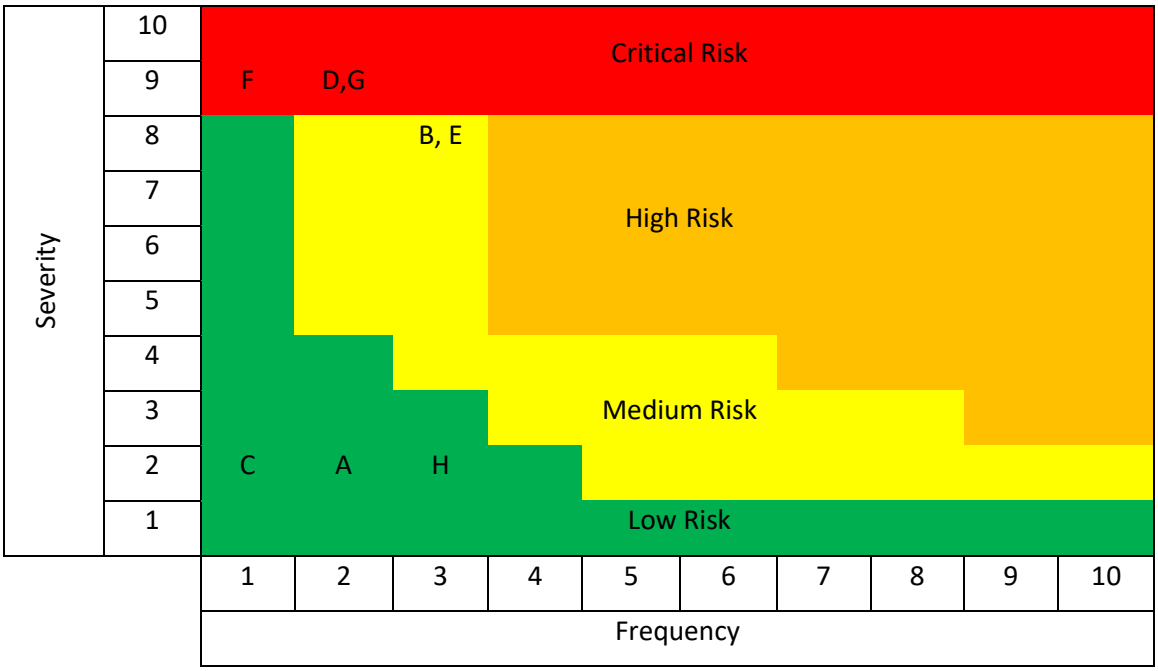


Figure 26: Criticality chart [33].

Thus, failure modes A, C and H are low risk, B and E are medium risk, while failure mode D and F are critical due to safety concerns. G is critical due to it having the potential to destroy the device, leaving it inoperable.

# 7 Future Works – Prototype and Testing Phase

The Prototype and Testing phase of this project officially begins on January 6th, 2020, with the beginning of the Winter 2020 academic semester. Although, in order to reduce idle time at the initiation of this phase, the team plans to manufacture the components for the initial device prototype during the final examination period. TABLE XXII below outlines the preliminary schedule for this phase, with the course deadlines highlighted in yellow. In order to meet the first deadline of the Testing Plan report and presentation, the team will use the FMEA as a starting point of identifying the different tests that must be conducted, leading to the design of these tests.

TABLE XXII: PROTOTYPE AND TESTING PHASE HIGH LEVEL PLAN

| Week | Primary Action Item |
|---|---|
| **Week 1, January 6th – 12th** | Prototype Assembly and Testing Plan Generation |
| **Week 2, January 13th – 19th** | Prototype and Testing Plan Report and Presentation |
| **Week 3, January 20th – 26th** | Conduct Testing |

| | |
|---|---|
| **Week 4, January 27th – February 2nd** | Conduct Testing |
| **Week 5, February 3rd – 9th** | Conduct Testing |
| **Week 6, February 10th – 16th** | Review Testing Results |
| **Week 7, February 17th – 23rd** | Device Engineering Changes |
| **Week 8, February 24th – March 1st** | Prototype Testing Update Presentation |
| **Week 9, March 2nd – 8th** | Implement Engineering Changes |
| **Week 10, March 9th – 15th** | Conduct Testing |
| **Week 11, March 16th – 22nd** | Conduct Testing and Device Engineering Changes |
| **Week 12, March 23rd – 29th** | Implement Engineering Changes |
| **Week 13, March 30th – April 3rd** | Final Report and Presentation, Client Handoff |

CancerCare Manitoba has printed a test piece of the spiral and was picked up by the team on December 2, 2019. From evaluating this initial piece, it was unable to support itself from its own weight. As per the FMEA we controlled this risk by printing a test piece. The team will make the initial design change for the prototyping phase using the defined control methods. The spiral will be tested by printing it with regular PLA in between the spiral that will not show up well under x-ray or by adding in a support plate made out of acrylic for it to rest on.

Additional testing will be done to evaluate the contrast on the device under x-ray. A test piece for the bismuth PLA filament in the shape of a staircase that gradually gets thicker will be imaged. This will confirm if the proposed thickness is sufficient to view under x-ray or if it needs to be adjusted. A similar test will be done with acrylic to determine how much contrast is lost due to the housing's interference.

# 8 Schedule Performance Review

Figure 27 and Figure 28 present the original and up to date project Gantt charts, with the changes made highlighted in yellow. A significant change concerned the initial rapid timeline for concept generation and development, which the client requested to be extended in order to investigate as many alternatives as possible and ensure due diligence. To accommodate, the team conducted their report writing for the concept development phase and the concept development itself in parallel. A similar change was incorporated during the final design phase, where the team

conducted the 3D modelling and manufacturing plan development in parallel with the report writing, to produce a fleshed-out draft which improves the value of the feedback received from the project's faculty advisor.

Additional client reviews and discussion were also added, highlighted in blue, particularly during the concept development phase, in order to receive more valuable feedback and to ensure that the client and team remained of like thought with regards to the project. Moreover, a feasibility study on the top concepts was added in, to further assist in the narrowing down of concepts and identify all potential short comings that should be taken into consideration.

| ID | % Complete | Task Name | Duration | Start | Finish |
|---|---|---|---|---|---|
| 1 | 33% | **FFRV Engineering Design** | 61 days | Tue 9/10/19 | Thu 12/5/19 |
| 2 | 100% | **Phase 1** | 13 days | Tue 9/10/19 | Mon 9/30/19 |
| 3 | 100% | Initial Client Meeting | 0 days | Tue 9/10/19 | Tue 9/10/19 |
| 4 | 100% | Project Schedule | 3 days | Wed 9/11/19 | Fri 9/13/19 |
| 5 | 100% | Project Background | 3 days | Wed 9/11/19 | Fri 9/13/19 |
| 6 | 100% | Preliminary Research And Concept Development | 8 days | Wed 9/11/19 | Fri 9/20/19 |
| 7 | 100% | Project Needs | 5 days | Wed 9/11/19 | Tue 9/17/19 |
| 8 | 100% | Project Specifications | 6 days | Sat 9/14/19 | Fri 9/20/19 |
| 9 | 100% | Problem Definition Report Development | 5 days | Wed 9/18/19 | Tue 9/24/19 |
| 10 | 100% | PDR Draft Submission | 0 days | Wed 9/25/19 | Wed 9/25/19 |
| 11 | 100% | PDR Draft Revision | 3 days | Thu 9/26/19 | Sat 9/28/19 |
| 12 | 100% | Presentation Development | 3 days | Thu 9/26/19 | Sat 9/28/19 |
| 13 | 100% | Project Definition Report Submission | 0 days | Mon 9/30/19 | Mon 9/30/19 |
| 14 | 100% | Phase 1 Oral Presentation | 0 days | Mon 9/30/19 | Mon 9/30/19 |
| 15 | 0% | **Phase 2** | 17 days | Wed 10/2/19 | Fri 10/25/19 |
| 16 | 0% | Concept Generation | 5 days | Wed 10/2/19 | Tue 10/8/19 |
| 17 | 0% | Concept Selection | 0 days | Wed 10/9/19 | Wed 10/9/19 |
| 18 | 0% | Preliminary Concept Submission | 0 days | Thu 10/10/19 | Thu 10/10/19 |
| 19 | 0% | Technical Analysis | 3 days | Fri 10/11/19 | Tue 10/15/19 |
| 20 | 0% | Concept Design Report Development | 5 days | Fri 10/11/19 | Thu 10/17/19 |
| 21 | 0% | CDR Draft Submission | 0 days | Tue 10/22/19 | Tue 10/22/19 |
| 22 | 0% | CDR Draft Revision | 3 days | Tue 10/22/19 | Thu 10/24/19 |
| 23 | 0% | Concept Design Report Submission | 0 days | Fri 10/25/19 | Fri 10/25/19 |
| 24 | 0% | **Phase 3** | 28 days | Mon 10/28/19 | Thu 12/5/19 |
| 25 | 0% | Concept Optimization | 7 days | Mon 10/28/19 | Tue 11/5/19 |
| 26 | 0% | Concept Additional Analysis | 7 days | Wed 10/30/19 | Thu 11/7/19 |
| 27 | 0% | Manufacturing  Development | 7 days | Wed 11/6/19 | Thu 11/14/19 |
| 28 | 0% | Cost Analysis Development | 7 days | Thu 11/7/19 | Fri 11/15/19 |
| 29 | 0% | Preliminary Draft Report Submission | 0 days | Sat 11/16/19 | Sat 11/16/19 |
| 30 | 0% | Initial Prototype Development | 5 days | Mon 11/18/19 | Fri 11/22/19 |
| 31 | 0% | Preliminary Draft Report Revision | 4 days | Wed 11/20/19 | Sun 11/24/19 |
| 32 | 0% | Draft Report Submission | 0 days | Mon 11/25/19 | Mon 11/25/19 |
| 33 | 0% | Draft Report Revision | 5 days | Wed 11/27/19 | Tue 12/3/19 |
| 34 | 0% | Poster Development | 7 days | Mon 11/25/19 | Tue 12/3/19 |
| 35 | 0% | Presentation Development | 7 days | Mon 11/25/19 | Tue 12/3/19 |
| 36 | 0% | Final Deliverable Submissions | 0 days | Wed 12/4/19 | Wed 12/4/19 |
| 37 | 0% | Final Presentation | 0 days | Thu 12/5/19 | Thu 12/5/19 |

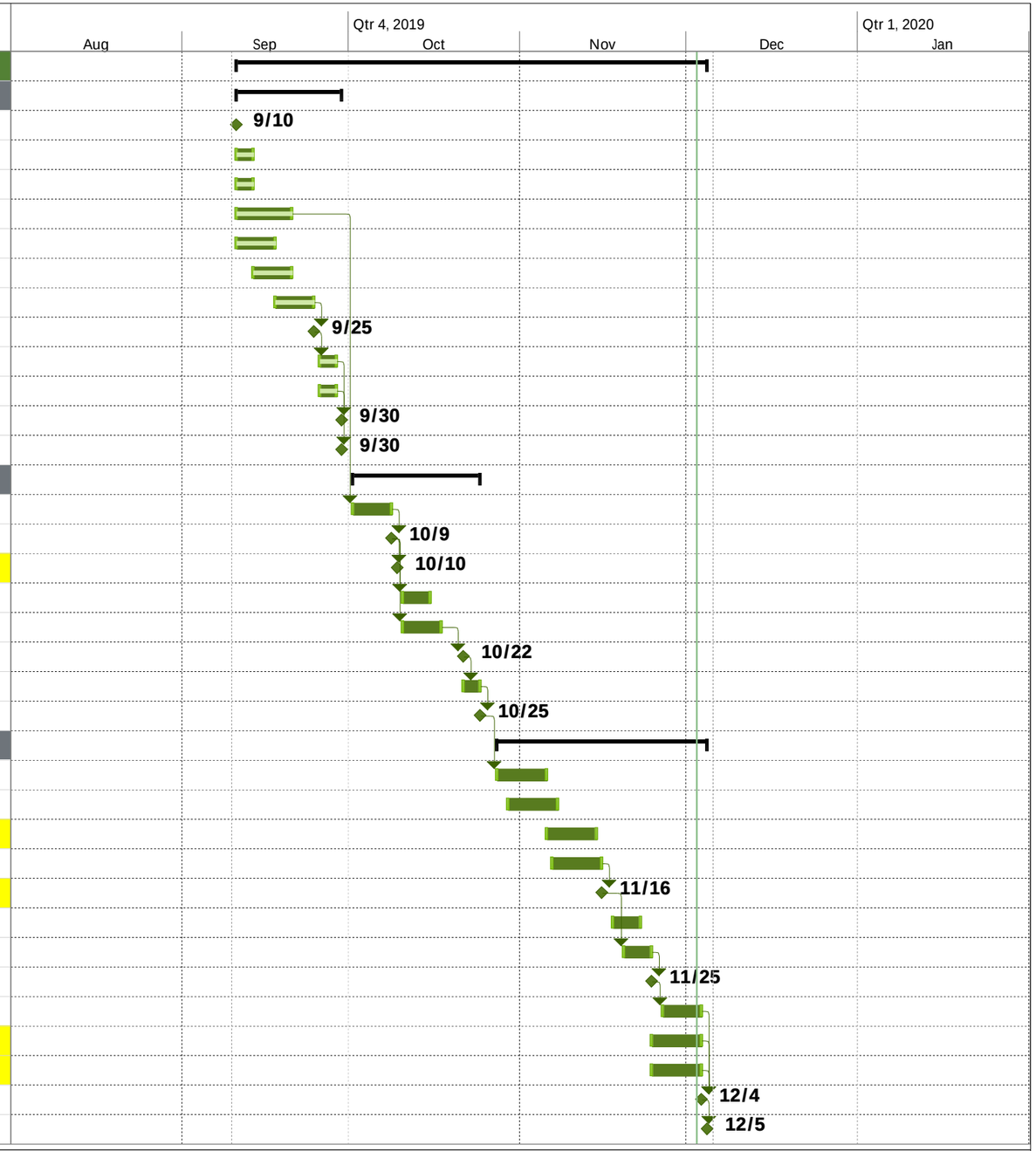


Project: Cancer Care Fluorosco
Date: Tue 12/3/19

| | | | | | | | |
|---|---|---|---|---|---|---|---|
| Task | Project Summary | Manual Task | Start-only | Deadline |
| Split | Inactive Task | Duration-only | Finish-only | Progress |
| Milestone | Inactive Milestone | Manual Summary Rollup | External Tasks | Manual Progress |
| Summary | Inactive Summary | Manual Summary | External Milestone | |

Figure 27: Initial Gantt chart.

| ID | % Complete | Task Name | Duration | Start | Finish |
|---|---|---|---|---|---|
| 1 | 100% | **FFRV Engineering Design** | **61 days** | **Tue 9/10/19** | **Thu 12/5/19** |
| 2 | 100% | **Phase 1** | **13 days** | **Tue 9/10/19** | **Mon 9/30/19** |
| 3 | 100% | Initial Client Meeting | 0 days | Tue 9/10/19 | Tue 9/10/19 |
| 4 | 100% | Project Schedule | 3 days | Wed 9/11/19 | Fri 9/13/19 |
| 5 | 100% | Project Background | 3 days | Wed 9/11/19 | Fri 9/13/19 |
| 6 | 100% | Preliminary Research And Concept Development | 8 days | Wed 9/11/19 | Fri 9/20/19 |
| 7 | 100% | Project Needs | 5 days | Wed 9/11/19 | Tue 9/17/19 |
| 8 | 100% | Project Specifications | 6 days | Sat 9/14/19 | Fri 9/20/19 |
| 9 | 100% | Problem Definition Report Development | 5 days | Wed 9/18/19 | Tue 9/24/19 |
| 10 | 100% | PDR Draft Submission | 0 days | Wed 9/25/19 | Wed 9/25/19 |
| 11 | 100% | PDR Draft Revision | 3 days | Thu 9/26/19 | Sat 9/28/19 |
| 12 | 100% | Presentation Development | 3 days | Thu 9/26/19 | Sat 9/28/19 |
| 13 | 100% | Project Definition Report Submission | 0 days | Mon 9/30/19 | Mon 9/30/19 |
| 14 | 100% | Phase 1 Oral Presentation | 0 days | Mon 9/30/19 | Mon 9/30/19 |
| 15 | 100% | **Phase 2** | **20 days** | **Mon 9/30/19** | **Fri 10/25/19** |
| 16 | 100% | Individual Concept Generation | 5 days | Mon 9/30/19 | Fri 10/4/19 |
| 17 | 100% | Pear Evaluation 1 | 1 day | Mon 10/7/19 | Mon 10/7/19 |
| 18 | 100% | Team Brainstroming and Formulating Concepts | 1 day | Wed 10/2/19 | Wed 10/2/19 |
| 19 | 100% | Reflection ON PDR | 1 day | Thu 10/3/19 | Thu 10/3/19 |
| 20 | 100% | Client preliminary Review on Concepts | 1 day | Thu 10/3/19 | Thu 10/3/19 |
| 21 | 100% | Feasibility Study on Preferable Concepts | 2 days | Fri 10/11/19 | Mon 10/14/19 |
| 22 | 100% | Concept Selection | 0 days | Wed 10/9/19 | Wed 10/9/19 |
| 23 | 100% | Preliminary Concept Submission | 0 days | Fri 10/11/19 | Fri 10/11/19 |
| 24 | 100% | Technical Analysis | 3 days | Fri 10/11/19 | Tue 10/15/19 |
| 25 | 100% | Concept Design Report Development | 5 days | Fri 10/11/19 | Thu 10/17/19 |
| 26 | 100% | CDR Draft Submission | 0 days | Tue 10/22/19 | Tue 10/22/19 |
| 27 | 100% | CDR Draft Revision | 3 days | Tue 10/22/19 | Thu 10/24/19 |
| 28 | 100% | Concept Design Report Submission | 0 days | Fri 10/25/19 | Fri 10/25/19 |
| 29 | 100% | **Phase 3** | **29 days** | **Fri 10/25/19** | **Thu 12/5/19** |
| 30 | 100% | Pear Evaluation 2 | 1 day | Fri 10/25/19 | Fri 10/25/19 |
| 31 | 100% | Bill of Material | 6 days | Fri 10/25/19 | Fri 11/1/19 |
| 32 | 100% | Preliminary Manufacturing Plan | 6 days | Fri 10/25/19 | Fri 11/1/19 |
| 33 | 100% | Concept Optimization | 7 days | Mon 10/28/19 | Tue 11/5/19 |
| 34 | 100% | Concept Additional Analysis | 7 days | Mon 11/4/19 | Tue 11/12/19 |
| 35 | 100% | Manufacturing Development | 7 days | Mon 11/4/19 | Tue 11/12/19 |
| 36 | 100% | Cost Analysis Development | 7 days | Wed 11/13/19 | Thu 11/21/19 |
| 37 | 100% | Preliminary Draft Report Submission | 0 days | Fri 11/22/19 | Fri 11/22/19 |
| 38 | 100% | Initial Prototype Development | 5 days | Fri 11/22/19 | Thu 11/28/19 |
| 39 | 100% | Preliminary Draft Report Revision | 4 days | Wed 11/20/19 | Sun 11/24/19 |
| 40 | 100% | Draft Report Submission | 0 days | Mon 11/25/19 | Mon 11/25/19 |
| 41 | 100% | Draft Report Revision | 5 days | Wed 11/27/19 | Tue 12/3/19 |
| 42 | 100% | Poster Development | 5 days | Thu 11/28/19 | Wed 12/4/19 |
| 43 | 100% | Presentation Development | 5 days | Thu 11/28/19 | Wed 12/4/19 |
| 44 | 100% | Final Deliverable Submissions | 0 days | Wed 12/4/19 | Wed 12/4/19 |
| 45 | 100% | Final Presentation | 0 days | Thu 12/5/19 | Thu 12/5/19 |

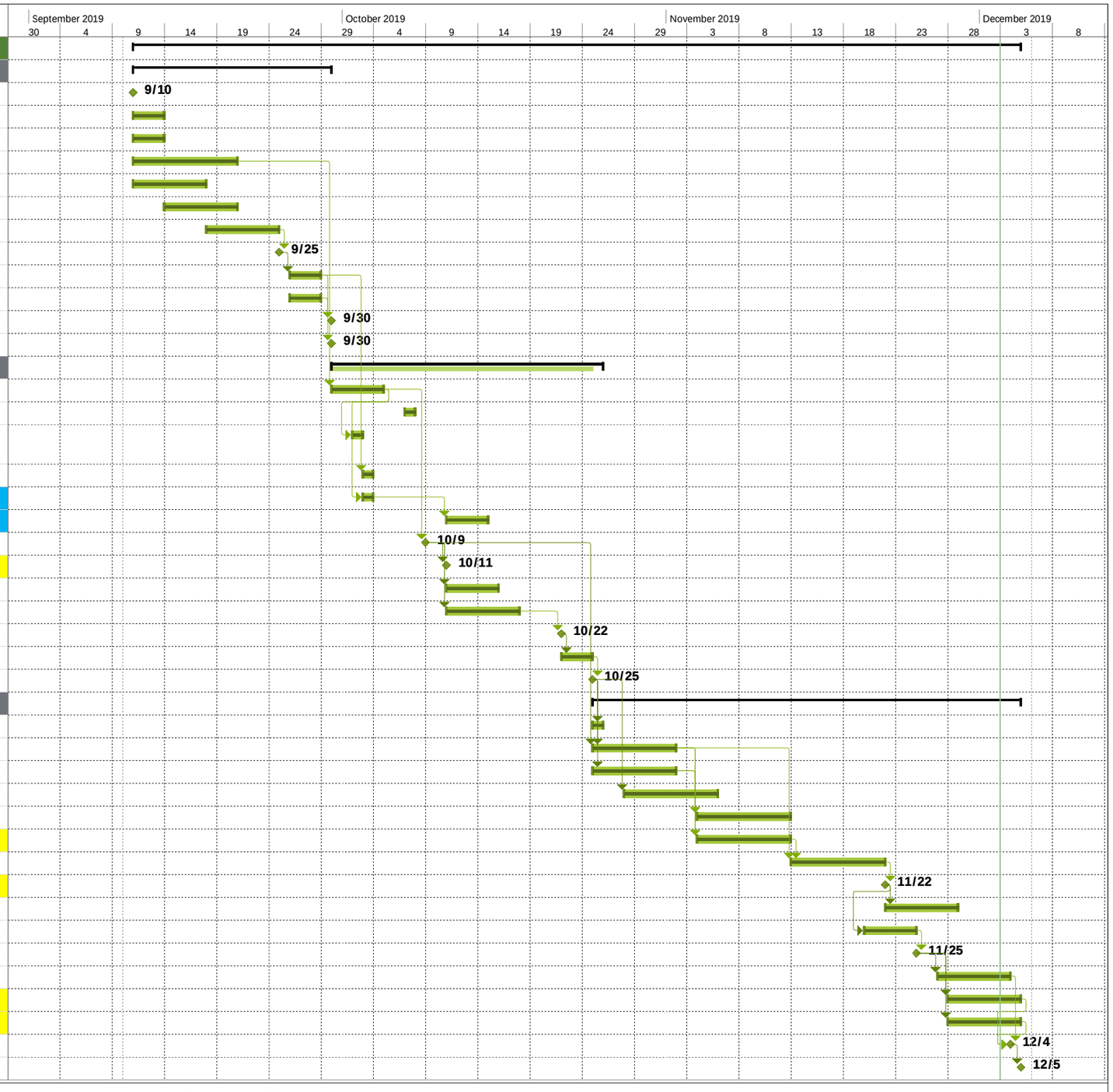


Project: Cancer Care Fluorosco
Date: Tue 12/3/19

Task, Split, Milestone, Summary, Project Summary, Inactive Task, Inactive Milestone, Inactive Summary, Manual Task, Duration-only, Manual Summary Rollup, Manual Summary, Start-only, Finish-only, External Tasks, External Milestone, Deadline, Critical, Critical Split, Progress, Manual Progress

Figure 28: Complete design phase Gantt chart.

# 9 Metric Review

TABLE XXIII tabulates the expected performance of the device versus the metrics defined earlier in section 1.6. The device meets all 19 marginal values and meets 15 of the ideal values. There is high confidence on all of the devices metric values except the ones highlighted in red.

TABLE XXIII: DEVICE PERFORMANCE VS MARGINAL AND IDEAL METRIC VALUES

| Needs # | Metric # | Engineering Metrics | Importance | Unit | Marginal Value | Ideal Value | Device Value |
|---|---|---|---|---|---|---|---|
| **1** | 1 | Position change distance between subsequent frames | 5 | mm | 0.5 - 1 | < 0.7 | 0.1 |
| **1** | 2 | Overlap percentage between subsequent frames | 5 | % | < 10 | <5 | 0 |
| **2** | 3 | Pattern frequency | 5 | Hz | 0.9-1.1 | 1 | 1 |
| **3** | 4 | Longest dimension | 5 | m | 0.5 - 1.0 | < 0.7 | 0.8 |
| **3** | 5 | Overall volume | 5 | m^3 | < 0.5 | < 0.25 | 0.12 |
| **3** | 6 | Total mass | 5 | kg | < 8 | < 4.5 | 2.0 |
| **4** | 7 | Mean number of photons transmitted | 5 | $mm^2$ keV | $<1.500\times10^8$ | $<1.300\times10^8$ | $1.313\times10^8$ |
| **5** | 8 | Image sharpness as measured by spatial frequency response | 5 | line pairs/mm | < 0.5 | <0.1 | 0.1 |
| **6** | 9 | Accepted hazard level determined through safety hazard analysis | 5 | # | 2 | 1 | 1 |
| **7, 8, 9, 10** | 10 | Degree of frame discontinuity | 4 or 5 | % | > 90 | 95-100 | 100 |
| **11** | 11 | Device operation intuitiveness, as judged by Harry Ingleby, on a subjective scale of 10 | 4 | # | 5-10 | 8-10 | Not yet judged. Expected to be high between 8-10 |
| **12** | 12 | Steady state operation time period | 3 | minutes | > 6 | > 10 | >30 |
| **13** | 13 | Time to appropriately clean and disinfect | 2 | minutes | < 5 | < 2 | 3 |
| **14** | 14 | Assembly time | 2 | minutes | < 5 | < 3 | 1 |

| Needs # | Metric # | Engineering Metrics | Importance | Unit | Marginal Value | Ideal Value | Device Value |
|---|---|---|---|---|---|---|---|
| **15** | 15 | Disassembly time | 2 | minutes | < 5 | < 3 | 2 |
| **16** | 16 | Accepted environmental hazard level as determined by an environmental effect's analysis. (Scale of 1-5) | 2 | # | 3 | 1 | 1 |
| **17** | 17 | Replacement parts lead time | 2 | days | 7-21 | 7-14 | 14 |
| **17** | 18 | Maximum maintenance duration | 2 | minutes | 10 - 20 | <10 | 5 |
| **17** | 19 | Accepted service complexity level as determined through product service analysis (from 1-10 with 1 the easiest) | 2 | # | 1-5 | 1-3 | 2 |
| **18** | 20 | Device operation aesthetics, as judged by Harry Ingleby, on a subjective scale of 10 | 2 | # | 5-10 | 8-10 | Not yet judged. Expected to be high between 8-10 |
| **19** | 21 | Device time in operation until maintenance is required | 2 | hours | >= 300 | >= 600 | 1560 |

The metrics that will be judged by Harry Ingleby have yet to be measured but are expected to meet or exceed the ideal target based on previous discussions. The expected mass is projected to be 2 [kg] but may decrease due to the 3D printed components being printed will an infill ratio less than 100%. Metric 8 will be evaluated during the testing phase but is expected to be better than the benchmark metronome value. Metric 12 is expected to consistently operate due to the selected stepper motor and will be quantifiable determined in the testing phase.

# 10 Conclusion

CancerCare Manitoba sought a simple mechanical device which motions in a periodically repeating pattern for the purpose of identifying frame quality losses in fluoroscopy, defined as missed, duplicated, averaged, and split frames, at a maximum frame rate of 30 [fps]. The primary feature of the proposed design is a Bismuth spiral whose profile varies radially and angularly in any given stationary position, and when rotated at 60 [rpm], produces a unique image for every frame captured by the fluoroscope. The spiral occupies an area 20 [cm] in diameter, maximizing use of the area captured by the fluoroscope's image intensifier. The rotation of the spiral is driven by a NEMA 6 Bipolar stepper motor, providing high precision at relatively low speeds, and the design eliminates the need for a drive mechanism by mounting the spiral directly onto the motor. The speed of the motor is controlled by an Arduino Uno – R3 control board and an Easy Driver – Stepper Motor Driver, all powered by a pair of 18650 Lithium Ion rechargeable batteries, providing a charge of up to 5.2 [hr] and a total lifespan of 300 charge cycles. The components described thus far are all enclosed in an acrylic housing to mitigate tampering, damage, and ensure spiral visibility when imaged by the fluoroscope. This assembly is then mounted on a tripod in order to allow for height adjustability during fluoroscopy studies. The final feature of note, which is a Bismuth grid, sized for a specific frame rate setting, in order to assist in the identification of the frame issues by serving as a reference point, like graph paper. This grid is attached using magnets to the outside of the acrylic housing.

For the purpose of economical and rapid prototyping, which also lends itself to design changes in the upcoming Prototype and Testing phase of this project, the components of the device are either 3D printed, laser cut, or bought off the shelf. The estimated cost of the initial prototype is $427.44 CAD, leaving room for additional design changes within the budget of $2,250 CAD.

For the assembly of the prototype, included with the design is the cost analysis, and assembly plan; which the team will initiate shortly after the submission of this report. Additionally, a preliminary Failure Modes and Effects Analysis has been conducted, in order to determine areas of testing, as well as identify the importance of each aspect to be tested relative to each other. The main aspects of the device to be tested include the consistency of the motor, the image quality of the device, and the overall structural integrity of the device.

# 11 References


[1] I. Ludlum Measurements, "Model L-629-15," Ludlum Measurements, Inc., 2019.

[2] M. Peladeau-Pigeon, Interviewee, *Conference Call: Frame Rate Verification Tool.* [Interview]. 13 September 2019.

[3] B. A. Schueler, "The AAPM/RSNA Physics Tutorial for Residents General Overview of Fluoroscopic Imaging1," Department of Diagnostic Radiology, Mayo Clinic, Rochester, 2000.

[4] M. Peladeau-Pigeon and C. Steele, "Understanding Image Resolution and Quality in Videofluoroscopy," *SIG Perspectives,* vol. 24, no. 3, pp. 115-124, 2015.

[5] McMaster-Carr, "Roller Chain," McMaster-Carr, 2019. [Online]. Available: https://www.mcmaster.com/roller-chain. [Accessed 5 November 2019].

[6] McMaster-Carr, "Chain Attachments," McMaster-Carr, 2019. [Online]. Available: https://www.mcmaster.com/chain-attachments. [Accessed 5 November 2019].

[7] McMaster-Carr, "Sprockets," McMaster-Carr, 2019. [Online]. Available: https://www.mcmaster.com/sprockets. [Accessed 5 November 2019].

[8] McMaster-Carr, "Precision Shafts," McMaster-Carr, 2019. [Online]. Available: https://www.mcmaster.com/precision-shafts. [Accessed 5 November 2019].

[9] McMasterCarr, "Standard Ball and Roller Bearings," McMasterCarr, 2019. [Online]. Available: https://www.mcmaster.com/standard-ball-and-roller-bearings. [Accessed 5 November 2019].

[10] McMaster-Carr, "Retaining Rings," McMaster-Carr, 2019. [Online]. Available: https://www.mcmaster.com/retaining-rings. [Accessed 5 November 2019].

[11] Home Depot, "Acrylic Sheets," Home Depot, 2019. [Online]. Available: https://www.homedepot.com/p/OPTIX-24-in-x-36-in-x-0-177-in-Clear-Acrylic-Green-Edge-Sheet-25529102/306516862. [Accessed 5 November 2019].

[12] B&Q, "MDF Board (Th)18mm (W)610mm (L)1220mm," B&Q, 2019. [Online]. Available: https://www.diy.com/departments/mdf-board-th-18mm-w-610mm-l-1220mm/1696266_BQ.prd. [Accessed 5 November 2019].

[13] McMaster-Carr, "Tensioner," McMaster-Carr, 2019. [Online]. Available: https://www.mcmaster.com/tensioners. [Accessed 5 November 2019].

[14] Siemens Healthineers, "Simulation of X-ray Spectra," Siemens Healthineers, 2019. [Online]. Available: https://www.oem-products.siemens-healthineers.com/x-ray-spectra-simulation. [Accessed 10 November 2019].

[15] Orion Telescope and Binoculars, "Orion Paragon-Plus XHD Extra Heavy-Duty Tripod," Orion Telescope and Binoculars, 2019. [Online]. Available: https://www.telescope.com/Orion/Orion-Paragon-Plus-XHD-Extra-Heavy-Duty-Tripod/rc/2160/p/5377.uts. [Accessed 20 November 2019].

[16] SparkFun, "Lithium Ion Battery - 18650 Cell (2600mAh, Solder Tab)," SparkFun, 2019. [Online]. Available: https://www.sparkfun.com/products/13189. [Accessed 20 November 2019].

[17] "OMC Stepper Online," OMC, [Online]. Available: https://www.omc-stepperonline.com/hybrid-stepper-motor/nema-6-bipolar-1-8deg-0-58ncm-0-82oz-in-0-3a-14x14x30mm-4-wires.html?mfp=184-frame-size-mm%5B14%20x%2014%5D&sort=p.price&order=DESC&limit=100. [Accessed 2019].

[18] J. Pena, "Stepper Motor Driver," SparkFun, 2019. [Online]. Available: https://learn.sparkfun.com/tutorials/easy-driver-hook-up-guide?_ga=2.157364730.1911766250.1573744042-1615281861.1572304856.

[19] *Cost of Acrylic from the University of Manitoba's FABLab,* Winnipeg, 2019.

[20] "TAP Plastics," [Online]. Available: https://www.tapplastics.com/product/plastics/handles_hinges_latches/acrylic_hinge_self_closing/609. [Accessed 01 12 2019].

[21] "Eliminator RC," [Online]. Available: https://webstore.eliminator-rc.com/catalogsearch/result/?q=epoxy. [Accessed 01 12 2019].

[22] SparkFun, "EasyDriver - Stepper Motor Driver," SparkFun, 2019. [Online]. Available: https://www.sparkfun.com/products/12779. [Accessed 20 November 2019].

[23] SparkFun, "Arduino Uno - R3," SparkFun, 2019. [Online]. Available: https://www.sparkfun.com/products/11021. [Accessed 20 November 2019].

[24] SparkFun, "Li-ion Power Pack Charger - 2 cell," Parallax, 2019. [Online]. Available: https://www.parallax.com/product/28986. [Accessed 20 November 2019].

[25] SparkFun, "Wall Adapter Power Supply - 5VDC, 2A (Barrel Jack)," SparkFun, 2019. [Online]. Available: https://www.sparkfun.com/products/15312. [Accessed 20 November 2019].

[26] McMaster-Carr, "Toggle Switch 2 Position, Round, Maintained, 2 Terminal, SPST-NO, 6A," McMaster-Carr, 2019. [Online]. Available: https://www.mcmaster.com/7343k184-7343K185. [Accessed 20 November 2019].

[27] McMaster-Carr, "Guard for Toggle Switches," McMaster-Carr, 2019. [Online]. Available: https://www.mcmaster.com/1143t1. [Accessed 20 November 2019].

[28] "Rare-Earth Magnets," Lee Valley, [Online]. Available: https://www.leevalley.com/en-ca/shop/hardware/rare-earth-magnets/magnets/disc/32065-rare-earth-circular-magnets. [Accessed 01 12 2019].

[29] "Socket Cap Screws," Home Depot, [Online]. Available: https://www.homedepot.ca/en/home/categories/building-materials/hardware/fasteners/screws/socket-cap-screws.html. [Accessed 01 12 2019].

[30] "1/4 Lock Nut," Home Depot, [Online]. Available: https://www.homedepot.com/p/Everbilt-1-4-in-20-tpi-Coarse-Stainless-Steel-Nylon-Lock-Nut-3-Pack-800131/204274167. [Accessed 01 12 2019].

[31] "M3 Hex Nut," Home Depot, [Online]. Available: https://www.homedepot.com/p/Everbilt-M3-5-Stainless-Steel-Metric-Hex-Nut-2-Piece-per-Bag-842318/204836105. [Accessed 01 12 2019].

[32] V. Campbell, "Risk Assessment and Mitigations: Failure Modes and Effects Analysis (FMEA)," University of Manitoba, 2019.

[33] V. Campbell, "Risk Assessment and Mitigation: Failure Modes and Effects Analysis (FMEA)," University of Manitoba, Winnipeg, 2019.

[34] R Nave , "Ferromagnetism," 2019. [Online]. Available: http://hyperphysics.phy-astr.gsu.edu/hbase/Solids/ferro.html.

[35] QUALITY CONTROL IN RADIOGRAPHY, " LIMITING SPATIAL RESOLUTION CR AND DR," Weebly, March 2015. [Online]. Available: http://qcinradiography.weebly.com/limiting-spatial-resolution. [Accessed 18 October 2019].

[36] M. Duarte, "Gear," [Online]. Available: https://thenounproject.com/term/gear/7137/. [Accessed 19 October 2019].

[37] "B&H Photo and Video," [Online]. Available: https://www.bhphotovideo.com/c/product/864575-REG/oben_ac_2361_3_section_aluminum_tripod.html. [Accessed 18 10 2019].

[38] "GrabCad," [Online]. Available: https://grabcad.com/library/simple-mechanism-of-camera-shutter-1. [Accessed 01 10 2019].

[39] P. chain, "ANSI Standard Roller Chain - K - 1 Attachment," [Online]. Available: https://www.peerchain.com/product/ansi-single-strand-chains-with-attachments-k-1/. [Accessed 20 October 2019].

[40] Mechanical Gifs, "Radial Engine," Mechanical Gifs, 2019. [Online]. Available: https://mechanicalgifs.com/mechanicalgifs/radial-engine. [Accessed 24 October 2019].

[41] "Types of Motors," SparkFun, 2019. [Online]. Available: https://learn.sparkfun.com/tutorials/motors-and-selecting-the-right-one?_ga=2.206289173.767166535.1573342818-1615281861.1572304856.

[42] "Power Supply," Amazon, [Online]. Available: https://www.amazon.com/BINZET-Adapter-Regulated-Supply-Copper/dp/B00PJZQDDO. [Accessed 2019].

[43] "Rechargeable Alkaline Battery," Amazon, [Online]. Available: https://www.amazon.com/Alkaline-Rechargeable-Battery-Controls-Electronic/dp/B07BPRHXYN. [Accessed 2019].

[44] "Power Pack Charger," Parallax, [Online]. Available: https://www.parallax.com/product/28986. [Accessed 2019].

[45] "Lithium Polymer Battery," SparkFun, [Online]. Available: https://www.sparkfun.com/products/13813. [Accessed 2019].

[46] "Power Pack and Charger 18650," Parallax, [Online]. Available: https://www.parallax.com/product/28986. [Accessed 2019].

[47] Electronics Hub, "DC Motor," Electronics Hub, 9 March 2015. [Online]. Available: https://www.electronicshub.org/dc-motor/. [Accessed 24 November 2019].

[48] Dejan, "How Brushless Motor and ESC Work," How to Mechatronic, 2019. [Online]. Available: https://howtomechatronics.com/how-it-works/how-brushless-motor-and-esc-work/. [Accessed 24 November 2019].

[49] OpenLab Pro, "OpenLab Stepper Motor Hookup Guide," OpenLab Pro, 2019. [Online]. Available: https://openlabpro.com/guide/openlab-stepper-motor-hookup-guide/. [Accessed 24 November 2019].

[50] J. Pena, "18650 Batteries," SparkFun, [Online]. Available: https://www.sparkfun.com/products/13189. [Accessed 2019].

[51] J. Pena, "Arduino," SparkFun, 2019. [Online]. Available: https://www.sparkfun.com/products/11021.

[52] J. Pena, "Continious Rotation Servo Trigger," SparkFun, 2019. [Online]. Available: https://learn.sparkfun.com/tutorials/continuous-rotation-servo-trigger-hookup-guide?_ga=2.227218843.767166535.1573342818-1615281861.1572304856.

[53] J. Pena, "DC Brushed Motor Driver," SparkFun, 2019. [Online]. Available: https://www.sparkfun.com/products/14450?_ga=2.206754453.767166535.1573342818-1615281861.1572304856.

[54] "M3 Hex Nut," Home Depot, [Online]. Available: https://www.homedepot.com/p/Everbilt-M3-5-Stainless-Steel-Metric-Hex-Nut-2-Piece-per-Bag-842318/204836105. [Accessed 01 12 2019].

# Appendix A – Specifications

## Table of Contents



## *List of Figures*

## A.1 House of Quality

Figure A - 1 below provides an overall summary of the project needs, metrics, target specification, and benchmarking in one image using a House of Quality. The highlighted needs and metrics have been identified as requiring additional explanation, provided immediately following the House of Quality.

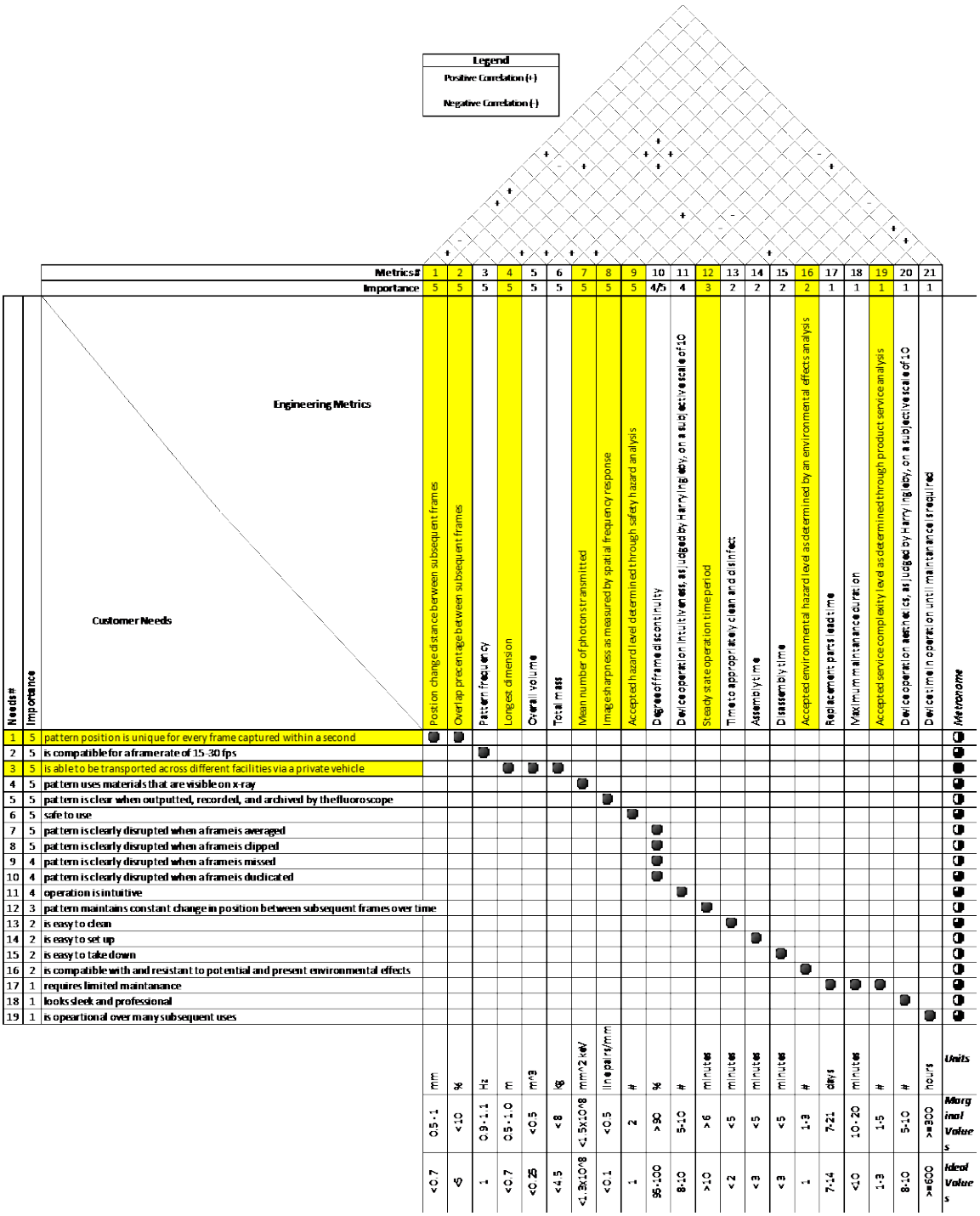


Figure A - 1: House of quality.

## A.2 Needs and Metrics Details

Need number 1 places the highest priority on ensuring that the device pattern position is unique for every frame captured within a second, which will be measured through metrics 1 and 2. Metric 1 measures the distance traveled by the pattern between two adjacent positions captured by the fluoroscope. Metric 2 measures the presence of a percentage overlap between

adjacent frames captured by the fluoroscope. The combination of these two metrics will ensure that every frame of the device's motion captured by the fluoroscope within a one second period, in the absence of any quality loss, is unique from one another.

Metric 4 measures the longest dimension of the overall device, in order to meet need 3, which puts a level 5 importance on ensuring that the device is easily transported via private vehicle and allows for assessment of a magnitude of fluoroscopes across Canada. Isolating the longest dimension as a metric, as opposed to considering metric 5 or 6, accounts for a design that is significantly longer than it is wide or tall, and penalizes it as it would be awkward to handle.

Metric 7 measures the mean number of photons transmitted through the material, measured in $mm^2$ keV. The higher this value is, more light is able to penetrate the object imaged by the x-ray, decreasing the image contrast. A lower value for the mean number of photons is desired for key pattern features of the device, in order to produce sufficient contrast.

Metric 8 measures the output image sharpness as defined by the spatial frequency response, measured in line pairs per millimeter, *lp/mm*. For any image one views this measures how well two objects with high contrast, placed directly adjacent to each other, can be distinctly differentiated [1]. Figure A - 2 below demonstrates differences in Spatial Frequency. That is, as lp/mm decreases, the more discernable two adjacent objects are from one another.

Figure A - 2: Examples of image spatial frequencies, measured by lp/mm [1].

The purpose of metric 9 is to assess the presence of safety hazards in the final design through a safety hazard analysis. As a result, an overall hazard level limit will be placed. Any hazards below the limit will be accepted as part of the design, as they will be low occurrence or impact hazards. Preventative measures will be implemented through labels and provided safety guidelines. The presence of any hazards above the limit will be rejected and design changes will

be incorporated to eliminate these hazards. Using a Failure Modes and Effects Analysis (FMEA) Severity rating scale, the following measurement guidelines have been defined for this metric.

1. Minor – Refers to things such as pinch point hazards while using the device.
2. Low – Refers to things such as any cuts or shocks experienced when interacting with the device.
3. Moderate – Refers to things such as the device exerting impact force on the operator or surrounding machinery due to falling over, etc. Result of the impact does not require attention, simply causes discomfort.
4. High – Refers to things such as the device damaging either the fluoroscope or the operator such that medical attention or machine repair is required.

Metric 12 measures the steady state operation time period of the device in minutes, resulting from need 12 which states that the pattern maintains constant change in position between subsequent frames over time. The metric acknowledges the possibility of synchronization errors over longer operation periods due to the error inherent in the mechanisms used to create the repeating pattern. If this issue is identified in the device, a reset mechanism will be added, and countermeasures will be built into the design to ensure that steady state operation time is maximized.

Metric 16 assesses potential environmental hazards that the design will be subjected to, very similarly to metric 9's assessment of safety hazards. The possible environmental hazards will come in many forms, such as dusk and grime in storage, snow and dirt during transportation, etc. Effect of radiation from the x-ray tube during device operation is not considered as an environmental hazard as the project primary contact, who is a subject matter expert in Radiology, stated it to be a non-issue. The effect of the environmental conditions on the device and its performance is measured on a scale of five as follows:

1. Cosmetic effect/damage – the hazard's effect does not impede the operation of the device
2. Non-critical effect – the hazard affects a component of the design that does not impede the primary function of the device

3. Easy to resolve – the hazard affects a critical component, but can easily be resolved through quick corrective measures (e.g. cleaning a component)
4. Difficult fix – the hazard affects a critical component, requiring substantial time and effort to correct (e.g. unscrewed spiral)
5. Component Replacement – the hazard's effect requires the replacement of the component

Metric 19 assesses the complexity of maintenance in a similar manner to the assessment of metrics 9 and 12, accounting for the need of limited maintenance. Maintenance including chain lube change, component replacement, battery replacement, etc. are considered. This metric is subjective and is based on cost, time and material of the service. Custom parts replacement for example would be most difficult and as such assigned a 10. Regular parts replacement is assigned an 8, chain lube replacement is a 6, and so on. The metric is scaled from 1 to 10 with 10 being a the most complex.

# References

[1] QUALITY CONTROL IN RADIOGRAPHY, " LIMITING SPATIAL RESOLUTION CR AND DR," Weebly, March 2015. [Online]. Available: http://qcinradiography.weebly.com/limiting-spatial-resolution. [Accessed 18 October 2019].

# Appendix B – Concept Development and Selection

## Table of Contents

## *List of Figures*

## *List of Tables*

## B.1 Preliminary Concepts

The following sections include the preliminary concepts of the different types of motions. They are categorized as rotational,

### B.1.1 Rotational Based Motion

This section includes concepts that use rotational motion about a point as its primary method for the periodically repeating pattern.

#### B.1.1.1 Clock Concept

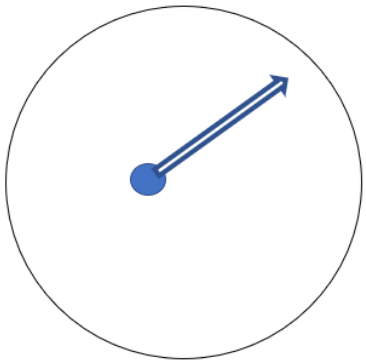

Figure B - 1: Simple clock sketch.

The idea was inspired by a simple cock set up as illustrated in Figure B - 1. The clock hand runs with continuous motion and speed.

#### B.1.1.2 Planetary Concept

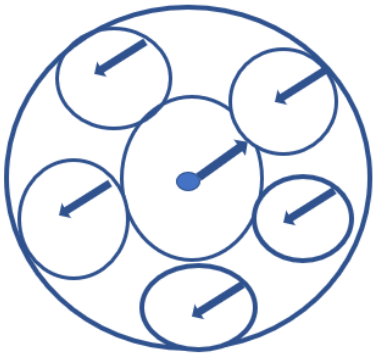

Figure B - 2: Planetary concept.

The idea here is inspired by motion of planetary gears as illustrated in Figure B - 2. On each gear, a clock hand is attached. Each smaller clock acts as a simple clock. The concept can identify 15 different frame rates if each clock can identify three different frame rates.

### B.1.1.3 Simple Gear Assembly

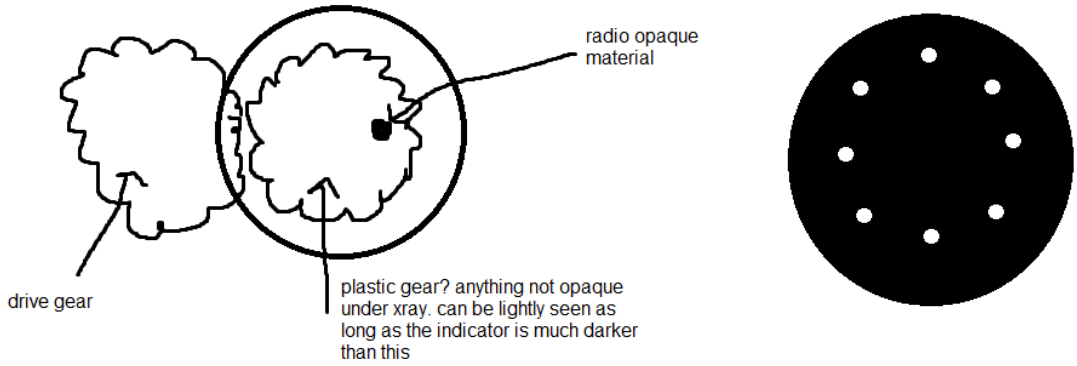


Figure B - 3: Simple gear assembly.

The concept shown in Figure B - 3 uses a driven gear that is made of plastic or a similar material that is radiotranslucent. The marker on the plastic gear will be of a radio opaque material. The cover of the material is made of a radio opaque material with holes. The marker on the driven gear will cover each hole as the driven gear spins. For adjustability, multiple covers can be made with varying holes, or one cover can be used with a variable motor speed.

### B.1.1.4 Archimedean Spiral

The periodic pattern used by this concept is the rotating spiral shown in Figure B - 4 which demonstrates the view captured by the intensifier. This spiral pattern can be implemented in two ways:

1. A continuous curve spiral
2. A discretized spiral with leveled sub-sections

The number of radial sub-sections can be increased, and an indicator can be placed on the perimeter of the circular plate on which the spiral lays, providing an indication of the current frame in the cycle, or percentage of cycle completed. A combination of materials would be used to achieve visible opacity and sufficient contrast in the fluoroscopy study.

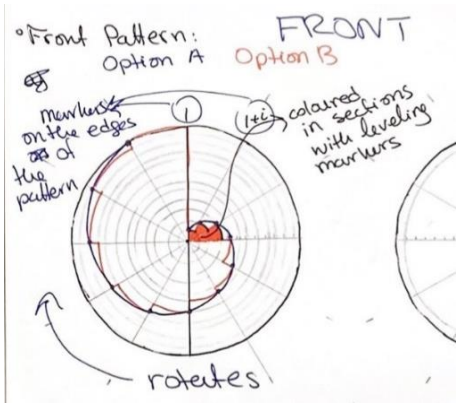


Figure B - 4: Archimedean spiral.

In order to achieve the circular motion of the spiral, a linearly moving bar that translates its motion to a pin, as seen in Figure B - 5, would be attached to the rear of the spiral plate. The speed of the linear bar is fastest when the pin is at the top and bottom of the circular plate, and slowest on the right and left edges of the circular plate.

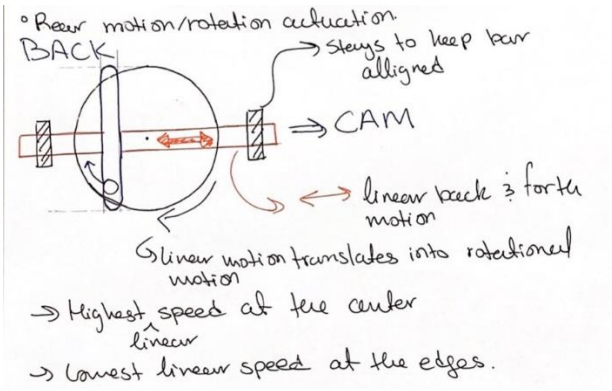


Figure B - 5: Slider-pin assembly.

In order to attain the varied linear speed of the bar, a pear-shaped cam, seen in Figure B - 6, would be used and driven by a motor.

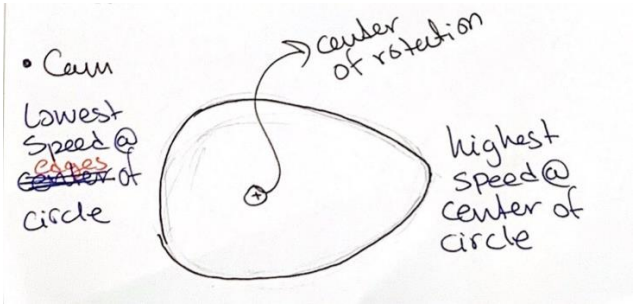


Figure B - 6: Cam motion.

#### B.1.1.5 Simple Clock

The clock pattern is very simple and very similar to the previous concepts that were presented. It will have one arm that moves 60 revolutions per minute and the dial will have 30 points. The 30 points and the dial will be radiopaque while the rest is radio translucent. The design was very similar to the other concepts and this concept was considered as a base concept instead in the selection process.

### B.1.2 Lateral Motion

The concepts in the following sections use unidirectional motion in which the object moves side to side across the imaged area.

#### B.1.2.1 Basic Chain Drive

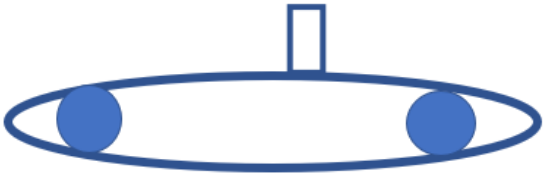

Figure B - 7: Simple belt drive assembly.

The idea is to have a belt or chain drive system as illustrated in Figure B - 7. On the belt or chain, a metallic object is attached and used as an indicator. The design is driven by an electrical motor where the motor is calibrated to a constant output speed.

#### B.1.2.2 Chain Elevator

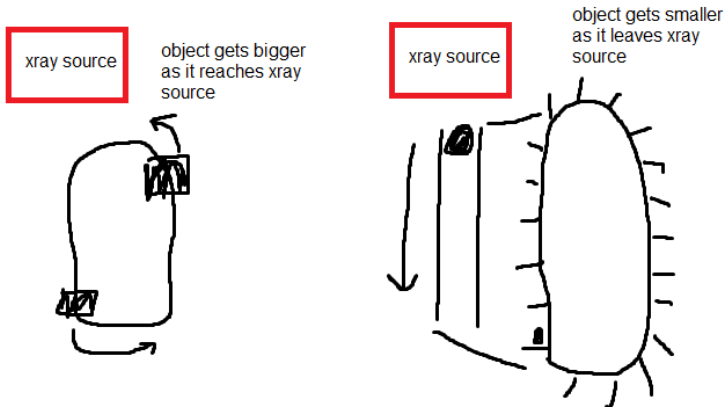


Figure B - 8: Chain elevator.

The above concept uses a chain drive for power transmission. X-rays behave similar to visible light. An object closer to the source will be larger but less defined while an object further away will be smaller but the image will be sharper. The design on the left of Figure B - 8 has an indicator that gets larger as it approaches the x-ray source while the indicator of the design on the right gets smaller as it gets further away from the source. The left design would have indicators attached to the chain while the right design would have buckets attached to the chain to carry the indicators as shown in Figure B - 9.

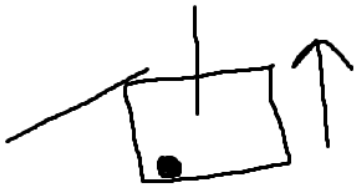

Figure B - 9: Bucket for chain elevator design.

As the bucket reaches the top, the ramp will force the bucket to rotate and therefore drop the ball out of the bucket

### B.1.2.3 Simple Chain Drive

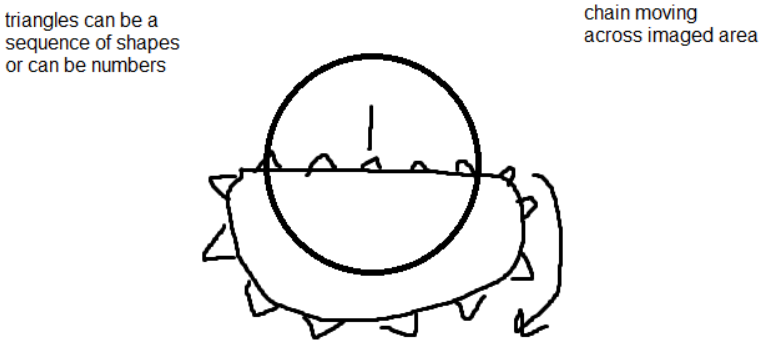


Figure B - 10: Simple chain drive assembly.

The design in Figure B - 10 uses a chain drive that moves laterally across the imaged portion of the fluoroscope. The chain has a pattern of shapes or numbers attached to it that moves across an indicator in the imaged area. Less shapes or numbers results in a faster chain speed to achieve the same frequency across the indicator, in turn introducing motion blur.

### B.1.2.4 Belt Conveyor

The belt conveyor design, illustrated in Figure B - 11 below, has equally spaced metallic hooks attached to the belt that is driven by an electric motor. The hooks will pass in front of an acrylic plate with equally spaced metallic markings that would be compatible with the frame rate to be investigated. The contrast between the radiopaque materials to illustrate the position on the x-ray. The plates would be interchangeable with markings for individual frame rates.

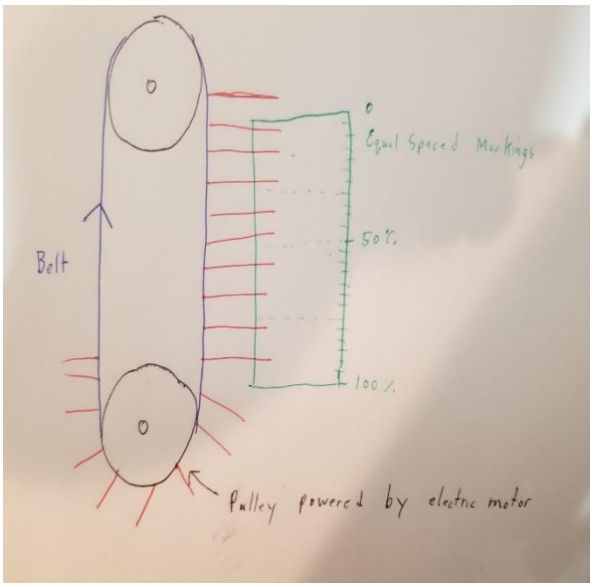


Figure B - 11: Belt conveyor.

## B.1.3 Miscellaneous

The following concepts were unable to be classified in a generic motion. As such, they are considered miscellaneous.

### B.1.3.1 Connect Four Shutters

The connect four shutter design has 30 equally spaced holes cut into a metal sheet as illustrated in Figure B - 12 below. To show contrast on the x-ray image, the holes would be covered up by flaps at a desired speed. For 30 frames per second (fps), 30 holes would be covered per second whereas 25 fps would have 25 holes covered per second.

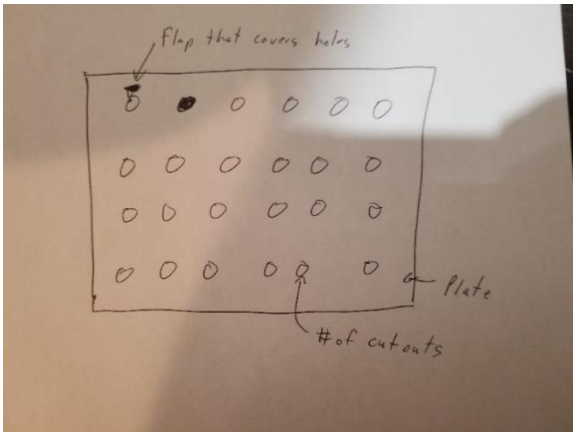


Figure B - 12: Connect four shutters.

### B.1.3.2 Noble Gas

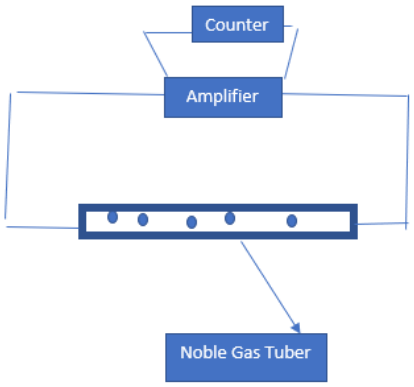


Figure B - 13: Noble gas counter.

This idea is inspired by the Geiger counter system as illustrated in Figure B - 13. As the x-ray particles passes through the noble gas tube, they will ionize the noble gas to electrons. Electrons will flow along the copper wire to the amplifier, converting into electrical signals to be counted.

### B.1.3.3 Flipping triangles

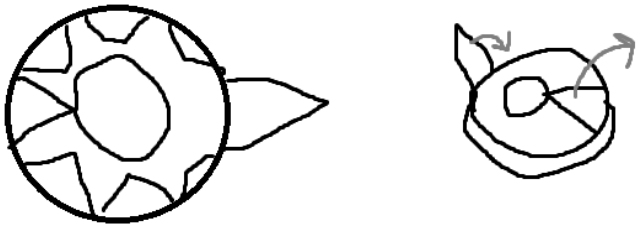

Figure B - 14: Flipping triangles.

The design in Figure B - 14 uses triangles that flip up and down. When a triangle's tip reaches the center circle line, the motion is complete and so the motion of the next triangle should be considered. Adjacent triangles will simultaneously "close" in a clockwise or counter clockwise direction.

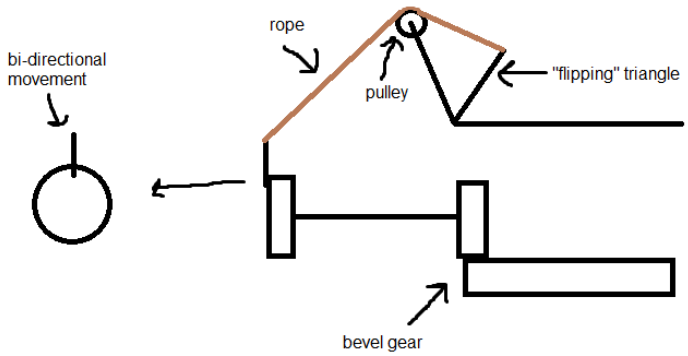


Figure B - 15: Flipping triangles motion mechanism.

The motion mechanism is shown in Figure B - 15 above. The mechanism consists of a bevel gear which transforms motion to a bilateral direction. The bilateral motion is then attached to a pulley through a rope that will raise and lower the triangles.

### B.1.3.4 Radial Engine

Using a planetary gear configuration, the multiple pistons seen in Figure B - 16 would translate radially within their housing. Each piston housing contains a marker to measure the motion of the pattern between subsequent frames.

Figure B - 16: Radial engine [1].

Additionally, a dial could be employed on the perimeter of the orbit gear of the planetary configuration, in order to provide a reference for the cycle's progress.

### B.1.3.5 Undeveloped Concepts

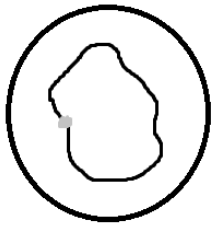

Figure B - 17: Radiopaque marker moving on a set path.

The concept in Figure B - 17 above uses a radiopaque ball that moves along a fluid path. The fluid used should be radio translucent. The fluid will be moved using a pump.

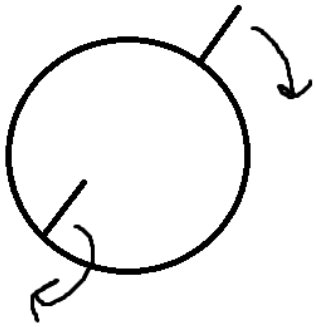

Figure B - 18: Rotating arms.

The design in Figure B - 18 consists of multiple rotating arms. As one arm leaves the captured view, another arm will enter.

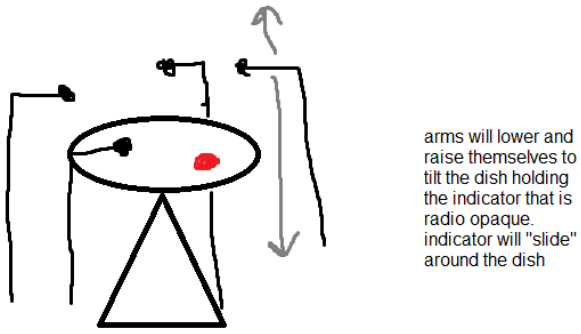


Figure B - 19: Rising arms.

In Figure B - 19 above, a plate is balanced on a pointed end. On the plate, a radio opaque marker is present. The plate is tilted in either a clockwise or counter clockwise direction through the up and down movement of adjacent arms.

## B.2 Selection Criteria

The selection process applies seven criteria, which originate from the project metrics, to each concept. TABLE B - I below lists the criteria and their assigned weights.

TABLE B - I: SELECTION FACTOR WEIGHT TABLE

| Design Criteria | 1 | 2 | 3 | 4 | 5 | 6 | 7 |
|---|---|---|---|---|---|---|---|
| **1. Device Simplicity** | | 2 | 3 | 1 | 1 | 1 | 1 |
| **2. Output Pattern Performance** | | | 2 | 2 | 2 | 2 | 2 |
| **3. Variable Frame Rate Compatibility** | | | | 3 | 3 | 3 | 3 |
| **4. Costs** | | | | | 4 | 6 | 4 |
| **5. Durability** | | | | | | 5 | 5 |
| **6. Ease of Operation** | | | | | | | 7 |
| **7. Maintenance** | | | | | | | |
| **Total Hits** | 4 | 6 | 5 | 2 | 2 | 1 | 1 |
| **Weight (%)** | 18.05 | 28.57 | 23.81 | 9.52 | 9.52 | 4.76 | 4.76 |

The criteria developed were based on the design requirements, needs and metrics. The following list details each criterion.

1. **Device Simplicity** – Considers the number of components, complexities of the component geometries, and the manufacturing processes involved.
2. **Output Pattern Performance** – Addresses metrics 7, 8, and 10, concerning the image contrast, special frequency response, and ability to demonstrate the four frame quality losses.
3. **Variable Frame Rate Compatibility** – Addresses metric 3 concerning the pattern frequency, which originates from the need for the device to be compatible with a fluoroscope frame rate range from 15 to 30 fps.
4. **Costs** – Considers manufacturing, material, testing, and other miscellaneous costs.
5. **Durability** – Considers operator blunders, such as drops from the minimum operational height of 1 [m], as well as regular wear and tear.
6. **Ease of Operation** – Considers the range of skillsets of operators.
7. **Maintenance** – Considers the need for simple and timely maintenance.

## B.3 Detailed Concept Generation

The team identified four possible motion mechanisms through which the periodic pattern of the device could be achieved: circular, lateral, linear, and fluid motion. Circular and lateral motion were identified as the best methods for achieving the periodic pattern.

### B.3.1 Motion Type

Using the preliminary concepts generated, four types of motion were identified to achieve the project objectives are circular, lateral, linear, and fluid motion and are illustrated in TABLE B - II.

TABLE B - II: DIFFERENT TYPES OF POTENTIAL MOTION PATTERNS

| *CIRCULAR* | *LATERAL* | *LINEAR* | *FLUID* |
|---|---|---|---|
| 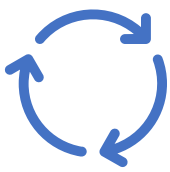 | 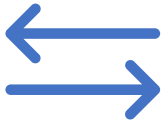 |  |  |

### B.3.1.1 Circular

An everyday instrument that moves in a periodic pattern is an analog clock. For every second, minute, and hour, within a 12-hour period, the hands of a clock have a unique position. Thus, a clock was one of the base ideas and inspirations used within circular motion concepts. These concepts could employ an object which moves circularly and does so with a specific speed such that for every frame captured by the fluoroscope during a second (maximum of 30 frames captured), the object has a unique position. Figure B - 20 and Figure B - 21 below provide an illustration of how this may be achieved, either with a conventional arm on a clock, or with two meshed gears that move a marker in a circular motion.

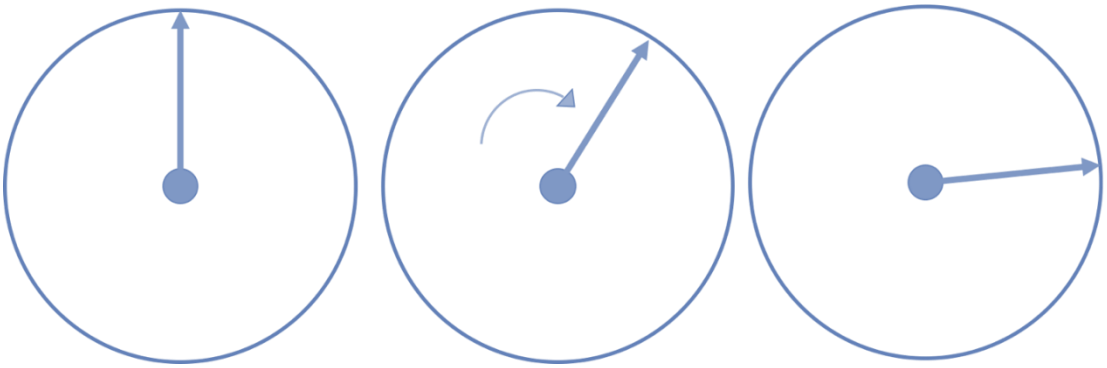

Figure B - 20: Circular clock mechanism.

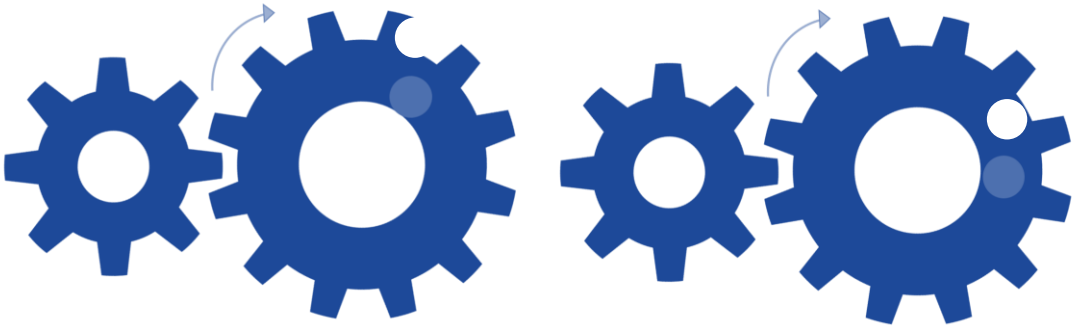

Figure B - 21: Rotating gear mechanism with marker [2].

### B.3.1.2 Lateral

Lateral motion is used to refer to an object that is moving in one direction. Lateral motion will move across the scanner face and can move discernable objects while maintaining constant offset. Additionally, the use of patterns that move along a single axis assists with the elimination of distractions within the field of view (FOV). To ensure constant periodic repetition of the lateral

motion, a closed loop mechanism, such as a belt or chain, could be employed. Figure B - 22 and Figure B - 23 illustrate how this may be achieved.

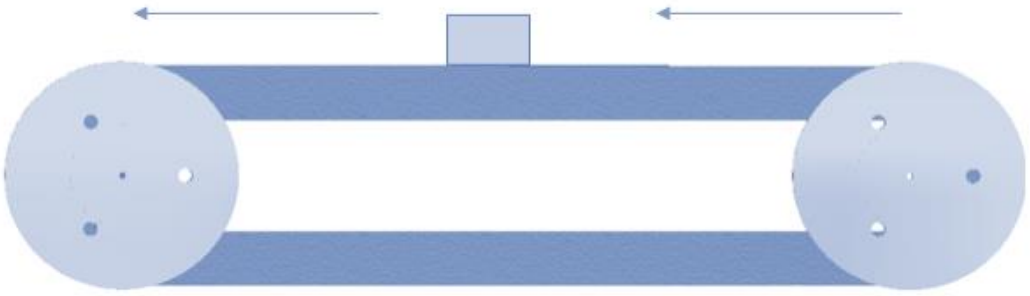

Figure B - 22: Simple belt drive mechanism with a metallic object attached to the belt.

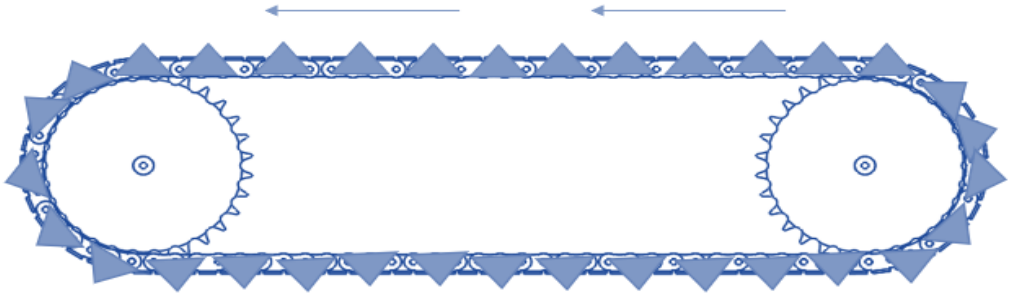

Figure B - 23: Simple chain drive mechanism with attached triangular objects.

### B.3.1.3 Linear

Like lateral motion, linear motion has a unidirectional movement. The main difference between the two being the direction of motion. The indicator of the device would move along the path of the electrons emitted by the x-ray tube, varying its distance away from the image scanner, shown in Figure B - 24 below.

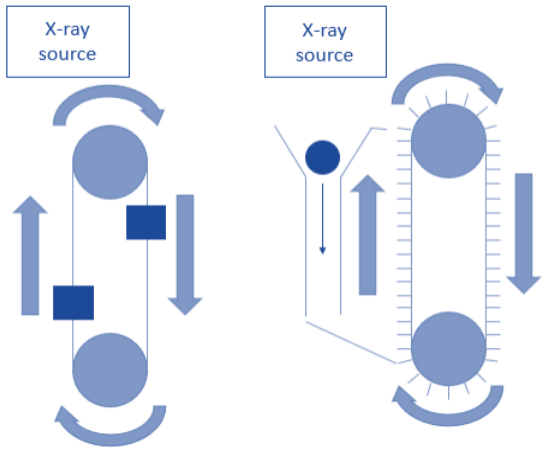


Figure B - 24: Device concept utilizing linear motion.

The left side of Figure B - 24 demonstrates an object moving away from the x-ray source (getting larger), while the right side demonstrates an object moving away from the x-ray source (getting smaller).

### B.3.1.4 Fluid

Pumps are a method of accurately and precisely moving a set amount of liquid at a desired flow rate. Pumps, in conjunction with Proportional-Integral-Derivative (PID) control, can be used to identify quality loss. A radiopaque liquid, such as mercury, would provide contrast to metallic markings on the fluid reservoir, when recorded by the fluoroscope. Figure B - 25 illustrates how this may be achieved from varying the levels between two reservoirs.

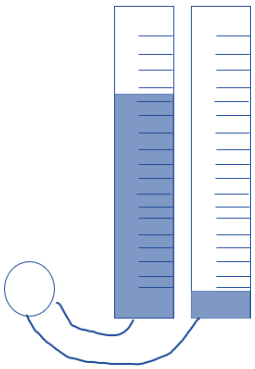

Figure B - 25: Initial base idea of radiopaque liquids varying in height over time.

### B.3.1.5 Motion Type Selection

TABLE B - III below details the assessment of the four motion types compared to the reference concept. Since the motion types were general ideas, their performance within each of

the selection criteria were assessed in comparison to the reference concept. A superior performance was assigned a "+", an inferior performance was assigned a "-", and an at par performance was assigned a "0".

TABLE B - III: MOTION TYPE SCORING AND SELECTION

| | | Reference Concept | Concept Motion | | | |
|---|---|---|---|---|---|---|
| | Criteria | Metronome | Linear | Circular | Lateral | Fluid |
| **1** | Device Simplicity | 0 | - | 0 | 0 | - |
| **2** | Output Pattern Performance | 0 | - | + | + | + |
| **3** | Variable Frame Rate Compatibility | 0 | + | + | + | + |
| **4** | Durability | 0 | 0 | 0 | 0 | - |
| **5** | Costs | 0 | - | - | - | - |
| **6** | Ease of Operation | 0 | - | + | + | 0 |
| **7** | Maintenance | 0 | - | 0 | 0 | - |
| | Sum +'s | 0 | 1 | 3 | 3 | 2 |
| | Sum 0's | 9 | 1 | 3 | 3 | 1 |
| | Sum -'s | 0 | 6 | 1 | 1 | 4 |
| | Net Score | 0 | -5 | 2 | 2 | -2 |
| | Rank | 2 | 4 | 1 | 1 | 3 |
| | **Continue** | | **No** | **Yes** | **Yes** | **No** |

The two motion types that tied for the top rank were circular and lateral motion, and thus were chosen to be used in further, more detailed, concept generation.

## B.4 Detailed Concepts

The preliminary ideas were combined and expanded upon to produce six detailed concepts, including all of their respective features, mechanisms, and manufacturing plans.

### B.4.1 Sinusoid

The sinusoid design creates a pattern in one plane through motion in another plane. Figure B - 26 below provides an overall view of what such a device may look like.

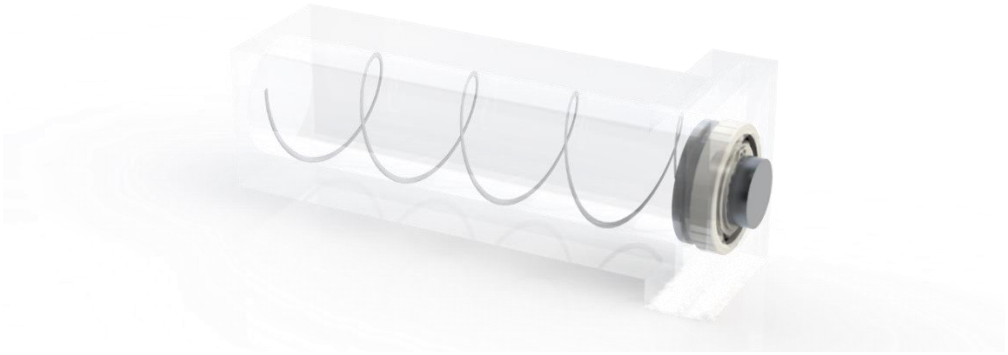

Figure B - 26: Sinusoid pattern concept – angled view.

The sinusoid pattern can be done by rotating a spring. The perspective of a moving sinusoid, as illustrated in Figure B - 27, can be seen from the side of the device. The spring is attached to a shaft held by a bearing and runs using a servo motor spinning at 60 rpm or more. The speed can be adjusted using a controller and the pattern can be distinguish by placing a grid behind the perceived motion.

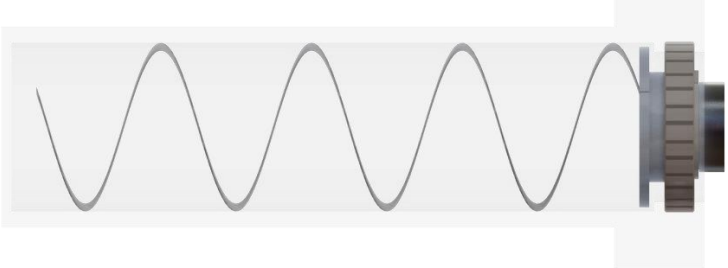

Figure B - 27: Sinusoid pattern concept - side view.

The casing is radiotranslucent, while the dial and the spring is radiopaque. The shaft will be made from aluminum using a lathe while the bearing and motor would be purchased. The controller and the power source separate from the pattern generating device.

### B.4.2 Archimedean Spiral

The Archimedean Spiral concept, shown in Figure B - 28, engages in circular motion similar to that of a clock. The use of a spiral pattern, as compared to a straight arm on a clock, improves on the ability of a circularly rotating device to produce unique frames, by combining position changes in both the angular and radial directions.

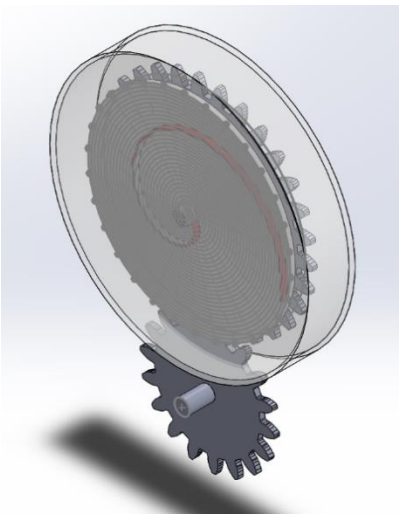

Figure B - 28: Archimedean spiral concept – overall angled view.

Figure B - 29 illustrates how the pattern captured by the fluoroscope evolves. The rotation of the meshed gears would cause the spiral pattern to rotate, creating continuous circular motion. To ensure every position of the spiral captured is unique, the larger upper gear would have to run at a rotational speed of at least 60 [rpm].

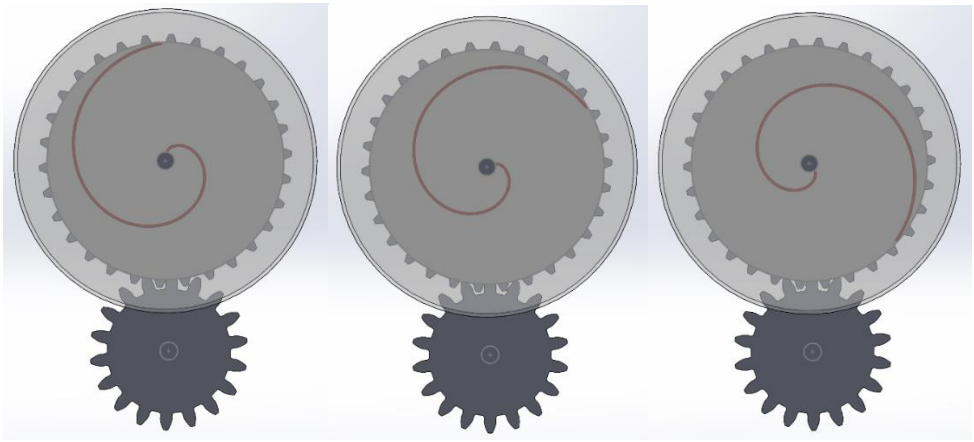

Figure B - 29: Archimedean spiral concept front view at different rotational positions.

The spiral could also be driven with a belt drive which would simply require more space for the drive mechanism. Figure B - 30 illustrates how the main gear drive shaft is attached to the clear casing, which encloses the mechanism and provides support for the shaft along which the mechanism rotates. Additional casings and support structures would be designed underneath and around the exposed pinion gear in order to enable the design to be positioned vertically between the x-ray tube and the image scanner.

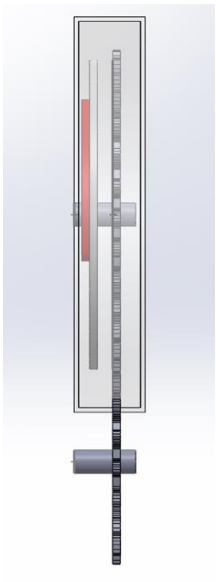

Figure B - 30: Archimedean spiral concept side view.

An additional feature of this design is the implementation of a grid as a backdrop to the spiral. One way to implement it would be a basic grid, seen in Figure B - 31, which shows the varied diameter circles and equally spaced radial subdivisions.

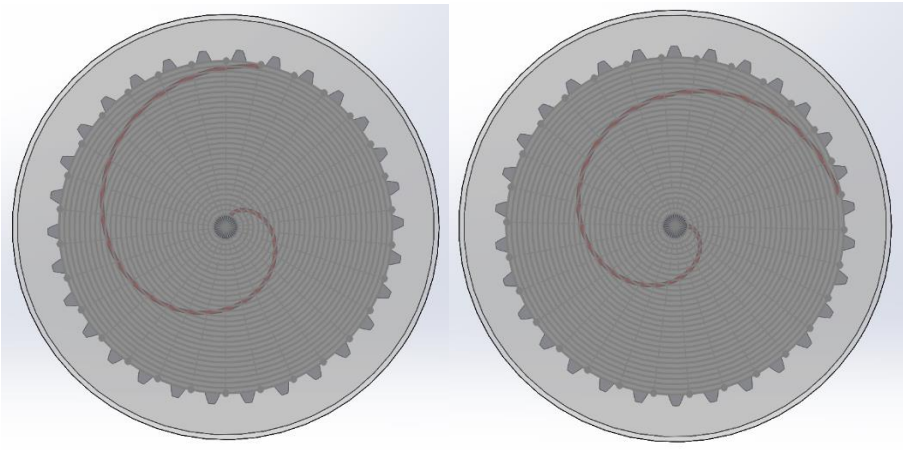

Figure B - 31: Basic grid backdrop to spiral pattern, at different spiral positions.

A secondary alternative, illustrated in Figure B - 32, would vary the distances between the radial subdivisions between each pair of adjacent circles. The number of subdivisions in each set would be equal to a given frame rate setting, within a discretized set between 15 and 30 fps, used for videofluoroscopic swallow studies (VFSS). This feature could provide some level of adjustability to assess the performance of fluoroscopes at different frame rates. The sub-divisions shown in Figure B - 32 are for frame rate settings of 15, 17, 20, 22, 25, 27, and 30 fps.

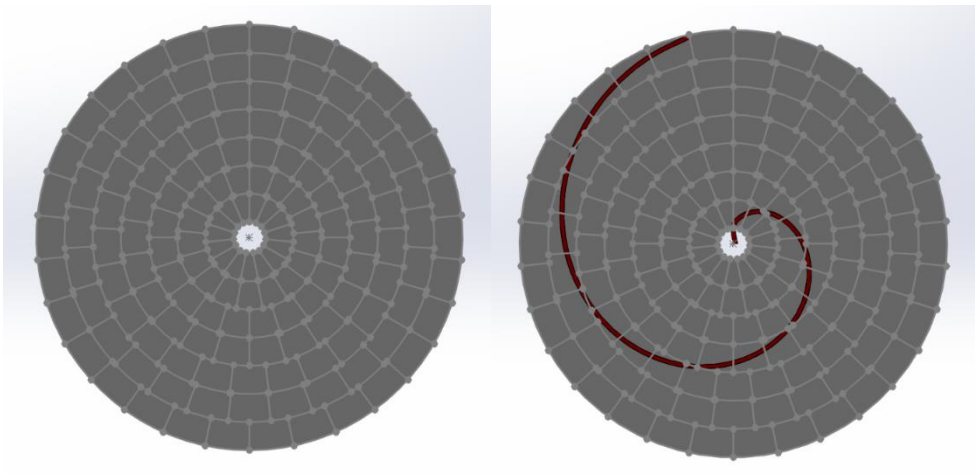

Figure B - 32: Spiral concept with varied radial subdivisions for frame rate identification.

To manufacture this concept, the primary consideration would be the materials used to ensure that the features that are of interest during the VFSS are easily discernable. By utilizing a combination of different materials, with varying radio-opacity, a high enough contrast may be achieved.

Since the spiral is of primary interest, it will be fabricated from a metal with the highest radio-opacity of the materials used within the imaged area. If the design were to implement either of the grid alternatives discussed, the grid would be made of a material with a low radio-opacity. The larger the difference, the better the contrast between the two will be. The radio-opacity of the grid should be high enough, however, to still be visible on the captured image. For all other parts of the design that are of no interest in the VFSS, low radio-opacity materials, such as aluminum or plastic, would be used depending on any strength requirements.

To manufacture the spiral shape and grid markings, a precise operation such as a laser etcher could be used to create the geometries into the rotating plate, after which the appropriate material would be deposited into the lasered voids. No other components of the concept would possess as high of a complexity and would use common manufacturing processes.

Lastly, Figure B - 30 illustrated the plate and main gear as separate components, but the two could be bonded together, or the design could eliminate the rotating plate completely, manufacturing the spiral and grid directly into the gear. This option is possible as the concept does not require a large amount of force transmission.

### B.4.3 Simple Gear Drive

To obtain continuous motion, the base concept of utilizing a simple drive gear was further developed. Figure B - 33 illustrates a gear made of clear plastic that has a darker indicator attached that contrasts with the gear when imaged by the fluoroscope. An additional plate would be placed underneath, fabricated with different sets of holes in a circular configuration, assisting in determination of the frame rate.

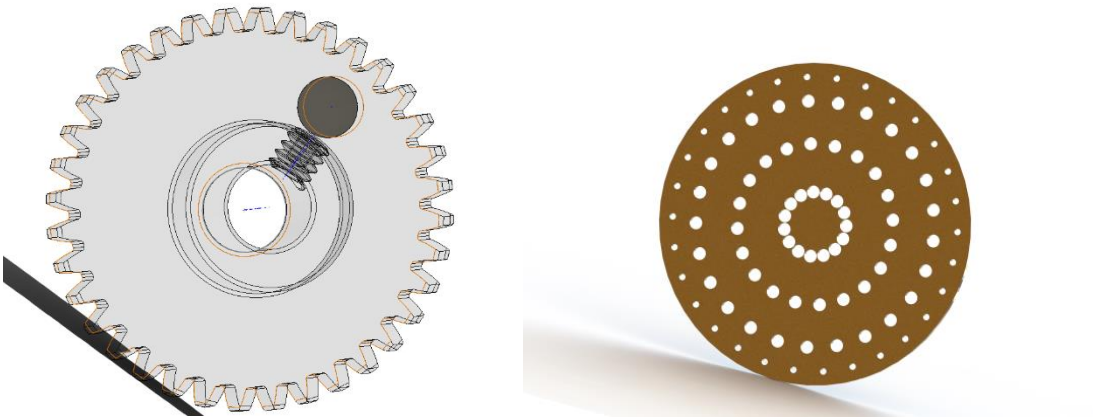

Figure B - 33: Front view of simple gear drive mechanisms.

The material on the plastic gear will cover the holes as it spins around. Two alternatives are considered to provide device adjustability:

Option A:

- The number of holes is 30, 25, 20, and 15 and are evenly spaced apart. These are potential FPS settings used by the fluoroscope.
- Motor rotates at a reference speed of 1 revolution per second for a frame rate setting of 30 fps.
- Variable motor speed is implemented such that if a lower frame rate, such as 25 fps was desired, the motor speed would be lowered and so the indicator will only reach 25 of the 30 circles within a second.

Option B:

- Motor is set to rotate the indicator at one revolution per second
- The number of holes can be varied with interchangeable plates placed underneath the plastic gear, with every frame rate setting having its own specific hole plate.

To drive the gear, a purchased motor will be used. To support the mechanism, the design will include a frame. For manufacturing the holed plate(s), 3D printing with Polyethylene terephthalate (PET) could be used. Finally, the plastic gear can be manufactured through 3D printing or laser cutting.

### B.4.4 Belt Conveyor

The concept of employing lateral motion using a belt was further developed. Figure B - 34 illustrates the belt conveyer concept where the periodically repeating pattern is obtained by attaching three objects to the belt, moving them laterally as the belt runs. At each revolution, only one of three objects will be within the FOV, at the top of the horizontal portion of the belt, which will contrast from the device background. Three objects are evenly distributed along the drive belt, and the horizontal portion at the bottom of the belt will be covered with a plate to avoid unnecessary distractions within the FOV.

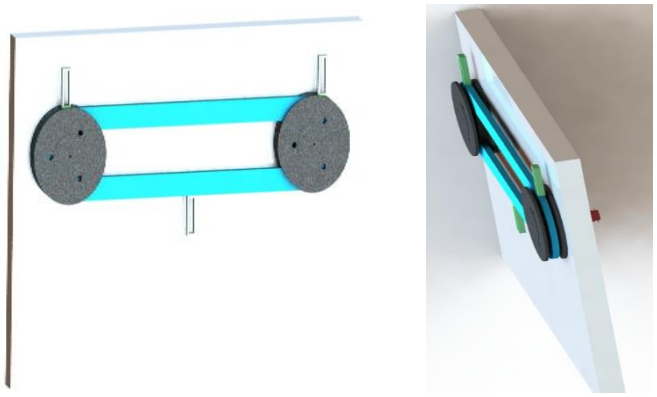

Figure B - 34: Front and side view of belt drive mechanisms.

For the drive system, belts and pulleys will be selected by referencing manufacturer's data. Two identical drive pulleys are required to be manufactured, potentially out of aluminum due to its remarkable properties in terms of being lightweight, durable, and possessing great tensile strength. One pulley will be manufactured with a shaft protruding out to allow the pulley to be driven. The belt would be a flat or timing belt (glass fiber) and will be purchased or manufactured based on the length required by the detailed design. To support the device, a frame would be designed to provide stability, mobility, and overall ease of operation. One possibility for the manufacturing of the frame are hollow stainless-steel tubes.

### B.4.5 Simple Chain Drive

As noted by its name, this design engages in lateral motion using a chain drive. There are numerous chain types to consider when using a chain drive. The simplest approach to the problem involves using a roller chain. Figure B - 35 below demonstrates a chain drive using a roller chain with attachment links.

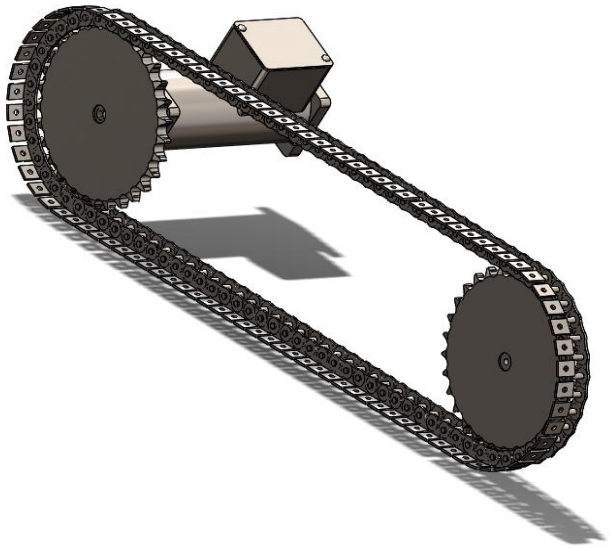

Figure B - 35: Side view of simple chain drive mechanisms.

The chain design will need a casing to account for safety. The indicator line will be marked on the outside of the casing. The roller link attachments allow for easy attachment of shapes with arrows, which will move past the indicator to create the periodic pattern. Although a timing belt drive would be lighter and quieter, the easy attachment of the indicating shapes makes the chain drive a viable choice. Figure B - 36 below shows a closeup of the roller link attachment.

Figure B - 36: Roller link attachment for easy attachment [3].

The slack side of the chain may not be used for the predictable periodic motion as the variation in movement perpendicular to the lateral movement (i.e. vibration) creates uncertainties and may introduce poor quality images when processed. Thus, the design should include a tensioner to eliminate any variation.

To account for split frames, the chain drive will be mounted diagonally. Figure B - 37 below demonstrates how the device will be mounted.

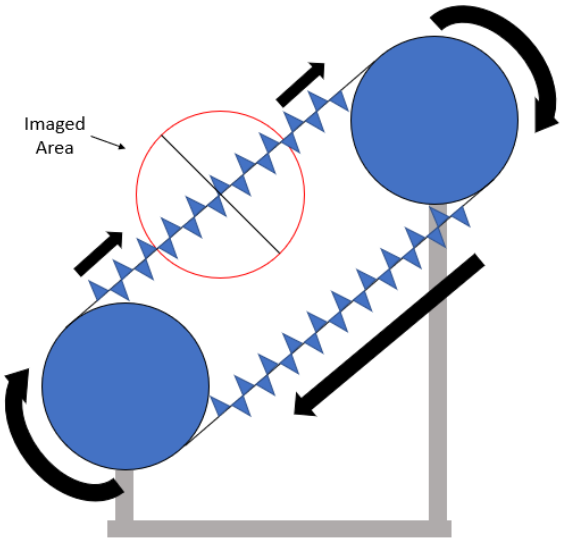


Figure B - 37: Diagonal mounting for chain drive.

Manufacturing considerations for the chain drive is very minimal. If any custom sprockets or shafts are needed, they will need to be considered. As well, the patterns to be attached to the roller link will need to be considered for manufacturing.

### B.4.6 Slider and Pin

After selecting circular and lateral motions to be utilized in the concept development, a combination of these two motions was considered and developed. Figure B - 38 demonstrates how a pin, seen in yellow, connected to a rotating plate, seen in red, will laterally drive the orange bar to achieve periodic lateral motion. This orange bar is supported by a bearing or universal joint that allows the orange bar to move laterally.

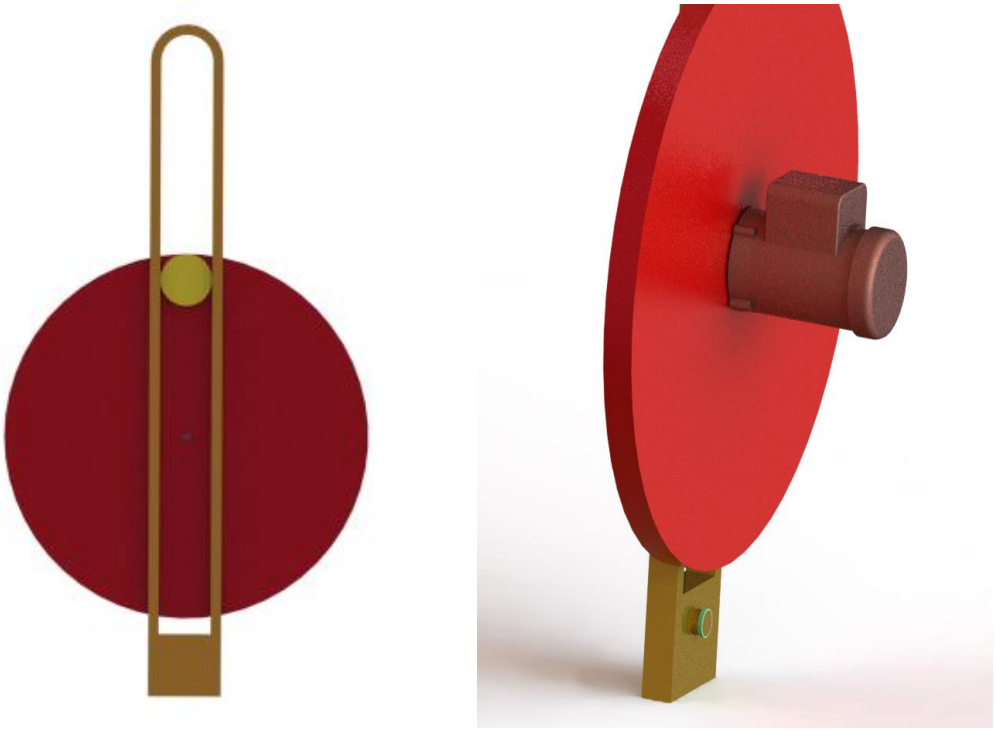

Figure B - 38: Front and side view of slider and pin mechanisms.

For the drive system, an electric motor with an output shaft is needed to drive the red circular plate. The electric motor must be calibrated in order to provide constant output speed of one cycle per second. An appropriate frame would be designed to support the device and would be made from hollow stainless-steel tubing. The rotating circular plate can be manufactured from a laser cutting acrylic. Lastly, the orange metal frame could be made of aluminum, and manufactured using casting.

### B.4.7 Mounting

The frame quality assessment device must securely operate at a height no lower than the minimum height of the fluoroscope's FOV. The chosen concept will be compatible with machine set ups in vertical or horizontal configurations. As each of the detailed concepts are similar in size and shape, the method for adjustable height will not be a factor to decide between them. The adjustability could be achieved by one of the following two methods depending on the x-ray machine set up:

1. The device will be operated in a horizontal position laying on top of the x-ray detector without the aid of additional mounting.

2. The device will have a universal mount incorporated into the housing such that it is able to mount to a tripod. This allows for the adjustment of the operational height of the device and to be used in various vertical set ups. An example is illustrated in Figure B - 39 below.

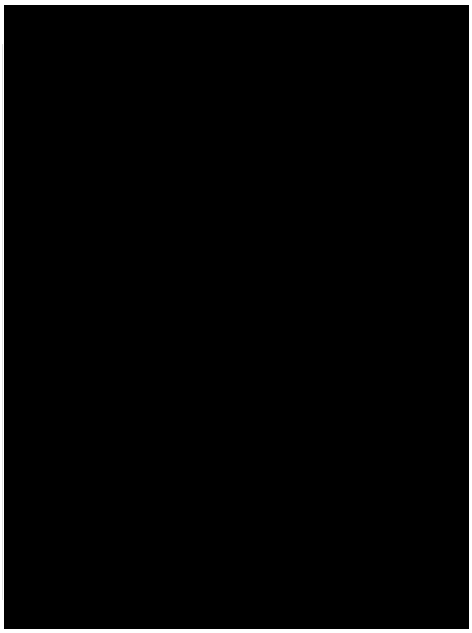

Figure B - 39: Tripod mounting for varying device operation height [4].

## B.5 Concept Screening

The team assessed the detailed concepts and determined that the top three concepts that will continue onto further analysis were the Archimedean spiral, simple chain drive, and sinusoidal pattern.

### B.5.1 Screening Process

Using the criteria presented in TABLE B - I detailed in section B.2, each team member reviewed the six detailed designs, and assigned a score out of five within each criteria. These individual scores were then averaged, and the standard deviation of each criterion for a given concept was calculated in order to identify areas of disagreement that the team needed to discuss prior to assigning the final scoring.

### B.5.2 Screening Results

TABLE B - IV shows a detailed list of the scoring and standard deviations of each concept. The scores are averaged values from each team member while the standard deviation allows the team to easily which scores should be discussed.

TABLE B - IV: DETAILED CRITERIA SCORING

| Criteria | Weight | Metronome | Concept | | | | | | | | | |
|---|---|---|---|---|---|---|---|---|---|---|---|---|
| | | | Sinusoid | | Archimedean | | Slider and Pin | | Belt Conveyor | | Simple Chain | |
| | | | Score | STD DEV | Score | STD DEV | Score | STD DEV | Score | STD DEV | Score | STD DEV |
| 1 | 19.05 | 5 | 3.4 | 0.89 | 3.6 | 0.55 | 3.8 | 0.45 | 3.2 | 0.84 | 3.6 | 0.55 |
| 2 | 28.57 | 2 | 3 | 1 | 4.2 | 0.84 | 2.3 | 0.84 | 2.6 | 0.65 | 3.4 | 0.42 |
| 3 | 23.81 | 1 | 3.2 | 0.84 | 4 | 0.71 | 2.4 | 0.89 | 3.2 | 0.84 | 3.4 | 0.42 |
| 4 | 9.52 | 2 | 3.6 | 0.55 | 3.6 | 0.55 | 3.4 | 0.55 | 3.2 | 1.10 | 3.4 | 0.55 |
| 5 | 9.52 | 5 | 3.4 | 0.55 | 3.6 | 1.14 | 3.5 | 0.50 | 3 | 0.35 | 3.2 | 0.45 |
| 6 | 4.76 | 4 | 3.8 | 0.45 | 3.4 | 0.89 | 3.6 | 0.55 | 3.2 | 0.84 | 3.2 | 0.84 |
| 7 | 4.76 | 2 | 3.4 | 0.55 | 3.4 | 0.55 | 3.2 | 0.45 | 2.3 | 0.45 | 2.4 | 0.55 |
| Total | | 2.71 | 3.28 | | 3.85 | | 2.93 | | 2.97 | | 3.36 | |

TABLE B - V below tabulates the average scores of the detailed concepts, in order of final ranking. The score of the reference concept is also included for comparison of the team's concepts. The top three concepts are determined to be the Archimedean spiral, simple chain drive, and sinusoidal pattern.

TABLE B - V: AVERAGED SCORING OF DETAILED CONCEPTS

| Concept | Averaged Score | Rank |
|---|---|---|
| **Metronome (Reference)** | 2.71 | - |
| **Archimedean Spiral** | 3.64 | 1 |
| **Simple Chain Drive** | 3.36 | 2 |
| **Sinusoid** | 3.06 | 3 |
| **Slider and Pin** | 2.97 | 4 |
| **Belt Conveyor** | 2.97 | 4 |

## B.6 Selected Concepts

The concept screening conducted by the team highlighted three top concepts: the chain, spiral, and sinusoid. All distinct from each other, it was difficult to commit to one concept due to uncertainty in the potential issues with these concepts. The continuation of this project to the prototyping and testing phase as well as a budget contribute to the difficulty in deciding. Given these factors, the top three concepts were developed further to ensure due diligence was taken and the best concept proceeded to full design, prototype, and testing.

### B.6.1 Archimedean Spiral

The Archimedean spiral is an evolution of the circular motion found within a clock. The hand of a clock falling between markings during image capture is a caveat to the simple clock. The spiral improves on this by having many continuous points to illustrate the position instead of one set arm as the pattern produced changes both angularly and radially.

To clearly indicate a change in position over a range of frame rates, the device will be outfitted with grid markings along the face of the spiral. Through further investigation, an optimal layout for the frame rate recording will be chosen using either a set face plate with equally distributed radial subdivisions, or varied distribution of radial subdivisions.

The spiral concept was also chosen due to the ability to rapidly prototype it using additive manufacturing for early concept validation. The gear structure can be 3D printed with a groove set into it for the spiral, into which a metallic wire can be pressed in to provide high radiopacity on the x-ray. To test multiple grid structures, patterns can be etched into acrylic sheets and metal deposited into the spaces.

### B.6.2 Simple Chain Drive

Using a chain allows for a no slip drive that is efficient and simple. Although timing belts may be used, chain drives allow for easy adjustability for the problem at hand.

The chain drive uses easy attachment roller links to mount the indicators on the chain. The indicators can be a series of distinguishable shapes or numbers. Given the size of the device, and thus the size of the indicators on the chain, the pattern used should take care in being unique. Using distinguishable and unique shapes, the chain drive can easily indicate when any frames are duplicated or averaged, while the diagonal mounting allows for accommodation for split frames.

In addition to the size, the speed of the chain should also be considered. As a benchmark, at least 30 unique shapes should pass the marked indicator to account for a maximum of 30 frames per second. The speed also plays a factor in determining if the pattern is distinguishable due to motion blur.

It is also important to consider the variation in speed. Chains experience chordal action due to the geometry of the sprocket and chain. Chordal action results in variation in chain speed. It is still unclear whether the speed variation is significant enough to be a problem. Chordal action will also introduce vibrations. To account for the vibrations, the chain drive concept should be mounted on a surface other than that of the fluoroscopic machine.

### B.6.3 Sinusoid

With its continuous motion and simplicity, the sinusoid was a popular concept. One of the main concerns was the manufacturability of the spring which creates the sinusoid pattern. A custom compression spring type of structure can only be manufactured through a spring manufacturer. The project Faculty Advisor suggested a local company that possessed the required capabilities.

Other possible issues of the design include the clarity of the pattern. The first iteration of the design shows a thin material being used with for the sinusoid. Further development was completed, and a standard thickness based on springs was used for a secondary conceptual design.

Development also included replacing the casing for the bearings with an aluminum material and adding a bearing on the opposing end in order to provide support for the spring. A grid was also added to have a visual reference. Figure B - 40 and Figure B - 41 below show the current conceptual design for the sinusoid that will move forward into further analysis and final selection.

Figure B - 40: Sinusoid device with aluminum embed grids and aluminum bearing casing.

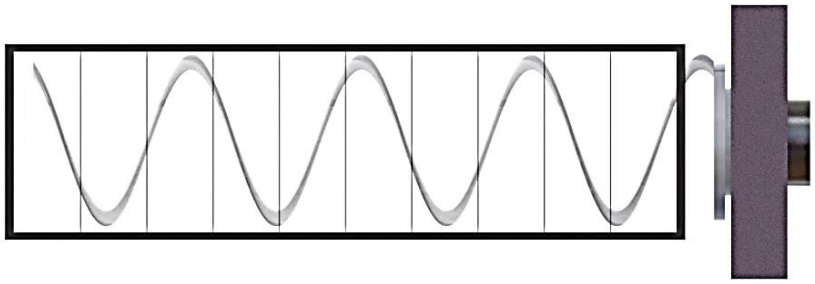

Figure B - 41: Sinusoid device with grid patterns for reference.

## B.7 Motor Selection

The following section outlines the criteria used for motor selection, information about the motors considered, and a scoring of the motors with respect to the selection criteria.

### B.7.1 Selection Criteria

The six criteria considered for the selection are detailed below and tabulated in TABLE B - VI.

1. **Ease of Control** - simplicity of the motor controller and how it interfaces with the motor.
2. **Maintenance** – effort required to maintain the motor's performance, minimize.
3. **Precision** – ability of the motor to maintain constant speed, with the aim to be maximized.
4. **Cost** – measured in $USD, minimize.
5. **Size** – width and diameter dimensions of the motor, minimize.
6. **Weight** – measured in grams, minimize.

TABLE B - VI: MOTOR CRITERIA WEIGHTING

| Design Criteria | | 1 | 2 | 3 | 4 | 5 | 6 |
|---|---|---|---|---|---|---|---|
| **1** | Ease of Control | - | 2 | 3 | 1 | 5 | 1 |
| **2** | Maintenance | | - | 3 | 4 | 5 | 6 |
| **3** | Precision | | | - | 3 | 3 | 3 |
| **4** | Cost | | | | - | 4 | 6 |
| **5** | Size | | | | | - | 5 |
| **6** | Weight | | | | | | - |
| | **Total Hits** | 2 | 1 | 5 | 2 | 3 | 2 |
| | **Weight %** | 13.33% | 6.67% | 33.33% | 13.33% | 20.00% | 13.33% |

## B.7.2 Motor Scoring

Based on types of motor options available, five specific motors were identified online as potential candidates to power the design. TABLE B - VII below outlines the specifications for these motors.

TABLE B - VII: MOTOR OPTIONS SPECIFICATIONS

| Motor Name | Type | Length [mm] | Width x Diameter | Shaft Diameter | Mass [g] | Cost [USD] | Other Information |
|---|---|---|---|---|---|---|---|
| **NEMA 11 Bipolar [5]** | Stepper | 51 | 28x28mm | 6mm | 290 | 32 | 1028 steps |
| **NEMA 6 Bipolar [6]** | Stepper | 30 | 14x14mm | 4mm | 30 | 55 | 200 steps |
| **Micro Gearmotor - 90 RPM (6-12V) [7]** | DC | 26 | 12x10mm | 3mm | 17 | 13 | |
| **Permanent Magnet AC Synchronous LYG35 Geared (LYG35115E04P) [8]** | Synchro-nous | | 35mm | | 260.8 | 108 | |
| **EzRobot Continuous Rotation HDD Servo [9]** | Servo | 20 | 40x35mm | | 40 | 15 | |

Based on the selection criteria outlined above, TABLE B - VIII details the assessment of the five motors considered.

TABLE B - VIII: MOTOR SCORING

| | Motors | | | | |
|---|---|---|---|---|---|
| **Design Criteria** | **NEMA 11 Bipolar** | **NEMA 6 Bipolar** | **Micro Gearmotor 90 RPM** | **Permanent Magnet AC Synchro** | **EzRobot Continuous Rotation HDD Servo** |
| **Ease of Control** | 5 | 5 | 1 | 1 | 5 |
| **Maintenance** | 5 | 5 | 5 | 5 | 5 |
| **Precision** | 5 | 5 | 2 | 4 | 4 |
| **Cost** | 4 | 3 | 5 | 1 | 5 |
| **Size** | 3 | 4 | 5 | 3 | 3 |
| **Weight** | 1 | 4 | 5 | 1 | 4 |
| **Score** | 3.93 | 4.40 | 3.47 | 2.67 | 4.13 |
| **Continue** | No | Yes | No | No | Yes |

# References


[1] Mechanical Gifs, "Radial Engine," Mechanical Gifs, 2019. [Online]. Available: https://mechanicalgifs.com/mechanicalgifs/radial-engine. [Accessed 24 October 2019].

[2] M. Duarte, "Gear," [Online]. Available: https://thenounproject.com/term/gear/7137/. [Accessed 19 October 2019].

[3] P. chain, "ANSI Standard Roller Chain - K - 1 Attachment," [Online]. Available: https://www.peerchain.com/product/ansi-single-strand-chains-with-attachments-k-1/. [Accessed 20 October 2019].

[4] "B&H Photo and Video," [Online]. Available: https://www.bhphotovideo.com/c/product/864575-REG/oben_ac_2361_3_section_aluminum_tripod.html. [Accessed 18 10 2019].

[5] StepperOnline, "11HS20-0674S-PG5 Full Datasheet," [Online]. Available: https://www.omc-stepperonline.com/download/11HS20-0674S-PG5.pdf. [Accessed 4 December 2019].

[6] StepperOnline, "6Hs12-0304S Full Datasheet," [Online]. Available: https://www.omc-stepperonline.com/download/6HS12-0304S.pdf. [Accessed 4 December 2019].

[7] SparkFun, "Micro Gearmotor - 90 RPM (6 - 12V) - ROB-12285," [Online]. Available: https://www.sparkfun.com/products/12285. [Accessed 4 December 2019].

[8] h. motors, "LYG35 35mm Geared Permanent Magnet AC Synchronous Motors," [Online]. Available: http://www.hurst-motors.com/lyg35geared.html. [Accessed 4 December 2019].

[9] RobotShop, "EzRobot Continuous Rotation HDD Servo," [Online]. Available: https://www.robotshop.com/en/ezrobot-continuous-rotation-hdd-servo.html. [Accessed 4 December 2019].

[10] QUALITY CONTROL IN RADIOGRAPHY, " LIMITING SPATIAL RESOLUTION CR AND DR," Weebly, March 2015. [Online]. Available: http://qcinradiography.weebly.com/limiting-spatial-resolution. [Accessed 18 October 2019].

[11] "GrabCad," [Online]. Available: https://grabcad.com/library/simple-mechanism-of-camera-shutter-1. [Accessed 01 10 2019].

# Appendix C – Data Sheets

## Table of Contents

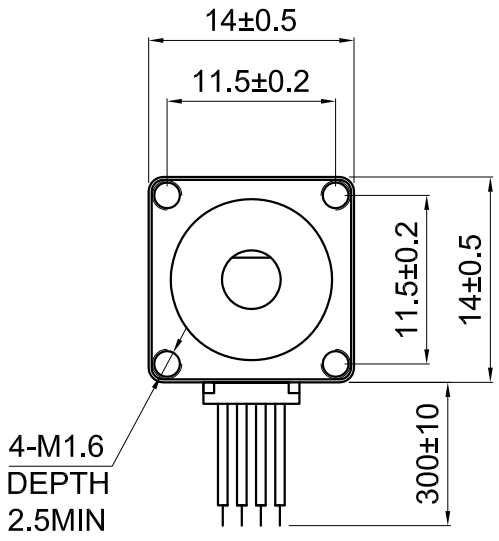


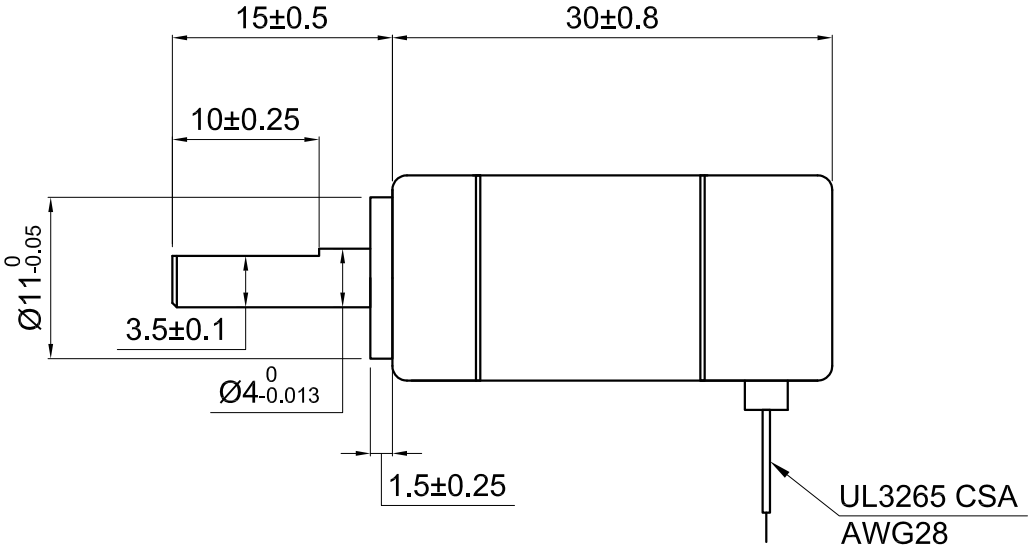


| SPECIFICATION / CONNECTION | BIPOLAR |
|---|---|
| AMPS/PHASE | 0.30 |
| RESISTANCE/PHASE(Ohms)@25°C | 22.00±10% |
| INDUCTANCE/PHASE(mH)@1KHz | 3.40±20% |
| HOLDING TORQUE(Nm)[lb-in] | 0.0058[0.051] |
| STEP ANGLE(°) | 1.80 |
| STEP ACCURACY(NON-ACCUM) | ±5.00% |
| ROTOR INERTIA(g-cm²) | 5.80 |
| WEIGHT(Kg)[lb] | 0.03[0.07] |
| TEMPERATURE RISE:MAX.80°C（MOTOR STANDSTILL;FOR 2PHASE ENERGIZED） | |
| AMBIENT TEMPERATURE -10°C~50°C[14°F~122°F] | |
| INSULATION RESISTANCE 100 Mohm（UNDER NORMAL TEMPERATURE AND HUMIDITY） | |
| INSULATION CLASS B 130°C[266°F] | |
| DIELECTRIC STRENGTH 500VAC FOR 1MIN.(BETWEEN THE MOTOR COILS AND THE MOTOR CASE ) | |
| AMBIENT HUMIDITY MAX.85%(NO CONDENSATION) | |

| TYPE OF CONNECTION (EXTERN) | | MOTOR | |
|---|---|---|---|
| PIN NO | BIPOLAR | LEADS | WINDING |
| 1 | A — | BLK | A |
| 2 | A\ — | GRN | A\ |
| 3 | B — | RED | B |
| 4 | B\ — | BLU | B\ |

FULL STEP 2 PHASE-Ex. ,
WHEN FACING MOUNTING END (X)

| STEP | A | B | A\ | B\ | | |
|---|---|---|---|---|---|---|
| 1 | + | + | - | - | ↓ | CCW |
| 2 | - | + | + | - | | ↑ |
| 3 | - | - | + | + | | |
| 4 | + | - | - | + | CW | |

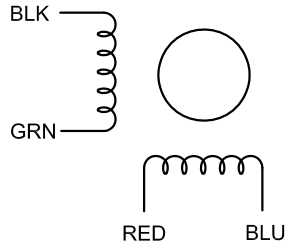


STEPPERONLINE®

| | | | |
|---|---|---|---|
| | APVD | | 4.11.2019 |
| | CHKD | | |
| 2:1 | DRN | | |
| SCALE | SIGNATURE | | DATE |

# STEPPER MOTOR

6HS12-0304S C-2

# Li-ion Power Pack / Charger – 2 Cell (#28986)

The Li-Ion Power Pack-Charger – 2 Cell is an integrated storage cell and charging system on a single 3" x 4" printed circuit board. Compatible with most 18650-size Li-ion cells, the total power output capability of the system is approximately 14–20 watt/hours, depending on the capacity of cells you choose. Although this Power-Pack/Charger is compatible with both protected and unprotected Li-ion 18650 cells, Parallax highly recommends using the protected types, such as Parallax part #28987.

## Features

- PCB-mounted cell holders with on-board charging circuitry
- Multiple power input/output options
- On-board output fuse protection
- Nominal 7.4 VDC output; 8.2 VDC maximum
- Standard 3" x 4" PCB footprint integrates well with the Board of Education® (#28150), Propeller™ Proto Board (#32212), or any application needing a reliable power supply with an integrated charging system
- Automatic charge/discharge switching circuitry
- Holds two rechargeable 3.7 volt Li-ion 18650-size cells
- Multiple LED indicators provide charge readiness information for each individual cell; a status key for the LED indicators is printed on the board.
- Aggressive holders retain cells in any board orientation and in moderate shock environments, such as mobile robotic applications. Cells are not permanent, and can be replaced.
- Dedicated circuitry continuously monitors the charging process to ensure safety, efficiency, and to maximize the number of charge/discharge cycles of each cell.

## Key Specifications

- Charging Power Requirements: +5–12 VDC @ 1amp (min.); 2.1 mm barrel jack, center positive supply (#750-00009 works well)
- Power Output: Unregulated nominal 7.4 VDC @ 1800—2600 mAh (depending on cells used)
- Dimensions: 3.0 x 4.0 x 1.0 in; 7.6 x 10.2 x 2.54 cm
- Charging Time: 1 – 6 hrs or more, depending upon the discharge level and capacity of the cells

## Application Ideas

- Portable power for data-logging applications
- Mobile robots
- Standby power / automatic power-switching
- Automatic charging circuits
- Stackable auxiliary power solutions
- Boe-Bot® / Board of Education / Propeller Proto Board Auxiliary Power Supplies
- Stingray™ Robot (#28980) battery pack upgrade

## Packing List

- (1) Li-ion Power-Pack / Charger – 2 Cell PCB, 3" x 4"
- (1) Li-ion Battery Cable (#802-00020)
- (2) 2-amp fuses; 1 pre-installed, 1 spare (#452-00065)
- (4) Black dome rubber feet (#700-00087)
- (4) Clear square rubber feet (#700-00037)

## Additional Items Required

- (2) Li-ion 18650-size cells (#28987 or equivalent)
- +5 to +12 VDC power supply, center positive, 2.1 mm barrel jack (#750-00009 or equiv.)
- Safety glasses
- Multi-meter (VOM)

## Assembly Instructions

**CAUTION: Before inserting the cells into the holder, two sets of rubber feet must be applied to the correct places on the bottom of the PCB, following the steps below.** Aside from applying the rubber feet and installing the cells into the holders, the PCB itself comes fully assembled and tested.

Lithium cells come pre-charged (to some extent), so treat them carefully—they already contain a significant amount of energy. Handle with care and do not short the terminals!

Step 1: Turn the PCB over so that it's oriented as shown in Figure 1 below.

**Figure 1**

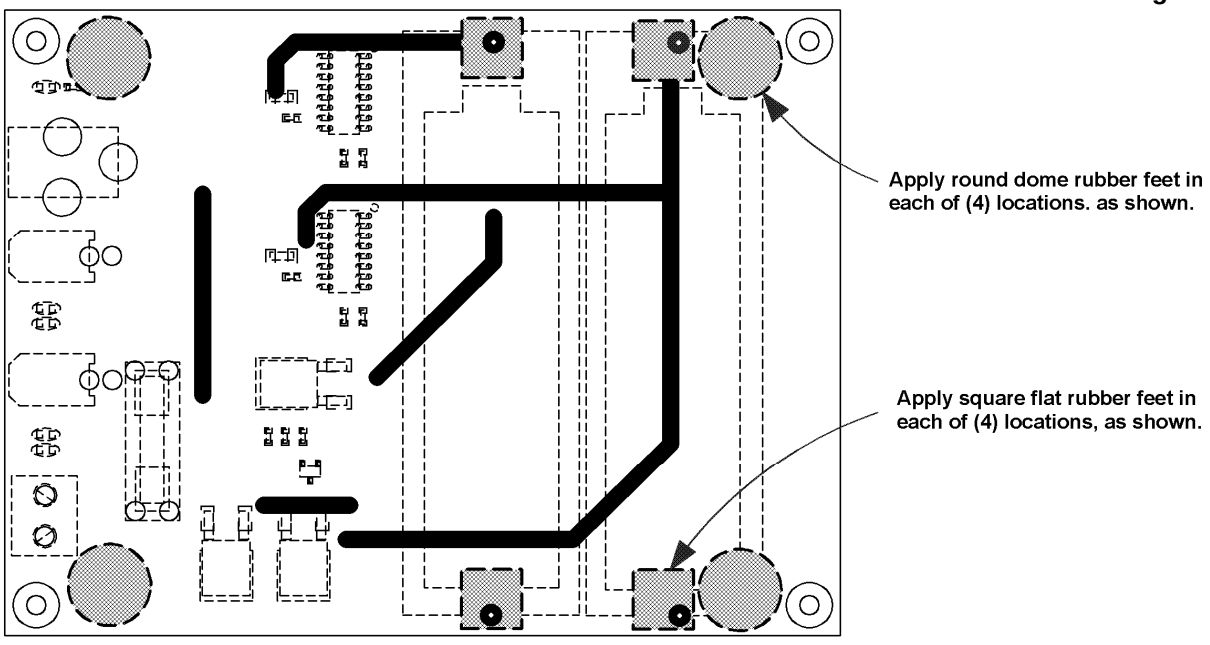


(Li-ion Power-Pack / Charger PCB) - Bottom View

Step 2: Place a clear flat rubber foot over each of the (4) soldered cell terminals as shown in Figure 1. These feet protect the cell holder terminals from being accidentally shorted. Remember: Li-ion cells have a lot of stored energy and rapid discharge can result in an unsafe condition. Even though the output of the board is fuse protected, direct shorting of these solder points is not within the fused portion of the circuit.

Step 3: Place a black domed rubber foot in each of the four locations designated by the dashed circles on the silk screen. These provide stability for the board if you set it on a flat surface. If you will be mounting this device on standoffs where the board traces cannot be shorted, then you can skip this step.

**Figure 2**

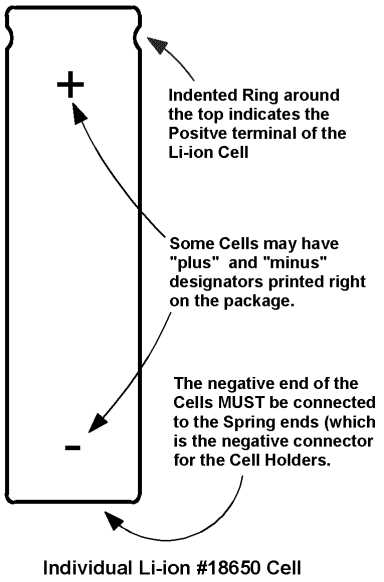

Individual Li-ion #18650 Cell

Step 4: Carefully remove the cells from their packaging. Note the positive cell polarity. Various brands of cells are marked differently. The positive terminal may be indicated by a ringed indentation near one end of the cell, or the packaging may be printed with "+" and/or "-" designators (as shown in Figure 2).

Step 5: Using a multi-meter (VOM), measure the voltage of each cell. Write down the sum total of the two voltages. If either cell measures less than 3 volts, it may be defective.

Step 6: Turn the board right-side up as shown in Figure 3.

Step 7: Carefully place the bottom (negative) end of a cell against the spring in Cell Holder "A", and then gently slide it down and in at a slight angle into the holder until it snaps into place. Repeat for Cell Holder "B."

Note: Cells without internal PCB's will snap into the holders easily.

Higher quality cells (those that have internal PCB protection such as Parallax #28987), are slightly longer. They will fit into the holder, but they are a very tight fit. The holder's ends will flex a bit as you insert the cell. Sight along the sides of the cells to make sure that they are completely seated into the cell holders.

**CAUTION: Removing the cells once they have been inserted into the holders is NOT recommended.** The holders are tight by design, and so the cells do not come out easily. Be aware that the body of a Li-ion cell is usually covered by a thin plastic wrapper that can be easily pierced. Furthermore, the negative terminal of a Li-Ion cell actually encompasses the entire body of the cell, to right up near the top of the Positive terminal of the cell itself. Attempting to pry a cell out of a holder with a sharp-edged screwdriver blade could pierce the cell's wrapper and short out the cell, damaging it.

However, if you ever do need to remove the cell, (i.e. when the cells wear out), a dull-edged, non-conducting prying tool, such as a chip-puller, is recommended. If such a tool isn't available, you can use a small, flat-bladed screwdriver covered in heat-shrink tubing or electrical tape. A small pair of needle-nose pliers (also covered in insulated material) works well too.

## Initial Testing

Step 8: Measure the voltage by placing your VOM's probes on the top two screw terminals on the green Cell Power Output terminal block. You should measure the same voltage as the sum of the two cells you measured in Step 5 (above).

Step 9: Plug the Battery Cable into the Cell Power Output jack (See Figure 3). Now measure the output voltage by inserting the positive VOM probe into the inside of the barrel plug on the end of the adapter cable, and touching the negative VOM probe to the outside ring of the barrel plug. Again, you should measure very close to the same voltage as the sum of the two cells you measured in Step 5 (above).

Step 10: Connect a “center positive” 2.1mm wall transformer (such as Parallax #750-00009) to the Charging Power Input jack as noted in Figure 3. The power supply should have a voltage output between +5 VDC and +12 VDC. The amount of current necessary to charge the cells is controlled automatically by the circuitry; however your wall transformer should be rated at 1 amp or more to minimize charging time. If the charging current supply is too low, the charging circuits may not operate. In addition, a lower current will not harm the cells; they'll just take longer to charge.

Step 11: Upon application of charging power, the green LED (next to the barrel jack) will turn on. After a few moments, the blue status indicator LEDs should come on. Solid blue means that the cells are being charged.

**Figure 3**

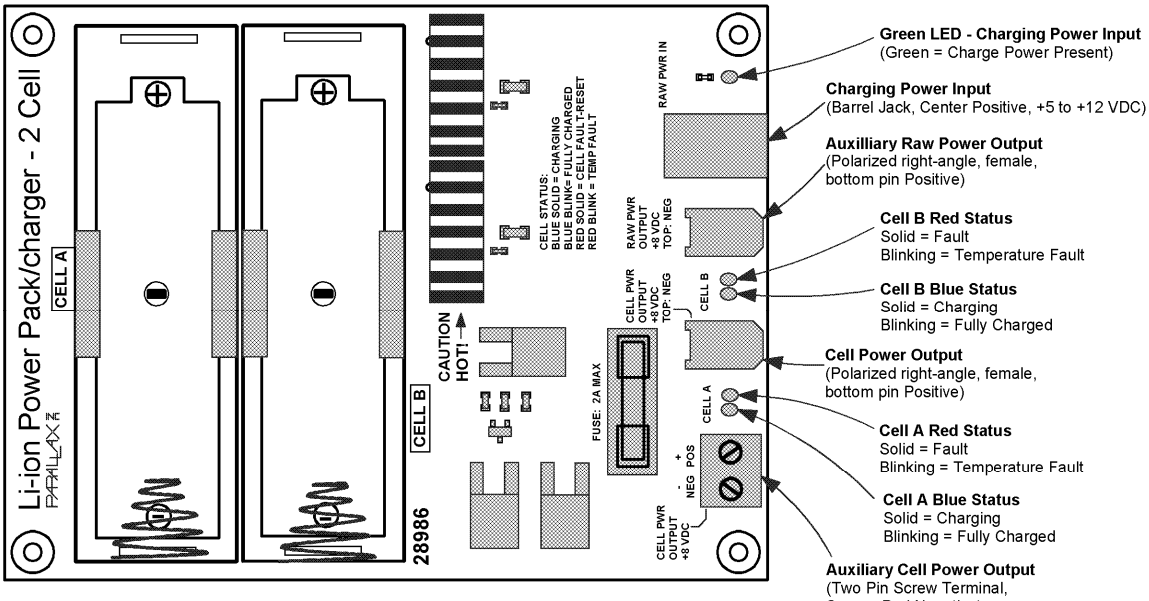


(Li-ion Power/Pack - Chager 2-cell PCB - TOP View)

## Circuit Description and Operation

**CAUTION: Due to the nature of the charging circuitry and the size and very high capacity of the cells, the heat-sinks near the cell holders may get hot!** The amount of heat generated depends on the length of charging time, the amount of charge on each of the cells, and the voltage input of the charging power source. For example, a 12 VDC transformer and/or completely drained cells will generate more heat than a 7.5 VDC charge input or near-fully charged cells.

With cells installed in their respective holders, and with no external connections to the input/output jacks, the circuitry is inactive and there is no current flow (other than some very, very small leakage current through the inactive charging circuits).

Upon application of +5 to +12 VDC to the Charging Power Input jack (J1), the following happens:

a) The Charging Power Input (Green LED) is activated.
b) The Auxiliary Raw Power Output has power that is directly from the charging source (wall transformer, solar panel, car battery, etc.). This power can be used to operate another circuit or application using the (included) Battery Cable.
c) Each cell is electrically disconnected and isolated from the other.
d) The Cell Power Output jacks are disconnected from the cells, and disabled.
e) The dual charging circuits begin a qualification mode to determine each cell's characteristics.
f) After checking the cells, LED status indicators are activated. If required, each cell begins charging their respective cells.

When Charging Power is removed, it results in the following:

a) The Auxiliary Raw Power Output jack is disabled.
b) Cell charging circuits are disabled and Status indicator LEDs are disabled.
c) The cells are electrically connected into a series configuration.
d) Cell Power Output jacks connect to the cells, resulting in a 7.4 to 8.2 VDC output.

## Jack/Plug/Indicators Functional Descriptions

**Green LED**: Charge Power Indicator—whenever charging power is applied to the Charging Power Input barrel jack, the board is receiving power.

**Charge Power Input**: 2.1mm barrel jack, center positive. +5 to +12 VDC input. Do not reverse the input voltage as this may damage the charging circuitry. Charging time is dependent on the amperage available from the power supply you choose, as well as the capacity of the cells you choose.

**Aux. Raw Power Output**: Polarized, right angle, female, bottom pin positive. This connection can be used to power another device. For example, you can charge the Li-ion cells and operate another device from the same power supply. When you plug in wall-transformer (to charge the Li-ion cells), you can use the Molex/barrel jack cable to provide power to another device (such as a Board of Education, Propeller Proto Board, etc.) This is not power from the cells. This is the same power that is charging the cells, via your charging supply input on the Charge Power Input barrel jack.

**Cell B Red Status**: This LED indicates a fault condition in Cell B.

- Solid = There is/was a fault in the cell, or there was a glitch during the charging process. Remove and then re-apply power to the board, to see if the condition persists.
- Blinking = The temperature of the cell is outside the safe charging zone. The safe charging zone is typically set for between 32 and 113 °F (0 to 45 °C).
- Off = There is no fault condition detected with Cell B, or there is no cell in the holder.

**Cell B Blue Status:** This LED indicates the charging status of Cell B.

- Solid = The cell is charging.
- Blinking = The cell is fully charged.
- Off = The cell was already fully charged and no charging was needed, there is no cell in the holder, or the cell is not fully-seated into the holder.

**Cell Power Output:** Polarized, right angle, female, bottom pin positive.
This Power Output jack is the output from the cells.

When there is no Charge Power Input (i.e. When the wall charger is disconnected from the PCB), the two 3.7 volt cells are electrically connected together in a series configuration, and the resulting power (3.7 VDC x 2 cells = 7.4 VDC) is available at this jack.

Upon application of Charge Power, Cell Power Output is disconnected from the on-board cells, and this jack is disabled.

**Cell A Red Status:** This LED indicates a fault condition in Cell A.

- Solid = There is/was a fault in the cell, or there was a glitch during the charging process. Remove and then re-apply power to the board, to see if the condition persists.
- Blinking = The temperature of the cell is outside the safe charging zone. The safe charging zone is typically set for between 32 and 113 °F (0 to 45 °C).
- Off = There is no fault condition detected with Cell A, or there is no cell in the holder.

**Cell A Blue Status:** This LED indicates the charging status of Cell A.

- Solid = The cell is charging.
- Blinking = The cell is fully charged.
- Off = The cell was already fully charged and no charging was needed, there is no cell in the holder, or the cell is not fully-seated into the holder.

**Auxiliary Cell Power Output:** Two-pin Screw Terminal Block, Square Pad Negative. This connection simply provides an alternative way to connect your application to the Cell Power Output. (No need to use the polarized cable). Be careful to check the polarity of your circuit, as this is not a polarized connector.

## Application Ideas and Sample Circuits

The following circuits represent some different combinations of charging and power delivery options. Figure 4 is an application that will simultaneously charge the cells, as well as provide Raw (wall-transformer) power to a separate application, such as a Board of Education, Propeller Proto Board, etc.

**Figure 4**

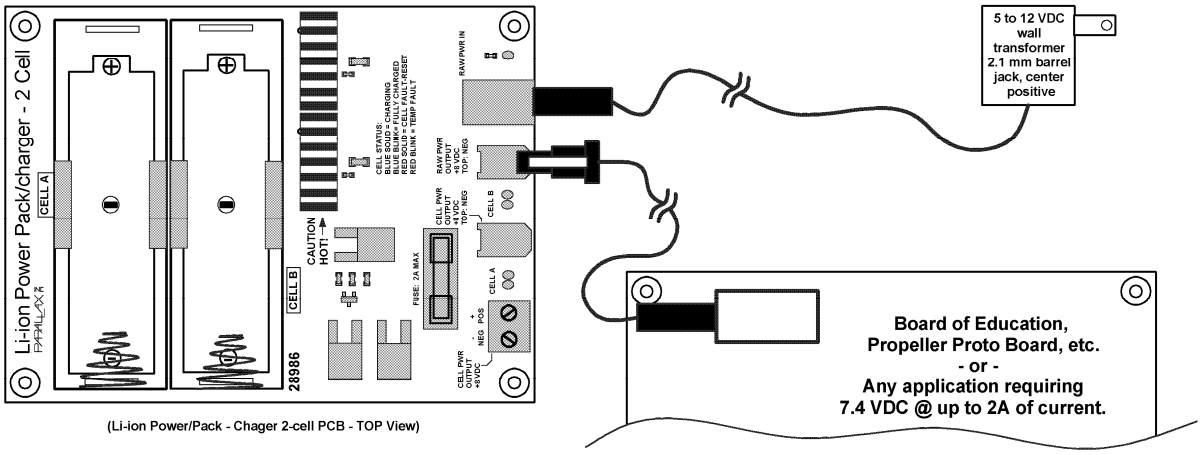


(Li-ion Power/Pack - Chager 2-cell PCB - TOP View)

Figure 5 is delivering cell power to an application and the cells are not being charged. This would be a common circuit in the case of a mobile robotics application.

**Figure 5**

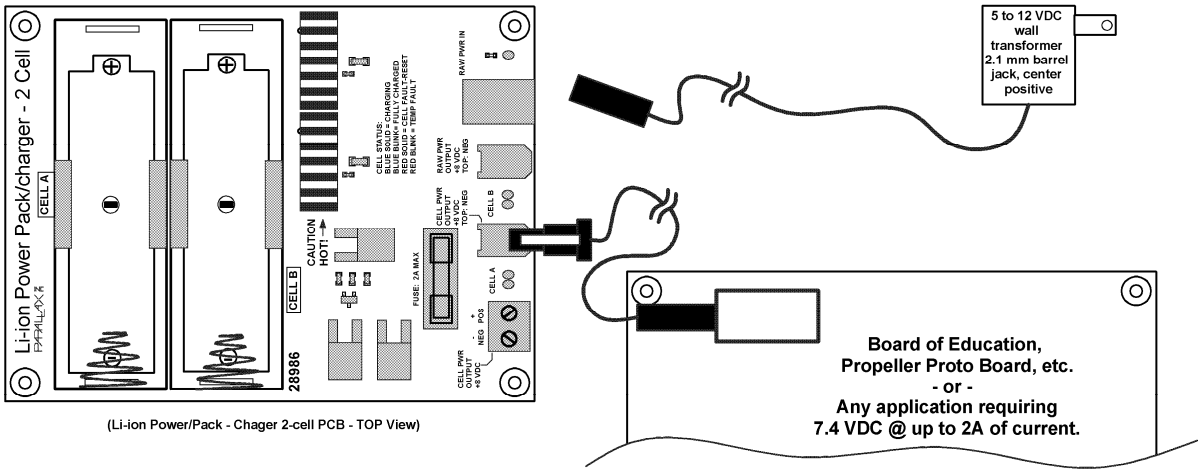


(Li-ion Power/Pack - Chager 2-cell PCB - TOP View)

Figure 6 is also delivering cell power, but through the two screw terminals instead of the polarized connector. Cell power is simultaneously available on the polarized connector as well.

**Figure 6**

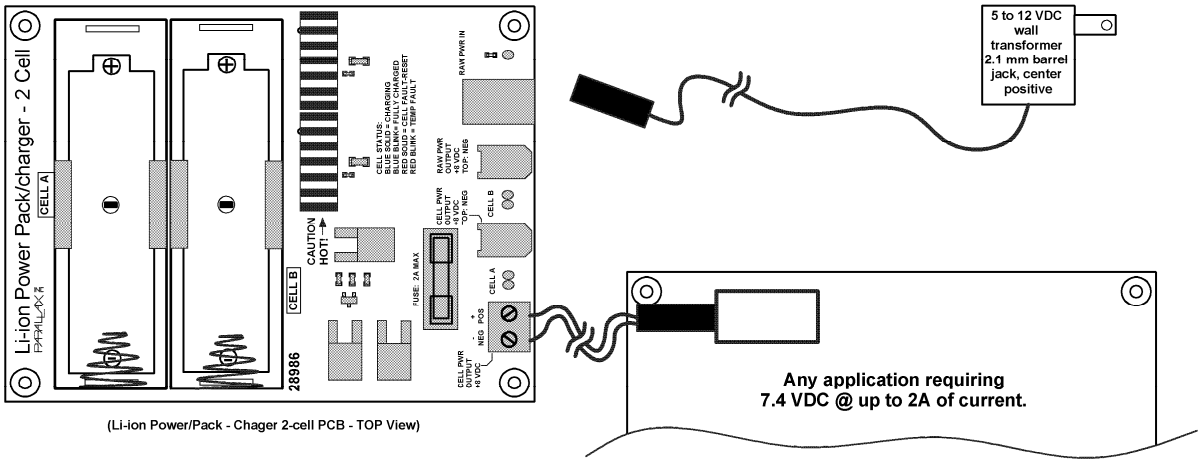


The circuit in Figure 7 operates as an uninterruptable power supply. All that is needed is the addition of a couple of diodes and an appropriately sized capacitor. When charging power is available, the cells are taken out of the circuit and they are being charged. That same charging input power is available through the Raw Power Output jack to power an application.

**Figure 7**

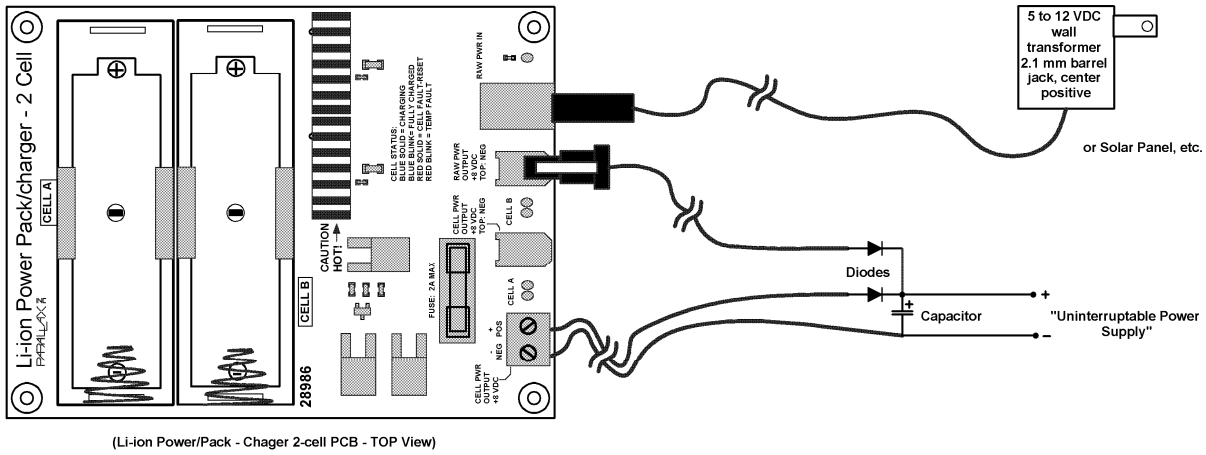


When the Charging Input Power is no longer available (for example, a solar panel at night), the Cell Power Output jack is activated. There will be a switch-over period, so be sure to use a capacitor large enough to span that time.

To minimize the diode's voltage drop, you could use a device like the STPS40L15CT which is designed especially for applications like this.

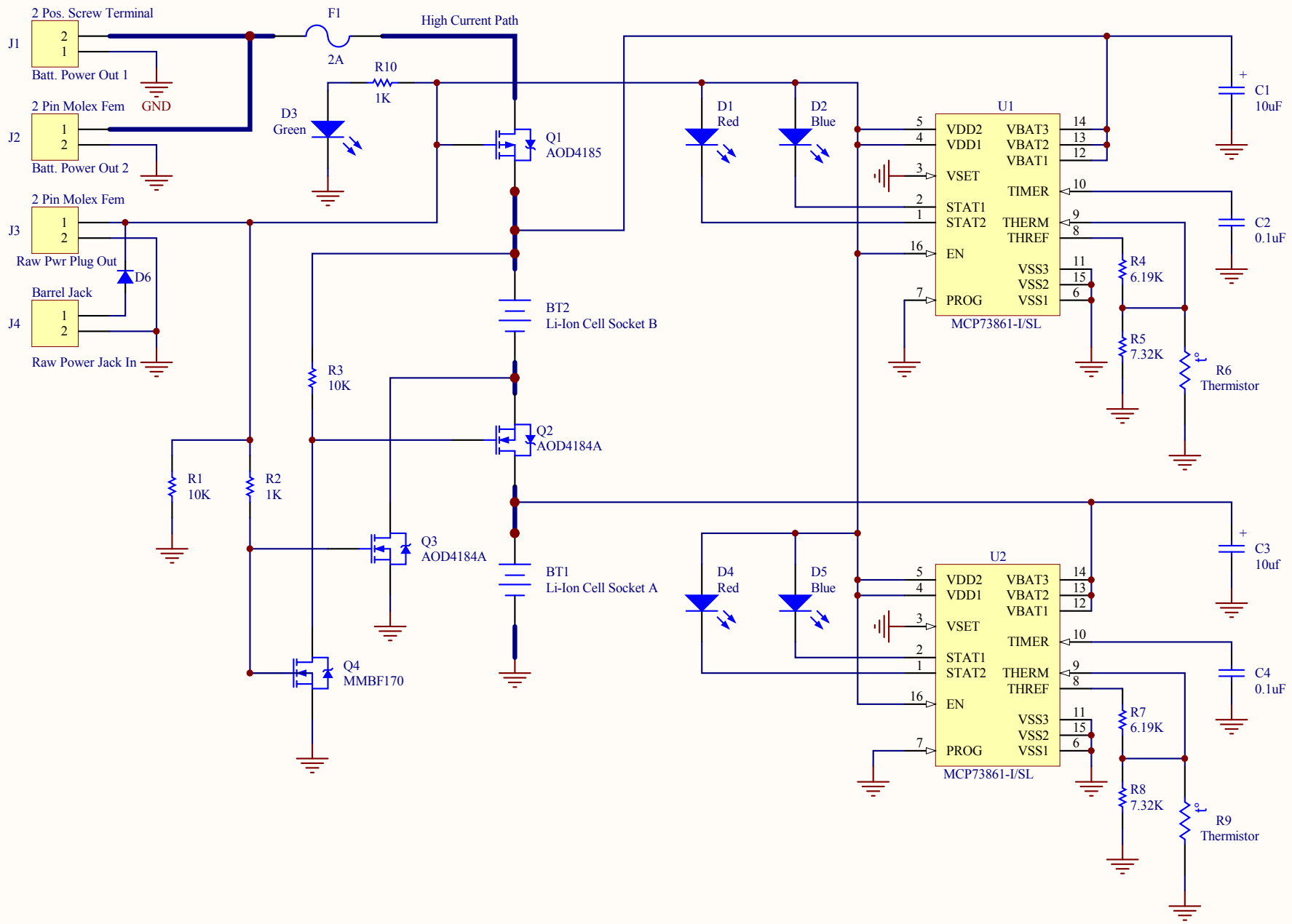


| | | |
|---|---|---|
| Title | Li-ion Power Pack/Charger-2 Cell | |
| Size: A | Number: 28986 | Revision: A |
| Date: 5/2/2011 | Sheet of | |
| File: F:\Altium Projects\..\Li-ion Power Pack-Charger-2 Cell_A.SchDoc | Drawn By: | |

# *Microstepping Driver with Translator*

## Features and Benefits

- ±750 mA, 30 V output rating
- Satlington® sink drivers
- Automatic current-decay mode detection/selection
- 3.0 to 5.5 V logic supply voltage range
- Mixed, fast, and slow current-decay modes
- Internal UVLO and thermal shutdown circuitry
- Crossover-current protection

## Package: 24-pin SOIC with internally fused pins (suffix LB)

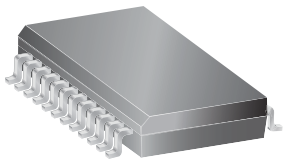

*Not to scale*

## Description

The A3967 is a complete microstepping motor driver with built-in translator. It is designed to operate bipolar stepper motors in full-, half-, quarter-, and eighth-step modes, with output drive capability of 30 V and ±750 mA. The A3967 includes a fixed off-time current regulator that has the ability to operate in slow, fast, or mixed current-decay modes. This current-decay control scheme results in reduced audible motor noise, increased step accuracy, and reduced power dissipation.

The translator is the key to the easy implementation of the A3967. By simply inputting one pulse on the STEP input the motor will take one step (full, half, quarter, or eighth depending on two logic inputs). There are no phase-sequence tables, high-frequency control lines, or complex interfaces to program. The A3967 interface is an ideal fit for applications where a complex µP is unavailable or over-burdened.

Internal circuit protection includes thermal shutdown with hysteresis, under-voltage lockout (UVLO) and crossover-current protection. Special power-up sequencing is not required.

The A3967 is supplied in a 24-pin SOIC, which is lead (Pb) free with 100% matte tin leadframe plating. Four pins are fused internally for enhanced thermal dissipation. The pins are at ground potential and need no insulation.

## Functional Block Diagram

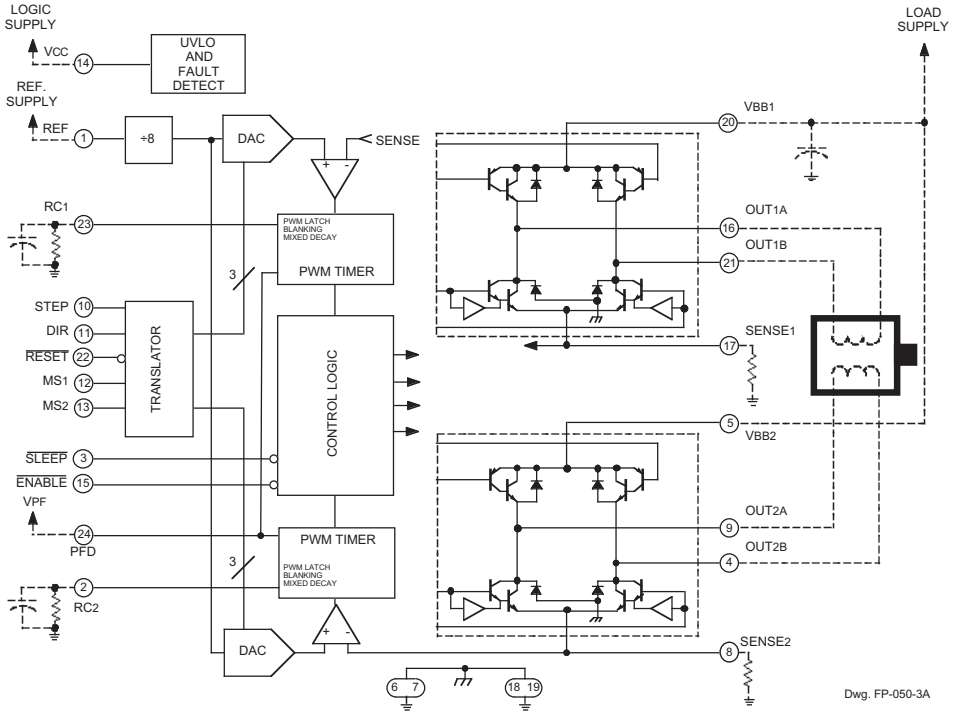

## Selection Guide

| Part Number | Packing | Package |
|---|---|---|
| A3967SLBTR-T | 24-pin SOIC with internally fused pins | 1000 per reel |

## Absolute Maximum Ratings

| Characteristic | Symbol | Notes | | Rating | Units |
|---|---|---|---|---|---|
| Load Supply Voltage | $V_{BB}$ | | | 30 | V |
| Logic Supply Voltage | $V_{CC}$ | | | 7.0 | V |
| Logic Input Voltage Range | $V_{IN}$ | $t_w$ > 30 ns | | –0.3 to 7.0 | V |
| | | $t_w$ < 30 ns | | –1 to 7.0 | V |
| Sense Voltage | $V_{SENSE}$ | | | 0.68 | V |
| Reference Voltage | $V_{REF}$ | | | $V_{CC}$ | mA |
| Output Current | $I_{OUT}$ | Output current rating may be limited by duty cycle, ambient temperature, and heat sinking. Under any set of conditions, do not exceed the specified current rating or a junction temperature of 150°C. | Continuous | ±750 | mA |
| | | | Peak | ±850 | mA |
| Package Power Dissipation | $P_D$ | See graph | | – | – |
| Operating Ambient Temperature | $T_A$ | Range S | | –20 to 85 | °C |
| Maximum Junction Temperature | $T_J$(max) | Fault conditions that produce excessive junction temperature will activate the device's thermal shutdown circuitry. These conditions can be tolerated but should be avoided. | | 150 | °C |
| Storage Temperature | $T_{stg}$ | | | –55 to 150 | °C |

## Thermal Characteristics

| Characteristic | Symbol | Test Conditions* | Value | Units |
|---|---|---|---|---|
| Package Thermal Resistance, Junction to Ambient | $R_{\theta JA}$ | 2-layer PCB, 1.3 in² 2-oz. exposed copper | 50 | °C/W |
| | | 4-layer PCB, based on JEDEC standard | 35 | °C/W |

*Additional thermal information available on Allegro website.

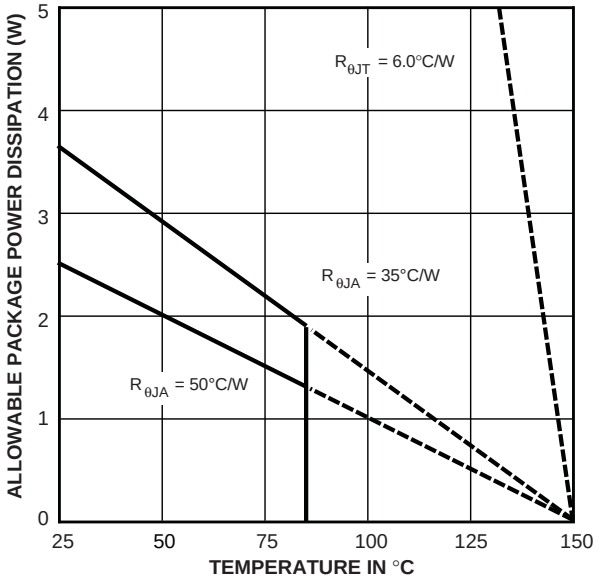

**ELECTRICAL CHARACTERISTICS at $T_A$ = +25°C, $V_{BB}$ = 30 V, $V_{CC}$ = 3.0 V to 5.5V (unless otherwise noted)**

| Characteristic | Symbol | Test Conditions | Limits | | | |
|---|---|---|---|---|---|---|
| | | | Min. | Typ. | Max. | Units |
| **Output Drivers** | | | | | | |
| Load Supply Voltage Range | $V_{BB}$ | Operating | 4.75 | – | 30 | V |
| | | During sleep mode | 0 | – | 30 | V |
| Output Leakage Current | $I_{CEX}$ | $V_{OUT}$ = $V_{BB}$ | – | <1.0 | 20 | µA |
| | | $V_{OUT}$ = 0 V | – | <-1.0 | -20 | µA |
| Output Saturation Voltage | $V_{CE(sat)}$ | Source driver, $I_{OUT}$ = -750 mA | – | 1.9 | 2.1 | V |
| | | Source driver, $I_{OUT}$ = -400 mA | – | 1.7 | 2.0 | V |
| | | Sink driver, $I_{OUT}$ = 750 mA | – | 0.65 | 1.3 | V |
| | | Sink driver, $I_{OUT}$ = 400 mA | – | 0.21 | 0.5 | V |
| Clamp Diode Forward Voltage | $V_F$ | $I_F$ = 750 mA | – | 1.4 | 1.6 | V |
| | | $I_F$ = 400 mA | – | 1.1 | 1.4 | V |
| Motor Supply Current | $I_{BB}$ | Outputs enabled | – | – | 5.0 | mA |
| | | RESET high | – | – | 200 | µA |
| | | Sleep mode | – | – | 20 | µA |
| **Control Logic** | | | | | | |
| Logic Supply Voltage Range | $V_{CC}$ | Operating | 3.0 | 5.0 | 5.5 | V |
| Logic Input Voltage | $V_{IN(1)}$ | | 0.7$V_{CC}$ | – | – | V |
| | $V_{IN(0)}$ | | – | – | 0.3$V_{CC}$ | V |
| Logic Input Current | $I_{IN(1)}$ | $V_{IN}$ = 0.7$V_{CC}$ | -20 | <1.0 | 20 | µA |
| | $I_{IN(0)}$ | $V_{IN}$ = 0.3$V_{CC}$ | -20 | <1.0 | 20 | µA |
| Maximum STEP Frequency | $f_{STEP}$ | | 500* | – | – | kHz |
| Blank Time | $t_{BLANK}$ | $R_t$ = 56 kΩ, $C_t$ = 680 pF | 700 | 950 | 1200 | ns |
| Fixed Off Time | $t_{off}$ | $R_t$ = 56 kΩ, $C_t$ = 680 pF | 30 | 38 | 46 | µs |

continued next page …

**Table 1. Microstep Resolution Truth Table**

| MS1 | MS2 | Resolution |
|---|---|---|
| L | L | Full step (2 phase) |
| H | L | Half step |
| L | H | Quarter step |
| H | H | Eighth step |

**ELECTRICAL CHARACTERISTICS (continued) at $T_A$ = +25°C, $V_{BB}$ = 30 V, $V_{CC}$ = 3.0 V to 5.5V (unless otherwise noted)**

| Characteristic | Symbol | Test Conditions | Limits | | | |
|---|---|---|---|---|---|---|
| | | | Min. | Typ. | Max. | Units |
| **Control Logic (cont'd)** | | | | | | |
| Mixed Decay Trip Point | PFDH | | – | $0.6V_{CC}$ | – | V |
| | PFDL | | – | $0.21V_{CC}$ | – | V |
| Ref. Input Voltage Range | $V_{REF}$ | Operating | 1.0 | – | $V_{CC}$ | V |
| Reference Input Impedance | $Z_{REF}$ | | 120 | 160 | 200 | kΩ |
| Gain ($G_m$) Error (note 3) | $E_G$ | $V_{REF}$ = 2 V, Phase Current = 38.37% † | – | – | ±10 | % |
| | | $V_{REF}$ = 2 V, Phase Current = 70.71% † | – | – | ±5.0 | % |
| | | $V_{REF}$ = 2 V, Phase Current = 100.00% † | – | – | ±5.0 | % |
| Thermal Shutdown Temp. | $T_J$ | | – | 165 | – | °C |
| Thermal Shutdown Hysteresis | $\Delta T_J$ | | – | 15 | – | °C |
| UVLO Enable Threshold | $V_{UVLO}$ | Increasing $V_{CC}$ | 2.45 | 2.7 | 2.95 | V |
| UVLO Hysteresis | $\Delta V_{UVLO}$ | | 0.05 | 0.10 | – | V |
| Logic Supply Current | $I_{CC}$ | Outputs enabled | – | 50 | 65 | mA |
| | | Outputs off | – | – | 9.0 | mA |
| | | Sleep mode | – | – | 20 | µA |

* Operation at a step frequency greater than the specified minimum value is possible but not warranteed.
† 8 microstep/step operation.

NOTES: 1. Typical Data is for design information only.
2. Negative current is defined as coming out of (sourcing) the specified device terminal.
3. $E_G = ([V_{REF}/8] – V_{SENSE})/(V_{REF}/8)$

## Functional Description

**Device Operation.** The A3967 is a complete microstepping motor driver with built in translator for easy operation with minimal control lines. It is designed to operate bipolar stepper motors in full-, half-, quarter- and eighth-step modes. The current in each of the two output full bridges is regulated with fixed off time pulse-width modulated (PWM) control circuitry. The full-bridge current at each step is set by the value of an external current sense resistor ($R_S$), a reference voltage ($V_{REF}$), and the DACs output voltage controlled by the output of the translator.

At power up, or reset, the translator sets the DACs and phase current polarity to initial home state (see figures for home-state conditions), and sets the current regulator for both phases to mixed-decay mode. When a step command signal occurs on the STEP input the translator automatically sequences the DACs to the next level (see table 2 for the current level sequence and current polarity). The microstep resolution is set by inputs $MS_1$ and $MS_2$ as shown in table 1. If the new DAC output level is lower than the previous level the decay mode for that full bridge will be set by the PFD input (fast, slow or mixed decay). If the new DAC level is higher or equal to the previous level then the decay mode for that Full bridge will be slow decay. This automatic current-decay selection will improve microstepping performance by reducing the distortion of the current waveform due to the motor BEMF.

**Reset Input ($\overline{\text{RESET}}$).** The RESET input (active low) sets the translator to a predefined home state (see figures for home state conditions) and turns off all of the outputs. STEP inputs are ignored until the RESET input goes high.

**Step Input (STEP).** A low-to-high transition on the STEP input sequences the translator and advances the motor one increment. The translator controls the input to the DACs and the direction of current flow in each winding. The size of the increment is determined by the state of inputs $MS_1$ and $MS_2$ (see table 1).

**Microstep Select ($MS_1$ and $MS_2$).** Input terminals MS1 and $MS_2$ select the microstepping format per table 1. Changes to these inputs do not take effect until the STEP command (see figure).

**Direction Input (DIR).** The state of the DIRECTION input will determine the direction of rotation of the motor.

**Internal PWM Current Control.** Each full bridge is controlled by a fixed off-time PWM current-control circuit that limits the load current to a desired value ($I_{TRIP}$). Initially, a diagonal pair of source and sink outputs are enabled and current flows through the motor winding and $R_S$. When the voltage across the current-sense resistor equals the DAC output voltage, the current-sense comparator resets the PWM latch, which turns off the source driver (slow-decay mode) or the sink and source drivers (fast- or mixed-decay modes).

The maximum value of current limiting is set by the selection of $R_S$ and the voltage at the $V_{REF}$ input with a transconductance function approximated by:

$$I_{TRIP}max = V_{REF}/8R_S$$

The DAC output reduces the $V_{REF}$ output to the current-sense comparator in precise steps (see table 2 for % $I_{TRIP}$max at each step).

$$I_{TRIP} = (\%\ I_{TRIP}max/100) \times I_{TRIP}max$$

**Fixed Off-Time.** The internal PWM current-control circuitry uses a one shot to control the time the driver(s) remain(s) off. The one shot off-time, $t_{off}$, is determined by the selection of an external resistor ($R_T$) and capacitor ($C_T$) connected from the RC timing terminal to ground. The off time, over a range of values of $C_T$ = 470 pF to 1500 pF and $R_T$ = 12 kΩ to 100 kΩ is approximated by:

$$t_{off} = R_T C_T$$

## Functional Description (cont'd)

**RC Blanking.** In addition to the fixed off-time of the PWM control circuit, the $C_T$ component sets the comparator blanking time. This function blanks the output of the current-sense comparator when the outputs are switched by the internal current-control circuitry. The comparator output is blanked to prevent false overcurrent detection due to reverse recovery currents of the clamp diodes, and/or switching transients related to the capacitance of the load. The blank time $t_{BLANK}$ can be approximated by:

$$t_{BLANK} = 1400C_T$$

**Enable Input ($\overline{\text{ENABLE}}$).** This active-low input enables all of the outputs. When logic high the outputs are disabled. Inputs to the translator (STEP, DIRECTION, $MS_1$, $MS_2$) are all active independent of the ENABLE input state.

**Shutdown.** In the event of a fault (excessive junction temperature) the outputs of the device are disabled until the fault condition is removed. At power up, and in the event of low $V_{CC}$, the under-voltage lockout (UVLO) circuit disables the drivers and resets the translator to the home state.

**Sleep Mode ($\overline{\text{SLEEP}}$).** An active-low control input used to minimize power consumption when not in use. This disables much of the internal circuitry including the outputs. A logic high allows normal operation and startup of the device in the home position.

**Percent Fast Decay Input (PFD).** When a STEP input signal commands a lower output current from the previous step, it switches the output current decay to either slow-, fast-, or mixed-decay depending on the voltage level at the PFD input. If the voltage at the PFD input is greater than $0.6V_{CC}$ then slow-decay mode is selected. If the voltage on the PFD input is less than $0.21V_{CC}$ then fast-decay mode is selected. Mixed decay is between these two levels.

**Mixed Decay Operation.** If the voltage on the PFD input is between $0.6V_{CC}$ and $0.21V_{CC}$, the bridge will operate in mixed-decay mode depending on the step sequence (see figures). As the trip point is reached, the device will go into fast-decay mode until the voltage on the RC terminal decays to the voltage applied to the PFD terminal. The time that the device operates in fast decay is approximated by:

$$t_{FD} = R_T C_T \ln (0.6V_{CC}/V_{PFD})$$

After this fast decay portion, $t_{FD}$, the device will switch to slow-decay mode for the remainder of the fixed off-time period.

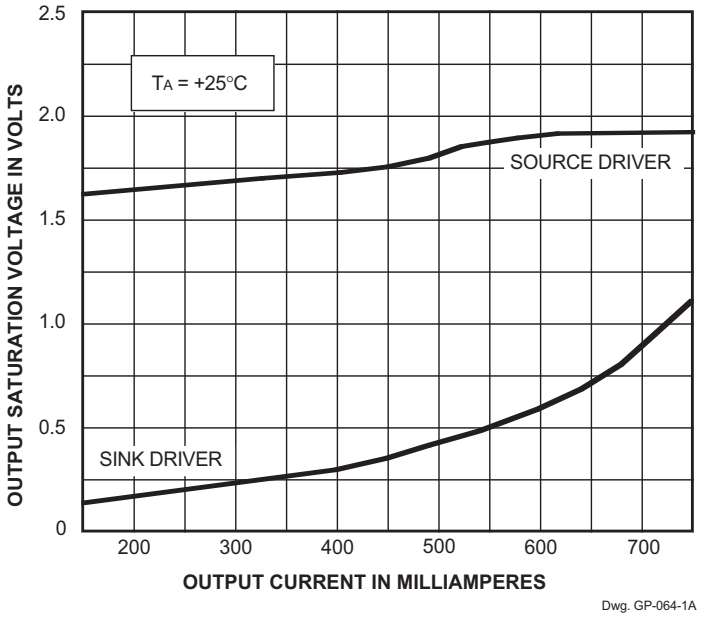


**Typical output saturation voltages showing Satlington sink-driver operation.**

**Timing Requirements**
($T_A$ = +25°C, $V_{CC}$ = 5 V, Logic Levels are $V_{CC}$ and Ground)

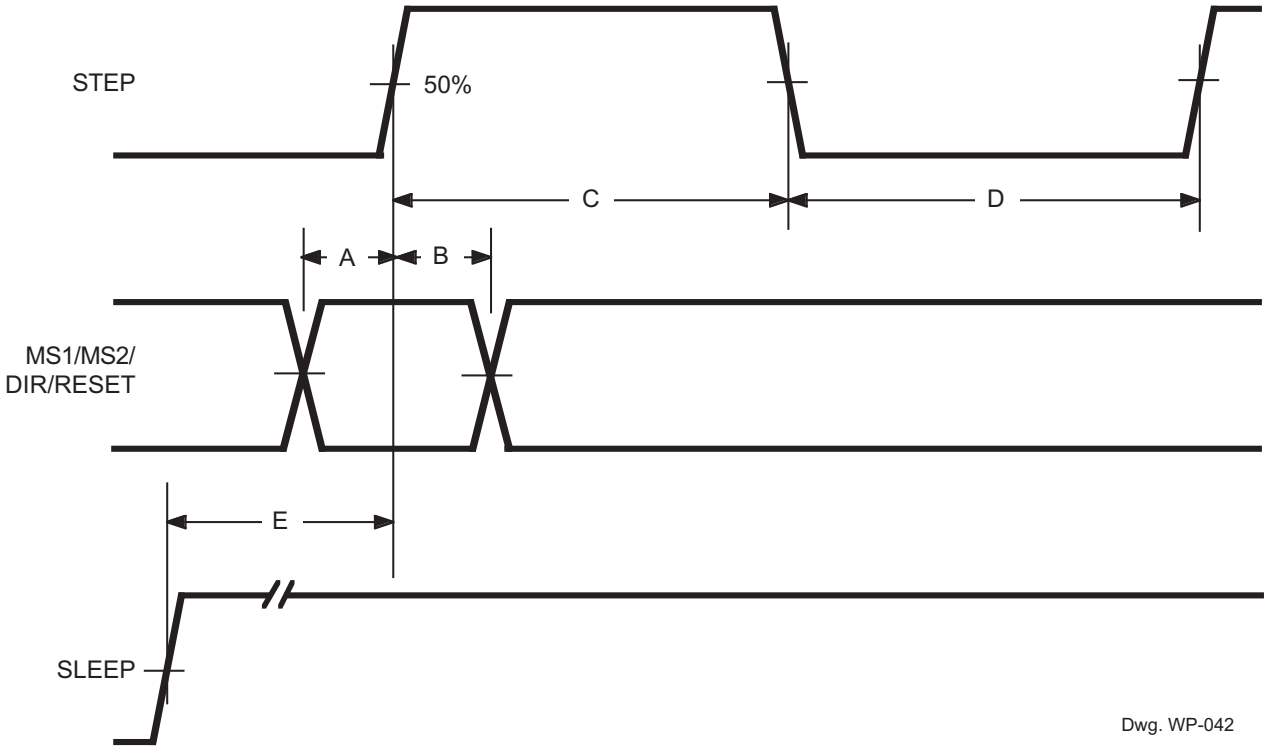


A. Minimum Command Active Time
Before Step Pulse (Data Set-Up Time) ..... 200 ns

B. Minimum Command Active Time
After Step Pulse (Data Hold Time) ..... 200 ns

C. Minimum STEP Pulse Width ..... 1.0 µs

D. Minimum STEP Low Time ..... 1.0 µs

E. Maximum Wake-Up Time ..... 1.0 ms

## Applications Information

**Layout.** The printed wiring board should use a heavy ground plane.

For optimum electrical and thermal performance, the driver should be soldered directly onto the board.

The load supply terminal, $V_{BB}$, should be decoupled with an electrolytic capacitor (>47 µF is recommended) placed as close to the device as possible.

To avoid problems due to capacitive coupling of the high dv/dt switching transients, route the bridge-output traces away from the sensitive logic-input traces. Always drive the logic inputs with a low source impedance to increase noise immunity.

**Grounding.** A star ground system located close to the driver is recommended.

The 24-lead SOIC has the analog ground and the power ground internally bonded to the power tabs of the package (leads 6, 7, 18, and 19).

**Current Sensing.** To minimize inaccuracies caused by ground-trace IR drops in sensing the output current level, the current-sense resistor ($R_S$) should have an independent ground return to the star ground of the device. This path should be as short as possible. For low-value sense resistors the IR drops in the printed wiring board sense resistor's traces can be significant and should be taken into account. The use of sockets should be avoided as they can introduce variation in $R_S$ due to their contact resistance.

Allegro MicroSystems recommends a value of $R_S$ given by

$$R_S = 0.5/I_{TRIP}max$$

**Thermal protection.** Circuitry turns off all drivers when the junction temperature reaches 165°C, typically. It is intended only to protect the device from failures due to excessive junction temperatures and should not imply that output short circuits are permitted. Thermal shutdown has a hysteresis of approximately 15°C.

**Table 2. Step Sequencing**

Home State = 45º Step Angle, DIR = H

| Full Step | Half Step | ¼ Step | ⅛ Step | Phase 1 Current ($\%I_{trip}$max) (%) | Phase 2 Current ($\%I_{trip}$max) (%) | Step Angle (º) |
|---|---|---|---|---|---|---|
| | 1 | 1 | 1 | 100.00 | 0.00 | 0.0 |
| | | | 2 | 98.08 | 19.51 | 11.3 |
| | | 2 | 3 | 92.39 | 38.27 | 22.5 |
| | | | 4 | 83.15 | 55.56 | 33.8 |
| 1 | 2 | 3 | 5 | 70.71 | 70.71 | 45.0 |
| | | | 6 | 55.56 | 83.15 | 56.3 |
| | | 4 | 7 | 38.27 | 92.39 | 67.5 |
| | | | 8 | 19.51 | 98.08 | 78.8 |
| | 3 | 5 | 9 | 0.00 | 100.00 | 90.0 |
| | | | 10 | –19.51 | 98.08 | 101.3 |
| | | 6 | 11 | –38.27 | 92.39 | 112.5 |
| | | | 12 | –55.56 | 83.15 | 123.8 |
| 2 | 4 | 7 | 13 | –70.71 | 70.71 | 135.0 |
| | | | 14 | –83.15 | 55.56 | 146.3 |
| | | 8 | 15 | –92.39 | 38.27 | 157.5 |
| | | | 16 | –98.08 | 19.51 | 168.8 |
| | 5 | 9 | 17 | –100.00 | 0.00 | 180.0 |
| | | | 18 | –98.08 | –19.51 | 191.3 |
| | | 10 | 19 | –92.39 | –38.27 | 202.5 |
| | | | 20 | –83.15 | –55.56 | 213.8 |
| 3 | 6 | 11 | 21 | –70.71 | –70.71 | 225.0 |
| | | | 22 | –55.56 | –83.15 | 236.3 |
| | | 12 | 23 | –38.27 | –92.39 | 247.5 |
| | | | 24 | –19.51 | –98.08 | 258.8 |
| | 7 | 13 | 25 | 0.00 | –100.00 | 270.0 |
| | | | 26 | 19.51 | –98.08 | 281.3 |
| | | 14 | 27 | 38.27 | –92.39 | 292.5 |
| | | | 28 | 55.56 | –83.15 | 303.8 |
| 4 | 8 | 15 | 29 | 70.71 | –70.71 | 315.0 |
| | | | 30 | 83.15 | –55.56 | 326.3 |
| | | 16 | 31 | 92.39 | –38.27 | 337.5 |
| | | | 32 | 98.08 | –19.51 | 348.8 |

**Full Step Operation**
$MS_1 = MS_2 = L$, DIR = H

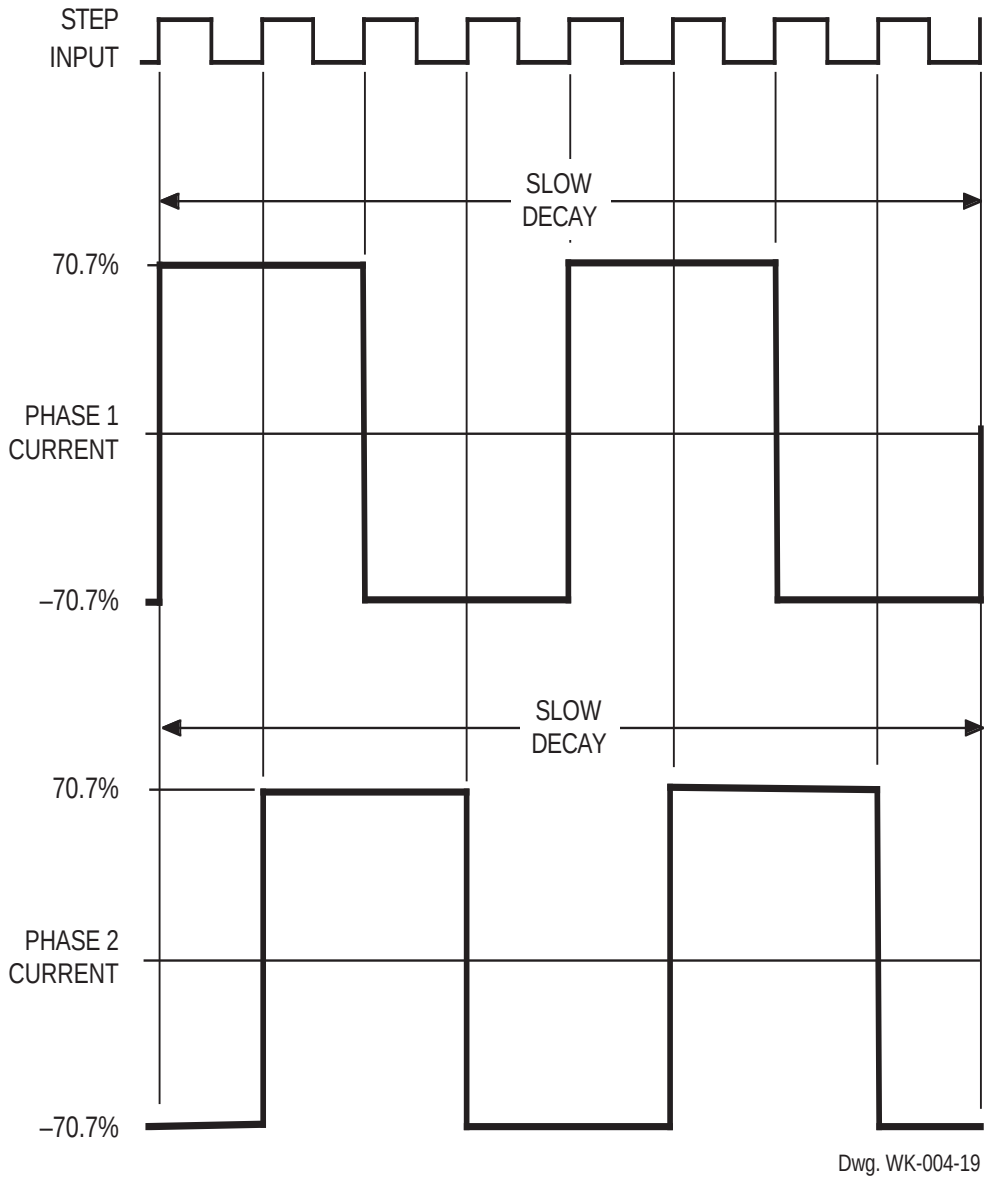


Dwg. WK-004-19

The vector addition of the output currents at any step is 100%.

**Half Step Operation**

$MS_1$ = H, $MS_2$ = L, DIR = H

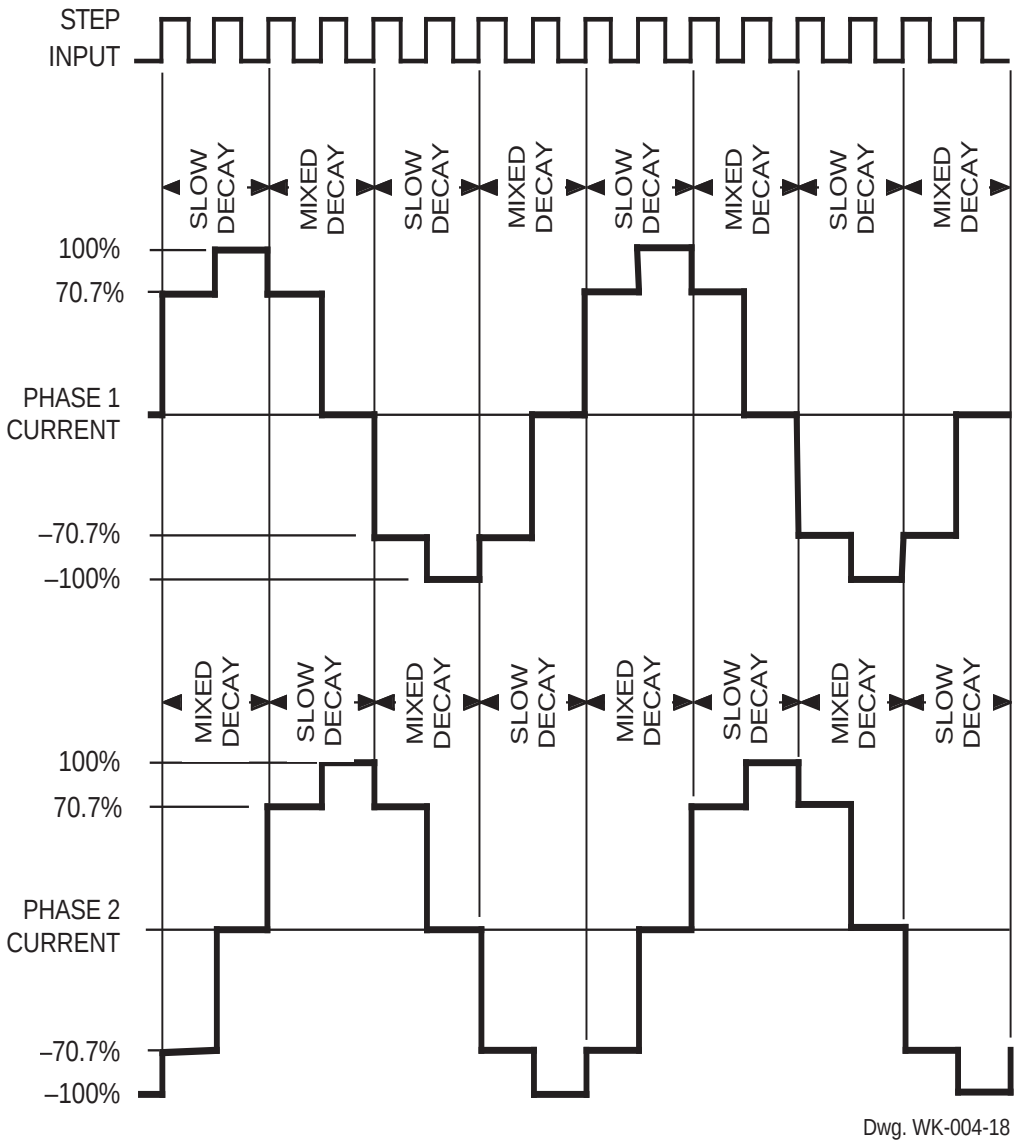


The mixed-decay mode is controlled by the percent fast decay voltage ($V_{PFD}$). If the voltage at the PFD input is greater than $0.6V_{CC}$ then slow-decay mode is selected. If the voltage on the PFD input is less than $0.21V_{CC}$ then fast-decay mode is selected. Mixed decay is between these two levels.

**Quarter Step Operation**
$MS_1$ = L, $MS_2$ = H, DIR = H

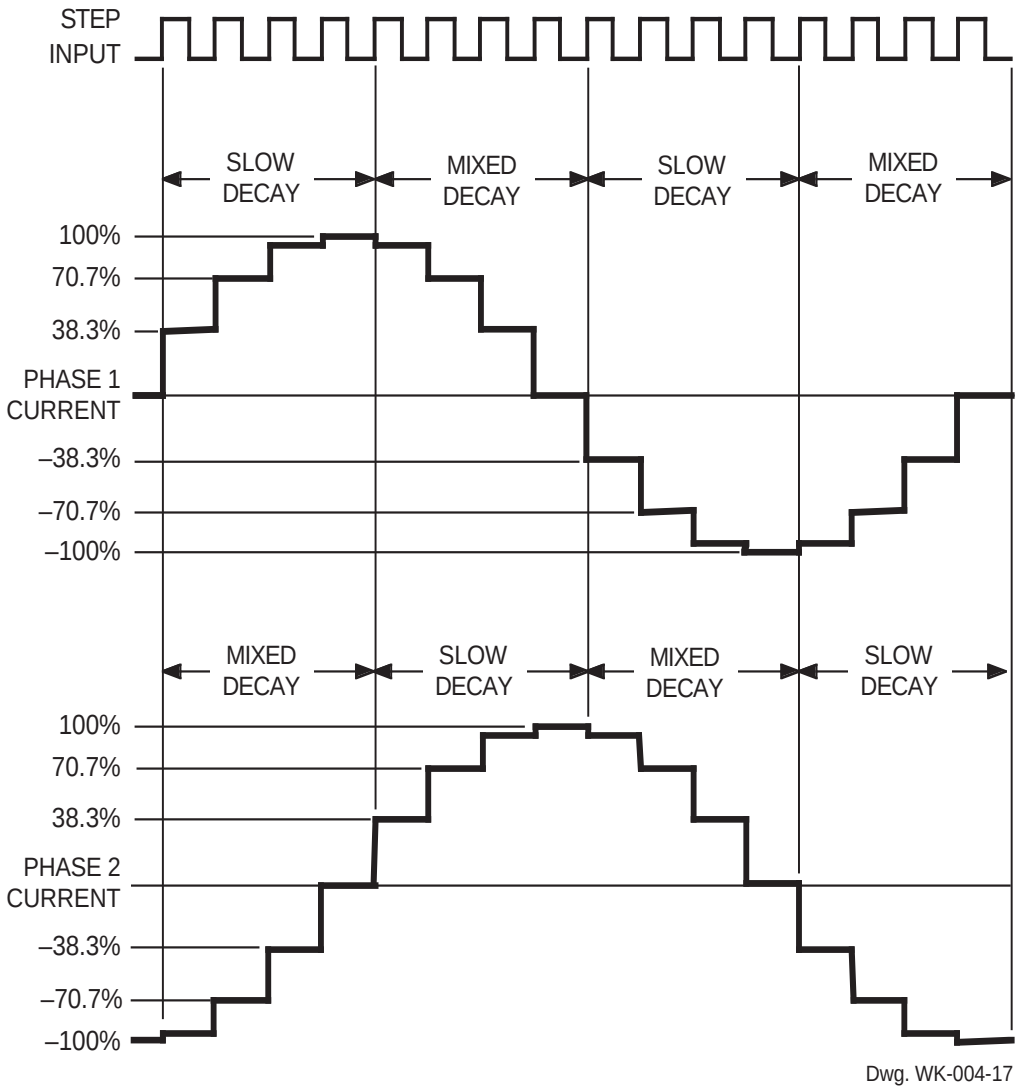


The mixed-decay mode is controlled by the percent fast decay voltage ($V_{PFD}$). If the voltage at the PFD input is greater than $0.6V_{CC}$ then slow-decay mode is selected. If the voltage on the PFD input is less than $0.21V_{CC}$ then fast-decay mode is selected. Mixed decay is between these two levels.

**8 Microstep/Step Operation**
$MS_1$ = $MS_2$ = H, DIR = H

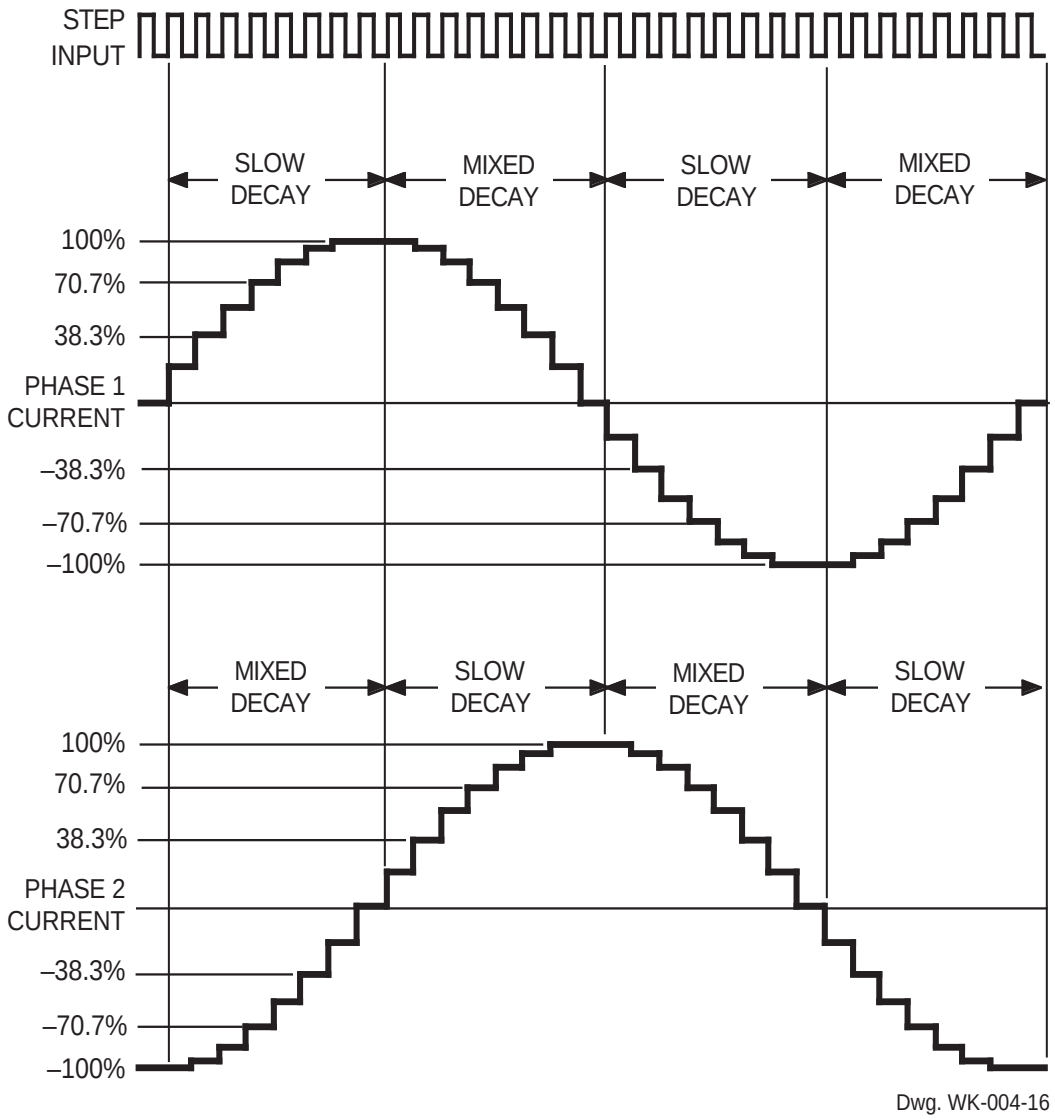


The mixed-decay mode is controlled by the percent fast decay voltage ($V_{PFD}$). If the voltage at the PFD input is greater than $0.6V_{CC}$ then slow-decay mode is selected. If the voltage on the PFD input is less than $0.21V_{CC}$ then fast-decay mode is selected. Mixed decay is between these two levels.

## Pin-out Diagram

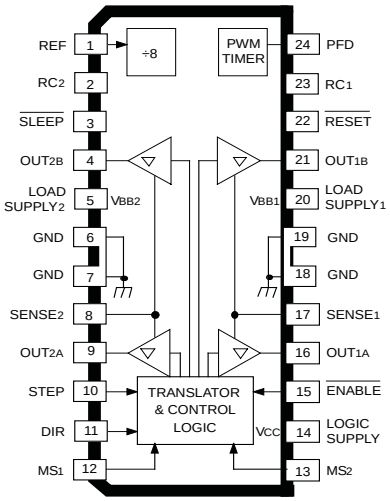


Dwg. PP-075-2

## Terminal List

| Terminal Name | Terminal Description | Terminal Number |
|---|---|---|
| REF | Gm reference input | 1 |
| RC2 | Analog input for fixed offtime – bridge 2 | 2 |
| SLEEP | Logic input | 3 |
| OUT2B | H bridge 2 output B | 4 |
| LOAD SUPPLY2 | VBB2, the load supply for bridge 2 | 5 |
| GND | Analog and power ground | 6, 7 |
| SENSE2 | Sense resistor for bridge 2 | 8 |
| OUT2A | H bridge 2 output A | 9 |
| STEP | Logic input | 10 |
| DIR | Logic Input | 11 |
| MS1 | Logic input | 12 |
| MS2 | Logic input | 13 |
| LOGIC SUPPLY | VCC, the logic supply voltage | 14 |
| ENABLE | Logic input | 15 |
| OUT1A | H bridge 1 output A | 16 |
| SENSE1 | Sense resistor for bridge 1 | 17 |
| GND | Analog and power ground | 18, 19 |
| LOAD SUPPLY1 | VBB1, the load supply for bridge 1 | 20 |
| OUT1B | H bridge 1 output B | 21 |
| RESET | Logic input | 22 |
| RC1 | Analog Input for fixed offtime – bridge 1 | 23 |
| PFD | Mixed decay setting | 24 |

## Package LB 24-Pin SOIC

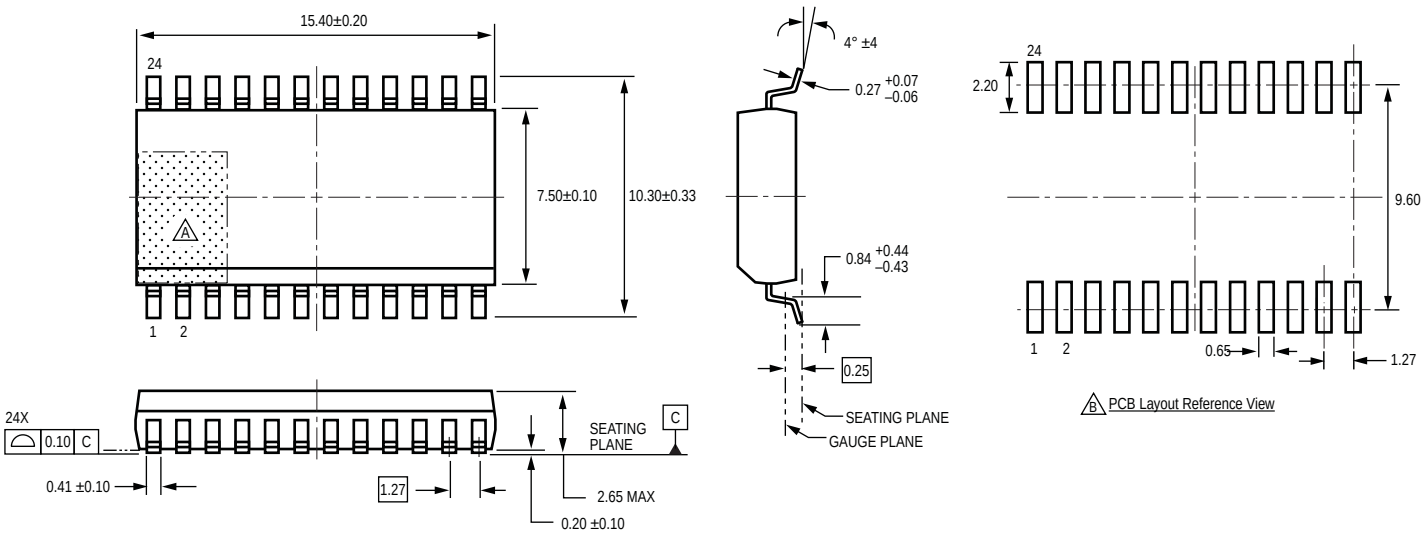


For reference only
Pins 6 and 7, and 18 and 19 internally fused
Dimensions in millimeters
(Reference JEDEC MS-013 AD)
Dimensions exclusive of mold flash, gate burrs, and dambar protrusions

A Terminal #1 mark area

B Reference pad layout (reference IPC SOIC127P1030X265-24M)
All pads a minimum of 0.20 mm from all adjacent pads; adjust as necessary to meet application process requirements and PCB layout tolerances



For the latest version of this document, go to our website at:
**www.allegromicro.com**

Allegro MicroSystems, LLC
115 Northeast Cutoff
Worcester, Massachusetts 01615-0036 U.S.A.
1.508.853.5000; www.allegromicro.com

# EasyDriver v4.5

www.schmalzhaus.com/EasyDriver

An easy to use bipolar stepper motor driver
Use 4 wire, 6 wire or 8 wire steper motors
From about 150mA/phase to about 750mA/phase
Defaults to 5V for Vcc (logic supply), settable to 3.3V
Supply 8V to 30V DC power input on JP1
Do not connect or disconnect motor
whlie EasyDriver is powered

DEFAULT OPTIONS
Short JP5, JP6, JP7 pins
to GND or Vcc to override

SLEEP = Vcc (awake)
MS1 = Vcc (1/8 microstep)
MS2 = Vcc (1/8 microstep)
ENABLE = GND (enabled)
RESET = Vcc (not reset)
PFD = Vcc (slow decay mode)

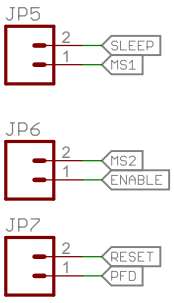


DIR is level sensitive
A rising edge on STEP
causes a step
Both take 0V to Vcc

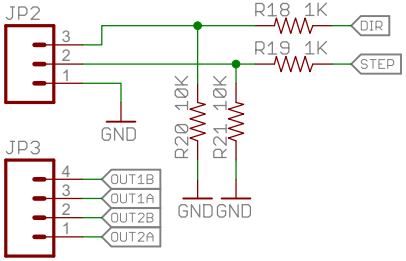


Coil 1 of motor across
OUT1B and OUT1A
Coil 2 of motor across
OUT2B and OUT2A




TP1 = Vref input to driver
Monitor this test point with meter
as you adjust current adj pot
Valid range 1.0V to Vcc
At Vref of 5V max current will be 833mA
At Vref of 2V max current will be 333mA
At Vref of 1V max current will be 166mA
Minimum current gives smoothest microsteps
Maximum current gives highest torque
Max Coil Current(in Amps) = Vref(in Volts)/6
Set R16 to 2.0V at factory = 333mA/phase

PFD intermediate voltage
Set for 'mixed-decay' mode.

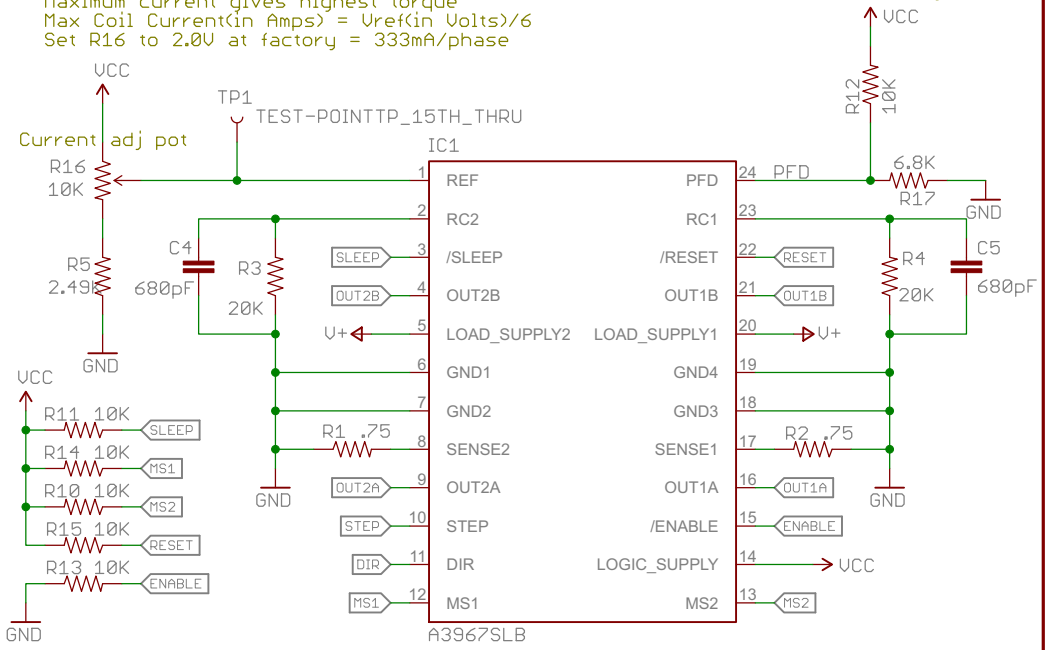


Power Input
8V to 30V (Vcc = 5V)
6.3V to 30V (Vcc = 3.3V)

Must use LM317
For 30V V+ input

SJ1 Normally Shorted
Cut to use your own
Vcc source from JP4

Vcc output

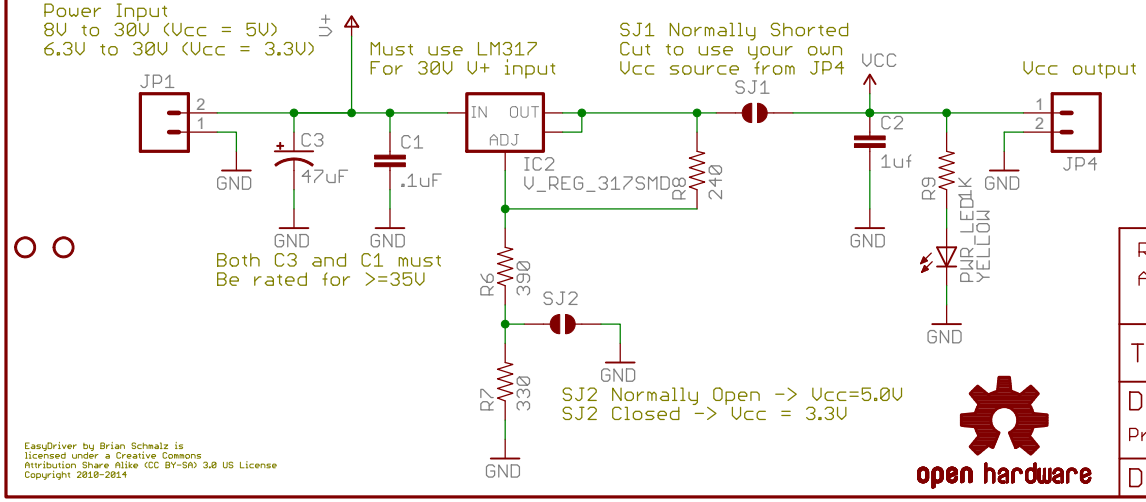


Both C3 and C1 must
Be rated for >=35V

Change List
v4.3 12/09/09 BPS Added mounting holes
v4.4 10/24/20 BPS
Fixed MIN/MAX silkscreen
All vias now .02"
v4.4 1/3/12 BPS : C3 now 47uF
v4.5 2/25/14 BPS



open hardware



TITLE: EasyDriver_v45 | SFE

Design by: Brian Schmalz
Produced by Spark Fun Electronics

REV: 4.5

Date: 12/18/2014 9:51:38 AM | Sheet: 1/1

Added series resistors and pull douns on STEP/DIR

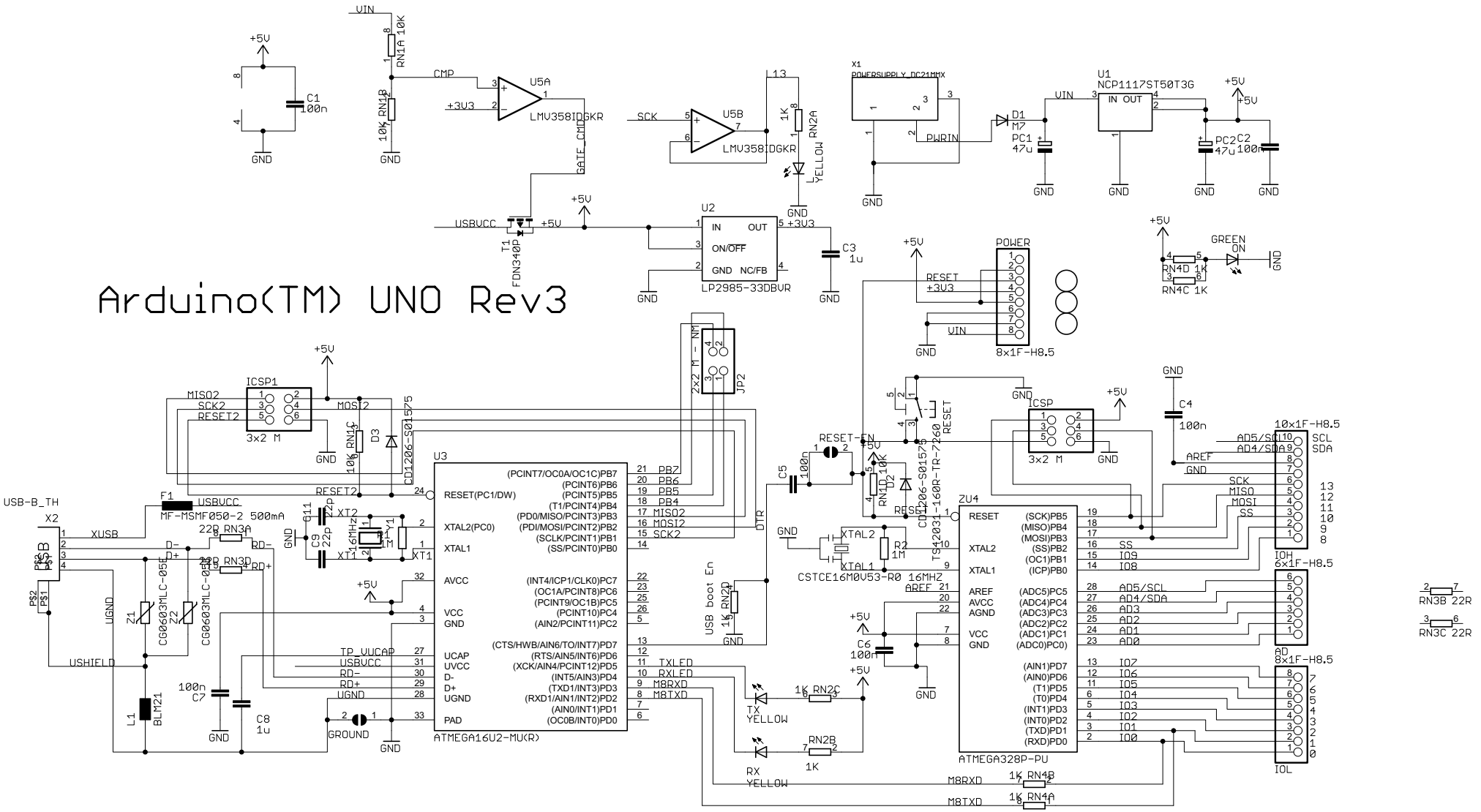

# References


[1] StepperOnline, "6Hs12-0304S Full Datasheet," [Online]. Available: https://www.omc-stepperonline.com/download/6HS12-0304S.pdf. [Accessed 4 December 2019].

[2] Parallax, "Microsoft Word - 28986-LiIonPowerCharger2cell-v1.0-Draft B.doc," [Online]. Available: https://www.parallax.com/sites/default/files/downloads/28986-Li-ion-Power-Charger2cell-v1.0.pdf. [Accessed 4 December 2019].

[3] Parallax, "No Title," [Online]. Available: https://www.parallax.com/sites/default/files/downloads/28986-Schematic-Li-ion-Charger-2Cell.pdf. [Accessed 4 December 2019].

[4] Allegro, "3967.indd," [Online]. Available: https://cdn.sparkfun.com/datasheets/Robotics/A3967-Datasheet.pdf. [Accessed 4 December 2019].

[5] B. Schmalz, "EasyDriver_v45.sch," 18 December 2014. [Online]. Available: https://cdn.sparkfun.com/datasheets/Robotics/EasyDriver_v45.pdf. [Accessed 4 December 2019].

[6] Arduino, "aruino_Uno_Rev3-02-TH.sch," [Online]. Available: https://www.arduino.cc/en/uploads/Main/Arduino_Uno_Rev3-schematic.pdf. [Accessed 4 December 2019].